Electroactive Supramolecular Systems for Informed Electrochemical Sensor Development

A thesis submitted to the Committee of Graduate Studies in Partial Fulfillment of the Requirements for the Degree of Master of Science in the Faculty of Arts and Science

TRENT UNIVERSITY
Peterborough, Ontario, Canada

Environmental and Life Sciences M.Sc. Graduate Program
January 2025

Abstract

Electroactive Supramolecular Systems for Informed Electrochemical Sensor Development

Carlos Quintero Arias

In an effort to improve upon existing analytical methods, electrochemical sensors offer portable, cost-effective alternatives to traditional lab-based techniques. Recent advances in supramolecular chemistry offer a unique alternative to achieve high selectivity while also benefitting from facile scaling for mass production. Thus, by incorporating host-guest chemistry with electrochemical sensors, the development of simple and selective sensors is possible. To that extent, novel hosts and electroactive ion pairs were investigated for their ability to transduce an electrochemical signal representative of host-guest complexation. Results demonstrated that the upper rim modifications of resorcinarene hosts attenuated their affinity for electroactive probes whilst maintaining structural integrity upon extended cycling. Further work revealed that guests may be directly quantified via their complexation with electroactive hosts. The sensing method was further validated by quantification of surfactant pollutants in the Otonabee River. Through a fundamental understanding of the electrochemical behaviour of host-guest systems a general sensing platform can be developed, where hosts are interchangeable for specificity towards any desired analyte. Therefore, moving away from expensive lab-based methods and significantly reducing the barriers for biological or environmental monitoring.

Keywords: Electrochemistry, Supramolecular Chemistry, Host-Guest, Resorcinarenes, Environmental monitoring, Pollutants, Ferrocene, Surfactants, PFAS, AMP

Acknowledgements

This work is the culmination of not only two years of research but also of an entire community's support. All work is a product of that which came before it, there is no such thing as a new idea free of inspiration; I am forever grateful for all the lessons I learned and all the help that went into completing my Master's. I want to thank the entire Martic Lab for their insightfulness; especially Dr. Martic, my supervisor, for encouraging me to ask "why?", to seize every opportunity, and for facilitating my discovery of electrochemistry. I wouldn't be the scientist I am today without it. To my Committee, Dr. Thompson and Dr. Keske, the breadth of knowledge you both brought to my project made me excited about how much more I have to learn. To Dr. Accettone, thank you for making the GTA experience so enjoyable, your teaching inspires. And to Dr. Beyeh, Dr. Twum and Frank, for being the supramolecular masterminds. Thank you for welcoming me in Oakland, your contributions can't be overstated.

I must thank my friends at Trent who levelled out the highs and lows of grad school. To Lance and Najia, the time spent around whiteboards and bickering about the finer points of electrochemistry were the best part of my work. To Lance, thank you, for teaching me how many doors a simple "Hello" will open (leading to my Linkedin connection with the Dr. Alex Peroff). To Jo, Tyra, Dev, and Meaghan, you each had priceless words of wisdom about the woes of grad school and life.

I'd like to thank my community, without their support, I may have given up a long time ago. Peterborough catches a lot of flak for being boring, but I learned that was a lie, a community of loving people could turn the Arctic into a Carnival. To Fede, David, Brooke, Edward VII, De, Ryan, Jake, Fin, Zach, Liv, David K, Cam, Matt, Clara, Adam and of course… Ryu and Keasby,

the cat, who was no help at all: thank you for making ptbo my home. I will always cherish the memories we made together.

To my family, who've put up with crazy schedules, whose love and insights inspire me, thank you. My mama, my dad, my brother Rudy, everything I am, is because of you. Thank you for always being in my corner, I can only repay you by making you proud. To Ryu, who I love and depend on more than I can say, thank you. Your unhesitating love and support always kept me going, thank you for always believing in me, thank you for being my rock. Los amo a todos mucho.

Table of Contents

List of Figures

Chapter 1 – Introduction to Supramolecular Systems and Electrochemical Sensing

1.1 Introduction

The design and development of modern analytical methods must consider the importance of accessibility. To that point, electrochemical sensors offer a unique opportunity to overcome barriers to entry; electrochemical sensors benefit from miniaturization, cost-effectiveness, and simplicity, all of which present hurdles to accessible analytical monitoring. Traditional lab-based analytical methods require trained personnel to develop rigorous standard operating procedures (SOPs) for an analysis suite. As a result, the analysis of environmental and biological samples is a time consuming and expensive process. Moving towards novel electroanalytical methods promises to empower the user by off-loading method development and allowing for simple "plug-and-play" analysis. Towards that goal, electrochemical sensing has received a lot of attention in academia with electrochemical sensor being developed across many fields including pharmaceuticals, environmental analysis, food quality inspection, and water quality monitoring.[1–4] Often, electrochemical sensors require complicated preparation to elicit a selective and sensitive response which may be achieved through the incorporation of supramolecular systems.

Synthetics molecular receptors with pre-organized cavities are central to supramolecular chemistry.[5] The self-assembly of supramolecular systems has been exploited for the highly specific recognition of various analytes. The formation of host-guest complexes can be deterministic through careful design of hosts to optimize non-covalent complementarity. Interestingly, the synthesis of host molecules is already practiced at an industrial scale, highlighting the molecule's

facile production. Host molecules have also seen applications across the same fields as electrochemical sensors; however, the detection of host-guest complexation is still reliant on traditional lab-based methods. By coupling the selectivity of host-guest complexes with the simplicity of electrochemistry the development of alternative analytical methods is possible.

Existing reports of host-guest electrochemical sensors are abundant given the clear benefits of connecting the two disciplines. Currently, sensors have focused on simplistic, early discovered host molecules such as crown ethers (CEs), cyclodextrins (CDs) and cucurbiturils (CBs).[4,6–9] Although, recent advancements in the synthesis of resorcinarene host molecules has vastly widened the library of available guests.[7] Resorcinarene hosts also benefit from a scalable synthesis whilst also being easily modified to complement any desired guest. Therefore, a general sensing platform can be developed where the resorcinarene host can be swapped out to fit the application.

Here, an introduction to electrochemical sensing methods and host-guest systems is reviewed. First, an overview of electrochemistry and electroanalytical methods is explained to understand the foundation of a sensing platform. This is followed by a review of host-guest systems, their design, functionality, and application. Finally, the integration of host-guest systems into electrochemical sensing is investigated to understand the advances in sensor development.

1.1 Electrochemical Sensing

Electrochemical sensors provide a powerful means to investigate electron transfer reactions. Reduction and oxidation reactions can be characterized through the application of a potential to an electrode via an external power supply. At the surface of the electrode, a species is reduced ($A + e^-$) if electrons in the electrode are at a higher energy than the lowest unoccupied molecular orbital (LUMO) or oxidized in the opposite case.[10,11] By monitoring these redox reactions and associated

standard redox potentials, electrochemical sensors can differentiate between molecules.[10,12] This simple principle can be exploited to gain insight into the analyte reactions or to quantify analytes.

Electrochemical sensors are abundant throughout industrial and consumer products given their low detection limits, cost-effectiveness, and miniaturization. The utility of electrochemical sensors is evident from their incorporation into various use cases, including wearables, bench-top sensing, or integrated into industrial electrochemical stacks for real time system analysis.[13,14] Throughout these applications, the fundamentals of electrochemical sensing are maintained; an analytical signal is gathered from the transduction of an electrochemical signal from the analyte.[15] However, beyond a simple electrical signal, sensors rely on various electroanalytical methods for detection and quantification. The various electroanalytical methods, their theory and advantages are covered in the following section.

1.1.1 Cyclic Voltammetry

Cyclic voltammetry (CV) is a popular electroanalytical method for the understanding of complicated electrochemical systems within seconds.[10,11] It is often employed as an initial method to gain a general understanding of an electrochemical system. In CV the potential is linearly swept across in the reverse and forward direction within the electroactive range of the analyte of interest around the standard electrode potential. [10,11] The potential is swept up to a switching potential (E_2) where the sweeping direction is reversed. The resulting current (i) is plotted against the voltage (V) in a voltammogram (Figure 1B).

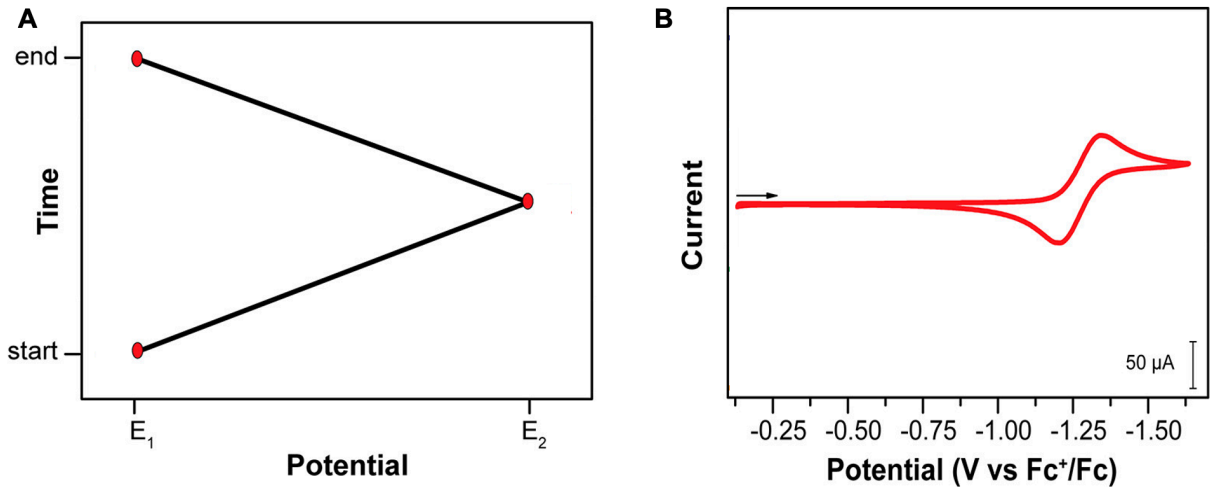

Figure 1.1. A) Cyclic potential sweep. B) Cyclic Voltammogram from potential sweep.[11] Reused under a creative commons license.

The initial current rise is dependent on the overpotential applied to the electrode and is limited by the electrochemical kinetics of the electrode. This region of the current response is described by the Butler-Volmer equation.[10,16]

$$j = j_0 \cdot \{e^{\left(\frac{(1-\alpha)zF\eta}{RT}\right)} - e^{-\left(\frac{\alpha zF\eta}{RT}\right)}\},$$

where j is the electrode current density (A m^{-2}), j_0 is the exchange current density (A m^{-2}), α is the charge transfer coefficient, z is the number of electrons involved in the reaction, F is the faraday constant (C mol^{-1}), η is the activation overpotential ($\eta = E - E^{0'}$) (V), R is the gas constant (J K^{-1} mol^{-1}), and T is the temperature (K).

The Butler-Volmer equation is a fundamental equation for electrochemical kinetics and demonstrates the relationship between current and voltage. The exchange current density provides insight into the efficiency of current output. For example, an exchange current density of $j_0 = 10^3$ µA/cm^2 appears as a straight line, parallel to the y-axis, compared to a $j_0 = 10^{-3}$ µA/cm^2, which extends further out before the exponential current behaviour is observed (Figure 2A). Simply, a

small j_0, requires significantly more potential for the same current output. The equation also reveals the symmetry between the anodic and cathodic reactions (oxidation and reduction) through the charge transfer coefficients, providing insight into the reversibility and kinetics of the redox reactions. As seen in figure 2B, the charge transfer coefficients impact the behaviour of the anodic or cathodic reactions. An α near 0 represents a favourable cathodic reaction, where values near 1 represent a favourable anodic reaction. This is obvious through the difference in steepness in the anodic and cathodic branches of the Butler-Volmer plot (Figure 2B). Therefore, with an understanding of the current behaviour, CV provides significant insights into the behaviour and kinetics of the electrochemical system.

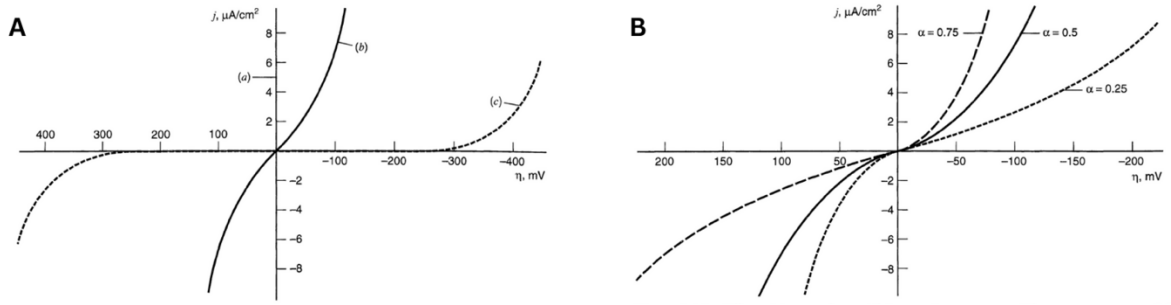

Figure 1.2. A) Impact of j_0 on activation overpotential, (a) $j_0 = 10^3$ μA/cm^2 (b) $j_0 = 10$ μA/cm^2, (c) $j_0 = 10^{-3}$ μA/cm^2, for a single electron reaction with a α of 0.5. B) Impact of α on the symmetry of the Butler-Volmer plot, for a single electron reaction with a α of 0.5. B) Impact of α on the symmetry of the Butler-Volmer plot, for a single electron reaction with a $j_0 = 10$ μA/cm^2.[10] Reproduced with permission, license number 5895361439938.

Eventually the CV current reaches a peak as all of the available analyte has been reduced to the oxidized species. Beyond this point, the current is limited by diffusion of the analyte to the electrode surface and is said to be under mass-transfer conditions and no longer behaves according

to the Butler-Volmer equation.[10,11] The rate or speed at which the potential is swept also greatly impacts the resulting voltammogram.

The speed at which the potential is scanned can also be altered and is known as the scan rate (υ). A common υ is 100 mV/s, where the potential sweep speed is sufficiently fast for results to represent a "stable" electrochemical system.[11] Modulation of υ is a common method of investigating the reversibility or a reaction and homogeneity of the reacting analyte via the Randles-Sevcik equation.

$$i_p = 0.4463nFAC\sqrt{\frac{nF\upsilon \mathrm{D}}{RT}},$$

where i_p is the peak current (A), n is the number of electrons involved in the reaction, F is faradays constant (C mol^{-1}), A is the surface area of the working electrode (cm^{-2}), C is the concentration of the electroactive species (mol cm^{-3}), υ is the scan rate (V s^{-1}), D is the diffusion coefficient (cm^2 s^{-1}) , R is the gas constant (J K^{-1} mol^{-1}), and T is the temperature (K). This equation is another fundamental aspect of the CV method as it provides insight into the electrode surface, the electroactive species, and quantification.

During sensing, the electrode surface can highly influence the resulting signal. Electrode fouling is the result of a passivation layer accumulating over the electrode surface, preventing further electron transfer.[10] To mitigate this issue, electrodes are cleaned regularly to polish the surface, ideally restoring an identical surface between measurements. However, the surface may be actively fouled during measurements as the analyte adsorbs to the surface, breaking the assumption of diffusion dependent current. This is apparent through by plotting the i vs $\upsilon^{1/2}$, where a linear relationship is expected for a freely diffusing species on an unfouled electrode surface (Figure 3). Therefore, the Randles-Sevcik equation can reveal the state of the electrode surface to

inform optimization of cleaning procedures or the utility of an electrochemical sensor for the analyte of interest.

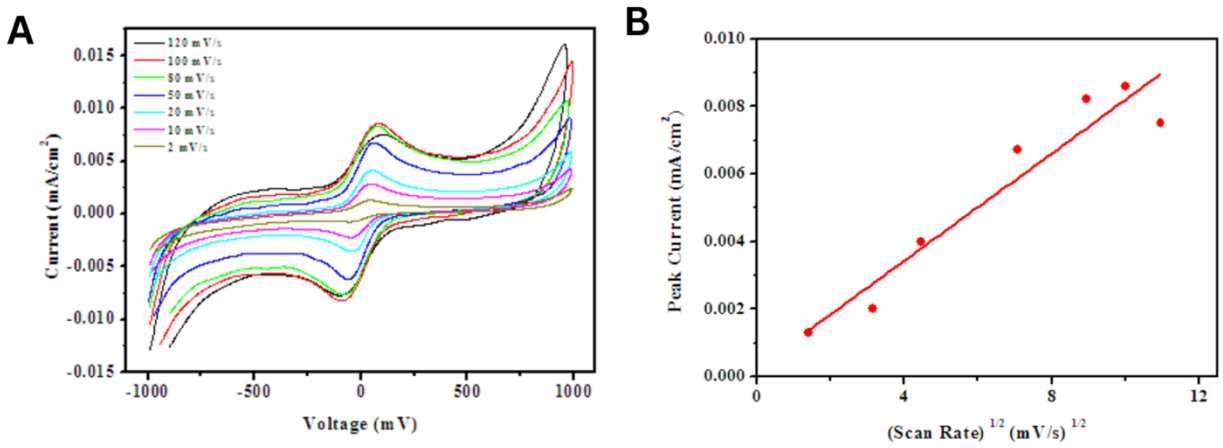

Figure 1.3. A) Cyclic voltammograms in a solution of potassium ferrocyanide at various scan rates; B) linear correlation of the peak current on the square root of the scan rate. All measurements taken on a carbon electrode.[17] Reused under a creative commons license

In more advanced electrochemical sensors, porous and functionalized surfaces are common, where the surface area cannot be geometrically determined. In these cases, the Randles-Sevcik equation is a powerful tool to isolate the area. The area can then be optimized during manufacturing to ensure a consistent current output between sensors.

While working with novel electroactive species or systems the Randles-Sevcik equation can also characterize and quantify the species. Primarily, the *D* is an important parameter when investigating an electroactive species. When a complex or electrosynthesis product is being studied, the *D* will vary and reflect in the current. It can serve as a parameter for optimization of industrial synthesis or a marker for quantification of a complex. Furthermore, at the core of sensing is quantification. The *C* can also be isolated in the Randles-Sevcik equation for rapid quantification

of the analyte. Thus, it is apparent how the straightforward, rapid CV method can provide extensive information regarding the species of interest.

Throughout literature CV has proven to be a central method for characterizing electrochemical sensors. Mathad *et al*. prepared β-cyclodextrin (β-CD) host modified carbon dots (C-dot), for the electrochemical detection of the anticancer drug lapatinib.[18] Here, carbon dots are prepared from *Azadirachta indica* leaf extract and modified with β-cyclodextrin through hydrogen bonding. They drop-casted their modified carbon dots onto a glassy carbon electrode (GCE) for sensing of lapatinib in solution. Given the complex modification of their electrode surface, they used CV and the Randles-Sevcik equation to prove the surface was indeed modified and subsequently determined the area; the Randles-Sevcik equation demonstrating a marked increase in the β-CD/C-dots modified electrode area (0.627 cm^2) compared to the bare electrode (0.0514 cm^2) (Figure 4A). CV was also employed for the characterization of the lapatinib oxidation on the various electrodes. Through CV they identified 3 oxidation peaks at 0.91, 1.12, and 0.55 V, along with one reduction peak at 0.50 V (Figure 4B). The CV also demonstrated that their β-CD/C-dots modified electrode had a 16-fold increase in the peak anodic current compared to the bare electrode. Therefore, CV provided necessary insight into the characterization of the electrochemical sensor and will serve a similar role in the characterization in this thesis.

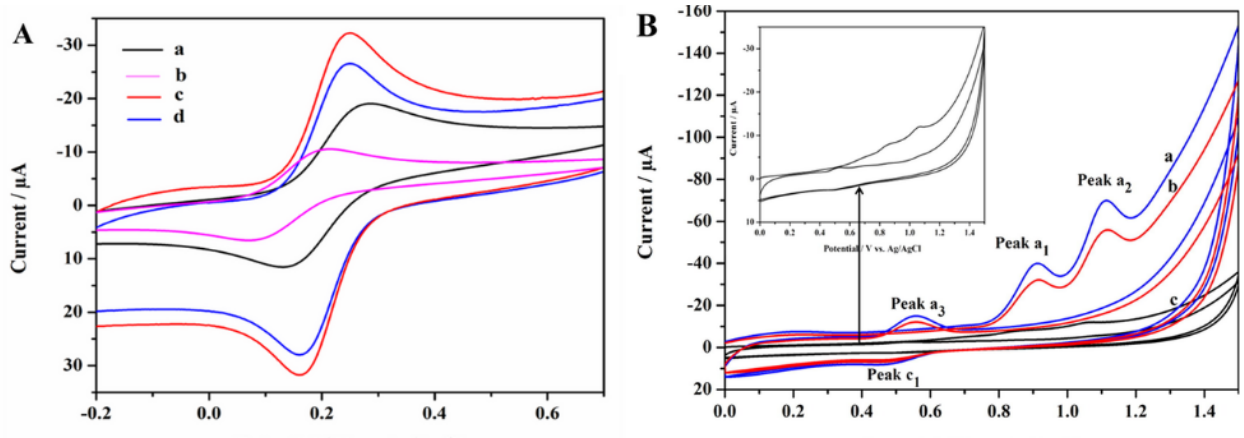

Figure 1.4. A) Cyclic Voltammograms on glassy carbon electrodes (GCE) (a), β-CD (b) C-dots (c) and β-CD/C-dots (d) in 0.1 M KCl all in 1 mM $[Fe(CN)_6]^{3-/4-}$. B) Cyclic Voltammograms of 10 µM LAP at β-CD@C-dots/GCE (a), C-dots/GCE (b), and bare GCE.[18] Reproduced with permission, license number 5895081303221.

While CV is a popular preliminary method the limited resolution and signal convolution require it to be used in tandem with other methods. While conducting a CV measurement, the faradaic current is the current generated by the reaction at the electrode surface and is the current of interest. However, the current in the voltammogram is representative of all contributing processes in the system. This presents an issue when detecting low concentrations of analyte as the faradaic current may be masked by other background current signals. Primarily, the current from the charging of the electrochemical double layer results in a large background current, capping limits of detection (LOD) to 10^{-5} M.[10] The charging and faradaic current cannot be isolated in CV. Furthermore, CV cannot distinguish between the electrode kinetic and chemical steps in a reaction. The current behaviour is modelled by the Butler-Volmer equation; however, the current may be limited by a preceding chemical step.[10] Thus, the current may be obstructed and incorrectly

attributed to slow electrode kinetics. In response to these limitations, several pulse techniques have been developed.

1.1.2 Pulse Voltammetry

Pulse voltammetry techniques have garnered attention given their ability to mitigate the charging current's presence during measurements. The methods arise from the voltametric method of polarography on dropping mercury electrodes (DME).[10] The DME, similar to a leaky faucet, relies on the continuous dropping of mercury to serve as a working electrode. However, the changing electrode area induces a charging current related to the rate of growth of the drop. Therefore, the faradaic current is the greatest, and the rate of drop growth the lowest at the end of the drops life cycle, just before falling off (Figure 5). The realization that the end of the drop's life cycle provided the highest sensitivity, and the best isolation of faradaic current resulted in the earliest pulse techniques. Tast polarography, an early pulse method, instead measured the current at discrete, constant intervals, just before a drop falls off, thus mitigating the charging current effects.

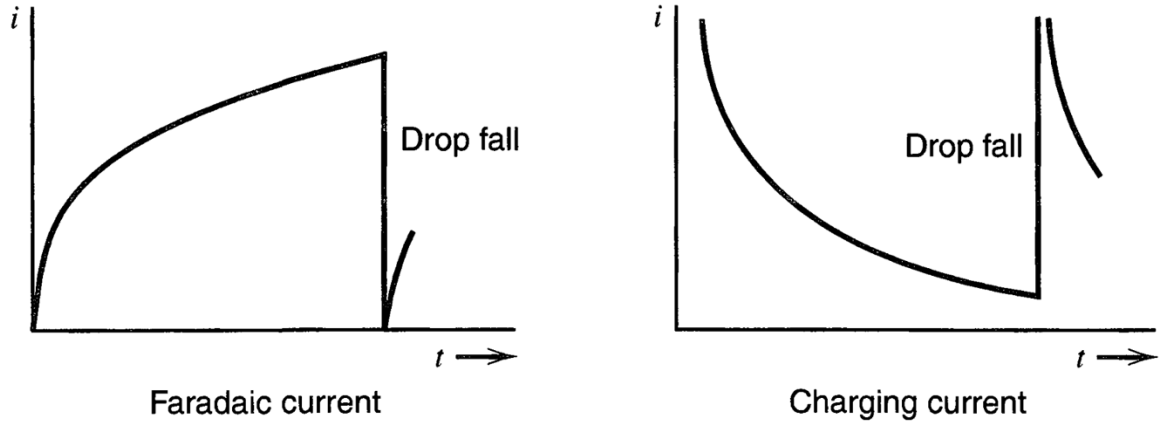

Figure 1.5. Schematic representation of faradaic and charging current of a dropping mercury electrode.[10] Reproduced with permission, license number 5895361439938.

A similar method based on the same principle has been developed for modern planar electrodes, known as differential pulse voltammetry (DPV). In DPV, a base potential is applied before a brief pulse of ~10 mV, then the potential is brought back to another base potential slightly greater than the previous (Figure 6A). The current is measured twice, once before the pulse (τ'), and a second time before the pulse end (τ). The difference in these two current measurements ($\delta i = i(\tau) - i(\tau')$) is plotted against the potential and the resulting voltammogram presents a peak around the E^0 (Figure 6B). The peak shape is unique to the pulse methods and unlike the current increase and plateau seen in CV. The voltammogram peak arises from the methods measurement of differences in current. At base potentials significantly more positive than the reduction potential no faradaic current flows and δi is near zero. At base potentials significantly more negative than E^0, the current has reached mass-transfer conditions and δi is again near zero. It is only at base potentials near E^0 where a small pulse can induce a large change in current, resulting in the peak shape. Importantly, the base potential sets up the electrochemical double layer and the pulse time is relatively small compared to the base potential application; therefore, the charging current is comparable, while the faradaic current is significantly different between τ' and τ. Thus, the subtraction in δi eliminated the charging current and the result is representative of only the faradaic current, increasing the sensitivity compared to CV. This method has proved useful for quantification with far lower LODs than CV, and boasts improved LODs over traditional spectroscopic and some chromatographic methods.[19] Similar pulse methods such as square wave voltammetry (SWV) rely on the same principle while varying the baseline potential hold. The pulse methods will be of great importance in the detection and quantification of surfactant pollutants which are often found at nanomolar concentrations. However, the increased sensitivity also requires careful consideration during experimental set-up due to the possibility of interference

from electrolyte or the sample solution background compound. Also, the pulse methods also suffer from the inability to resolve complex systems and their individual elements.

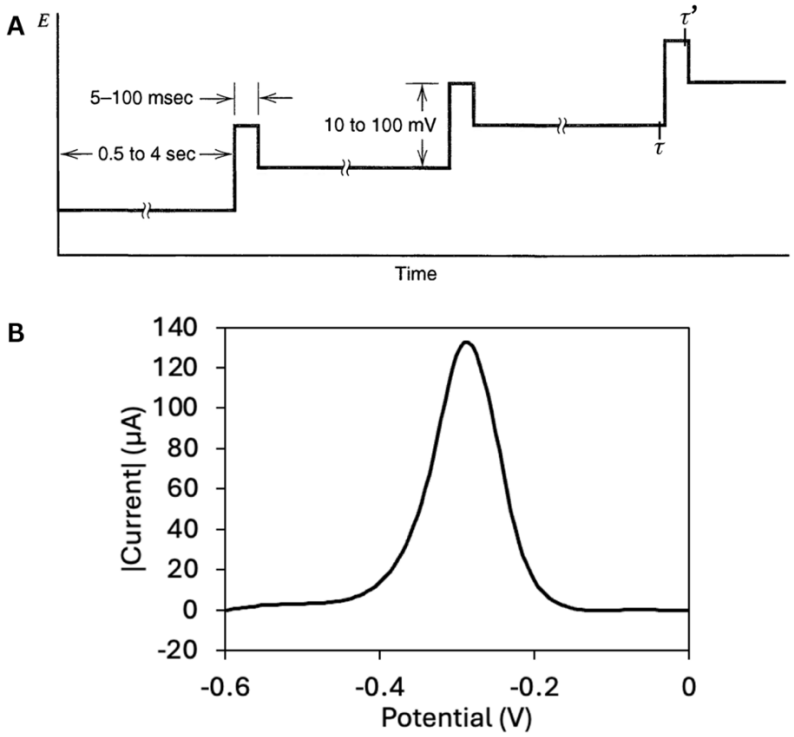

Figure 1.6. A) Potential program differential pulse experiment. B) example differential pulse voltammogram from 100 μM methylene blue in 100 mM phosphate buffer.[10] Reproduced with permission, license number 5895361439938.

Due to the increased sensitivity of DPV, it has been used throughout literature for the quantification of various analytes. In the article previously mentioned, *Mathad et al.* recognize the lack of sensitivity of CV for quantification. Despite the extensive use of CV for characterization, they used DPV to develop calibration curves for lapatinib with an LOD of 8.56×10^{-10} M, significantly lower than the 10^{-5} M LOD possible with CV. Another group developed a molecularly imprinted polymer (MIP)-electrode for the detection of caffeine in sports drinks.[20] They also recognize the power of the pulse methods for quantification of caffeine and developed a calibration

curve with a reported LOD of 2.5 x 10^{-6} M using DPV (Figure 7). Therefore, DPV has served as an effective method for quantification given its increased sensitivity and inherent charging current subtraction. The method will serve the same purpose in this thesis to quantify analytes of interest.

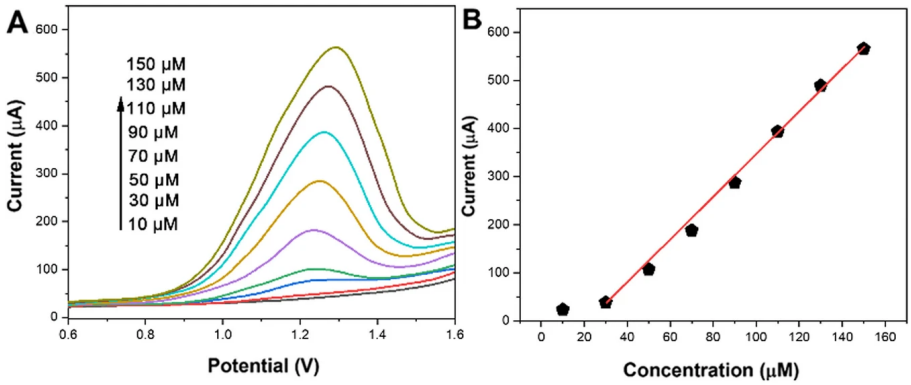

Figure 1.7. A) Differential pulse responses of different concentrations of caffeine. B) corresponding calibration curve.[20] Reproduced with permission, license number 5895090007215.

1.1.3 Electrochemical Impedance Spectroscopy

Electrochemical impedance spectroscopy (EIS) is a unique method that has recently become popular for its ability to isolate individual elements of a complex electrochemical system. Unlike the methods discussed hitherto, EIS relies on the perturbation of various ac voltage frequencies around an applied voltage (E_{app}) and the subsequent monitoring of an output sinusoidal current (Figure 8).[10,21,22] Since different components of an electrochemical system operate at different time scales, by applying a range of frequencies, EIS can probe each individual element of the system at their respective time constants. For example, the charging of the electrical double layer happens at faster time scale than the diffusion of analyte to the electrode surface, thus their characteristic frequencies are unique. While CV or DPV cannot distinguish the current from either process, by applying a range of frequencies EIS can isolate the two phenomena. To better understand EIS, a review of the origin of impendence and the fundamental circuit elements is necessary.

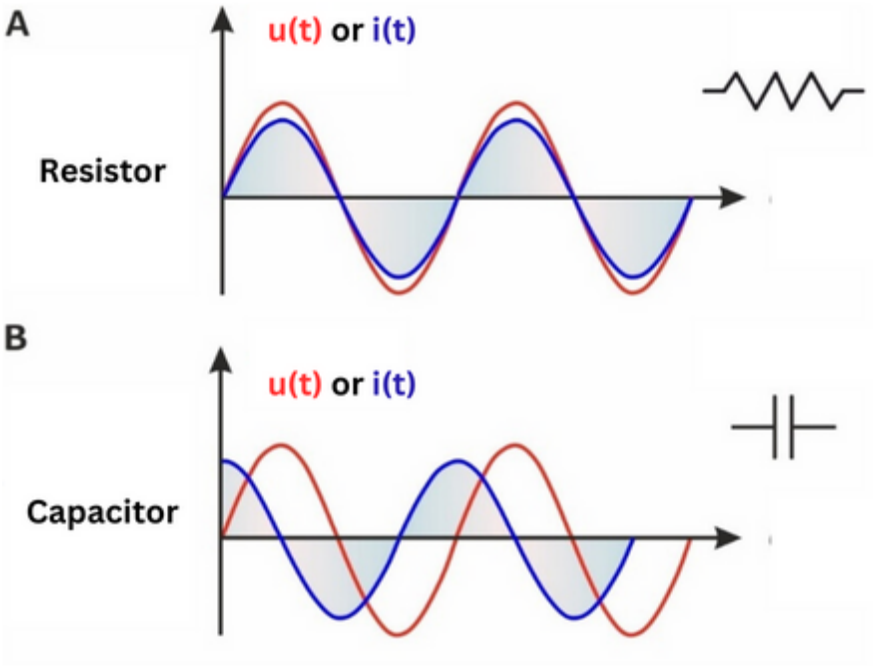

Figure 1.8. Sinusoidal waveforms u(t) and i(t) when an alternating voltage is applied to A) a resistor or B) a capacitor.[22] Reused under a creative commons license.

The resistor and capacitor are fundamental circuit elements that are most often encountered and used to describe an electrochemical system. The components behave according to their fundamental equations:

Table 1. Resistor and Capacitor circuit element representations, current, and impedance formulas.

	Resistor	**Capacitor**
Symbolic Representation		
Current Output	$I_R = \frac{U_R}{R}$	$i_C = C\frac{dU_C}{dt}$
Impedance	$Z_R = R$	$Z_C = \frac{1}{j\omega C}$ $\omega = 2\pi f$

From the equations for current, it is clear that across a resistor, the output current is proportional and in phase to the input voltage amplitude (Table 1, Figure 8A). However, with a capacitor, the output current is dependent on the rate of change of the input voltage, resulting in a phase shifted output current (Table 1, Figure 8B). Therefore, the relationship between the input and output is inconsistent; ironically, complex terms simplify the relationship. By first writing the voltage and current in their phasor notation, given Euler's formula, the voltage and current can be represented as their real components:

Euler's formula:

$$e^{\pm j\varphi} = \cos(\varphi) \pm j\sin(\varphi)$$

Voltage:

$$U(t) = |U|\cos(\omega t + \varphi_U)$$

$$\underline{U} = \left|\underline{U}\right| e^{j(\omega t + \varphi_U)}$$

Current:

$$I(t) = |I|\cos(\omega t + \varphi_I)$$

$$\underline{I} = \left|\underline{I}\right| e^{j(\omega t + \varphi_I)}$$

Considering that the impedance is analogous to resistance, we can then move away from time dependence and a constant proportionality between the input and output signals is revealed.

Impedance:

$$\underline{Z} = \frac{\left|\underline{U}\right|}{\left|\underline{I}\right|} e^{j(\omega t + \varphi_U - \omega t - \varphi_I)}$$

$$\underline{Z} = \left|\underline{Z}\right| e^{j\varphi_Z}$$

Finally, given Euler's formula the impedance can be broken up into its real and imaginary components for a graphical interpretation in an impedance spectrum.

Impedance:

$$\underline{Z} = |\underline{Z}|\cos(\varphi) + |\underline{Z}|j\sin(\varphi)$$

$$Real\ Impedance\ (Z'): |\underline{Z}|\cos(\varphi)$$

$$Imaginary\ Impedance(Z''): |\underline{Z}|j\sin(\varphi)$$

Impedance is often graphically represented through Nyquist and Bode plots. Given the unique impedimetric behaviour of the various components, the Nyquist and Bode plot allow the user to distinguish between the different components of the system.[10,21,22] The Nyquist plot plots the real component of impedance on the x-axis and the imaginary component on the y-axis (Figure 9). Whereas the bode plot has the frequencies on the x-axis, and two y-axes for the magnitude of impedance and the phase shift (Figure 9). For example, a resistor modulates the amplitude of the input current, therefore it only has a real component of impendence; the impedance is independent of frequency and the resulting Nyquist plot would be a single point. The Bode plot supports the Nyquist plot with a straight line representing the same magnitude of impedance across all frequencies without a phase shift (Figure 9A).

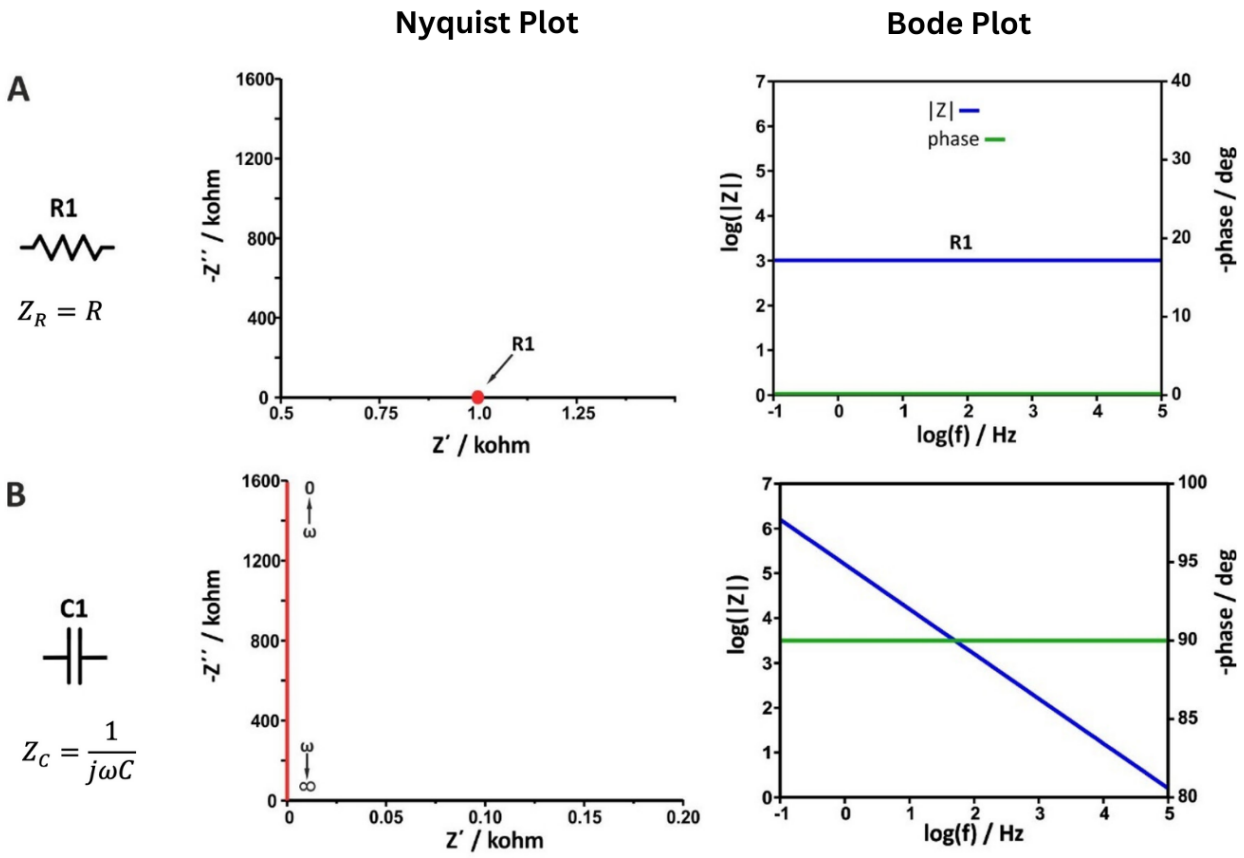

Figure 1.9. Nyquist and Bode plots of model A) resistor (1 kΩ) and B) capacitor.[22] Reused under a creative commons license.

Whereas a capacitor is only represented by imaginary impedance and is highly dependent on frequency. As frequency decreases, the impedance increases infinitely on the Nyquist plot. The supporting Bode plot helps illustrate the increasing impedance while maintaining a constant phase shift. With these two plots, the circuit elements can be combined in any number of ways to represent an electrochemical system and to characterize the components.

EIS has also played an integral role in electrochemical sensing, for both quantification and characterization. Recently an impedimetric sensor for the detection of melatonin on a gold nanoparticle-polydopamine GCE (AuNP/PDA/GCE) was developed.[23] Through the identification

of the resistor representing the resistance to charge transfer, the melatonin could be quantified. As the concentration of melatonin is increased, it binds to the AuNP/PDA on the surface, increasing the resistance to charge transfer, widening the "semi-circle" on the Nyquist plot (Figure 10). Through the impedimetric sensing on the modified surface, picomolar sensitivity was achieved. In a review by *Aguedo et al.* they demonstrate how EIS can be implemented for increased sensitivity and characterization of an electrochemical system.[24] Importantly, EIS was demonstrated to serve as an effective method for the characterization of a sensor's stability. Through EIS, the oxidation of nanomaterials is evident through the increased resistance to charge transfer. As a result, the sensor is incompatible with voltages above +200 mV vs Ag^{+}/AgCl. Therefore, EIS is a powerful tool that will serve to characterize the stability of interactions between hosts and guests in this thesis, while also modelling the equivalent circuit of any sensors.

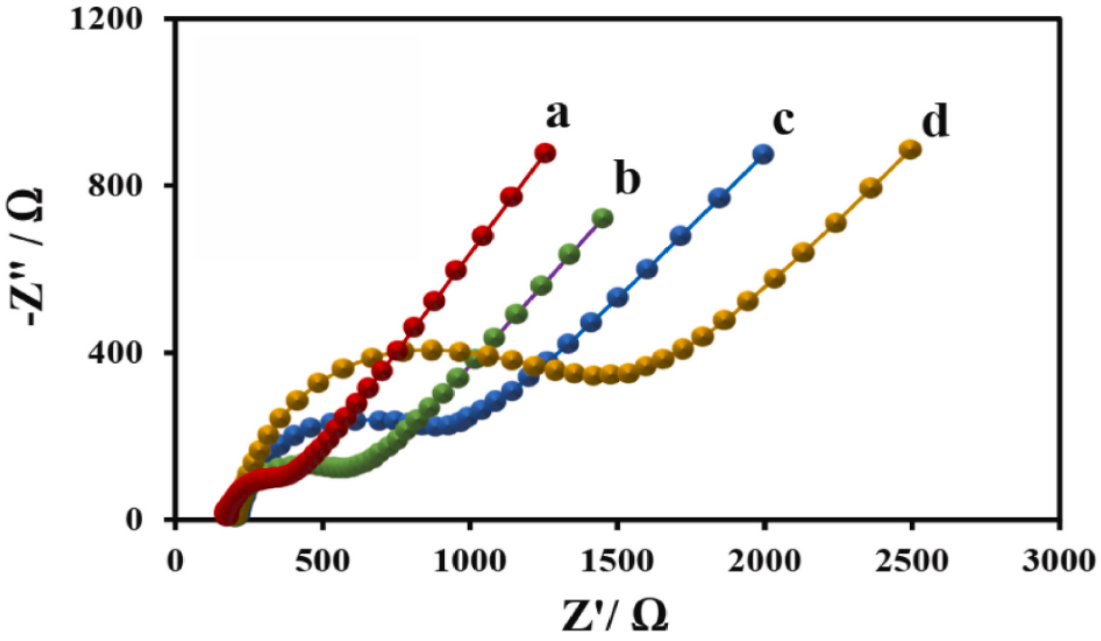

Figure 1.10. Nyquist plots of AuNPs/PDA/GCE in 5 mM $Fe(CN)_6^{3-/4-}$ (1:1) solution containing 0.1 M KCl at different concentrations of ME (a-d: 0 pM, 2 pM, 8 pM, and 18 pM).[23] Reproduced with permission, license number 5895081303221.

1.1.4 Electrochemical sensing

Electrochemical sensing offers a unique alternative to traditional analytical methods for quantification and characterization of electrochemical systems. CV, pulse voltammetry, and EIS all offer unique advantages to gain a holistic understanding of a sensor and its behaviour. CV has been employed as a rapid method for a general characterization of electron transfer reactions in a system, however, its background signals prevent effective quantification. Pulse methods such as DPV apply potential in a unique pulsing method to account for background signals, allowing for high sensitivity and quantification of analytes. Finally, EIS applied a range of frequencies of alternating voltage to independently characterize the components of an electrochemical system. In tandem, these methods will be crucial for the characterization of sensors and electrochemical systems in this thesis.

1.2 Host-Guest Systems

Supramolecular chemistry centers around the formation of discrete higher-order systems through non-covalent interaction between molecules. Central to this branch of chemistry is the development of host-guest (HG) complexes where synthetic receptors, hosts, are developed to complex with an analyte, guest, specifically and sensitively by exploiting hydrogen bonding, π-π stacking, cation-π bonding, and more. Interestingly, the modification of hosts allows for modulation of HG complexes in response to changes in temperature, pH, redox state, enzyme presence, or light. As a result, HG chemistry has seen use in a variety of applications including sensing, separation, and catalysis. Here, the various types of host molecules are covered and followed by their various applications. Then, a specific class of hosts, resorcinarenes, and the recent advances in their design are covered. Finally, the applications of resorcinarene hosts are covered. In this thesis there is an overarching goal of developing novel electroanalytical methods

by incorporation of HG chemistry, specifically novel resorcinarenes. It is necessary to understand the fundamentals of host design and synthesis to incorporate both HG and electrochemistry into functional sensors.

1.2.1 Types of Host molecules

The earliest hosts discussed in literature are the CEs and their sensitivity towards alkali metals.[25] Considered as first-generation macrocycles, first synthesized in 1967, CEs are cyclic polyether with oxygen lined cavities.[25,26] The ability to expand the cavity has made them popular options for ion sensing as they can distinguish between sodium or potassium ions.[27] However, in general, the CEs lack the specificity of newer hosts due to limitations of their modifications and sensing applications often rely on more advanced host molecules.

As some of the earliest hosts with encapsulating hydrophobic cavities and hydrophilic exteriors, CDs are some of the most well studied of the host molecules (Figure 11).[26,28] CDs are composed of glucopyranosides linked together by α-1,4 glycosidic linkages; they are formed through the digestion of starch. The CDs vary in the number of units in their rings, with α, β, and γ-cyclodextrins containing 6,7, and 8 glucose subunits respectively.[28] While first synthesized in 1891, it was not until 1950s that the importance and applications of CDs were appreciated.[28] In the mid 1900s, CDs were praised for their ability to encapsulate guests for the delivery of drugs, to protect oxidizable substances, and their ability to improve solubility of guests. Importantly, their natural precursors made them biocompatible and allowed for their "green" industrial synthesis. CDs form a cone frustrum with a slightly hydrophobic cavity, hydrophilic exterior, and hydroxyl-decorated rims. These hydroxyl groups are available for modification to improve selectivity for guests.

Another popular class of hosts are the CBs, first synthesized and structurally identified in 1981 (Figure 11).[29] Their synthesis involves the acid-catalyzed condensation of glycouril and formaldehyde. The group of hosts is most notably recognized for their pumpkin-shape structure and various homologues.[26,29] Similar to previous hosts, the CBs contain a hydrophobic cavity and negatively charged carbonyl rims. Interestingly, CBs have been previously reported to bund well to various electrochemical probes including ferrocene and cobaltocene.[30] They reveal an opportunity to impart an electrochemical signal to non-electroactive hosts. While selectivity is limited, the opportunity to form HG complexes with electroactive guests has brought about the incorporation of CBs into electrochemical sensors for competitive binding assays.[31] However, solubility issues, and limited selectivity prevent wide applicability of the host class.

The calix[n]arenes, named after their bowl shape, were first discovered in the 1940's.[32] Synthesized by the condensation of phenols and formaldehyde, these hosts have an electron-rich hydrophobic cavity with hydrophilic rims. They have seen the most use because of the ease of modification.[33] This includes incorporation into electrochemical sensors, optical sensors, used for solid extraction, and more. The hosts also benefit from easy large-scale synthesis with calixarenes of 4, 6, and 8 subunits being prepared with high yields and purity at kilogram scales. There has been focus on the modification of the hosts, specifically modification of the upper rim at the para position, the lower rim phenolic hydroxyl groups, and extension of the cavity to accommodate larger guests.

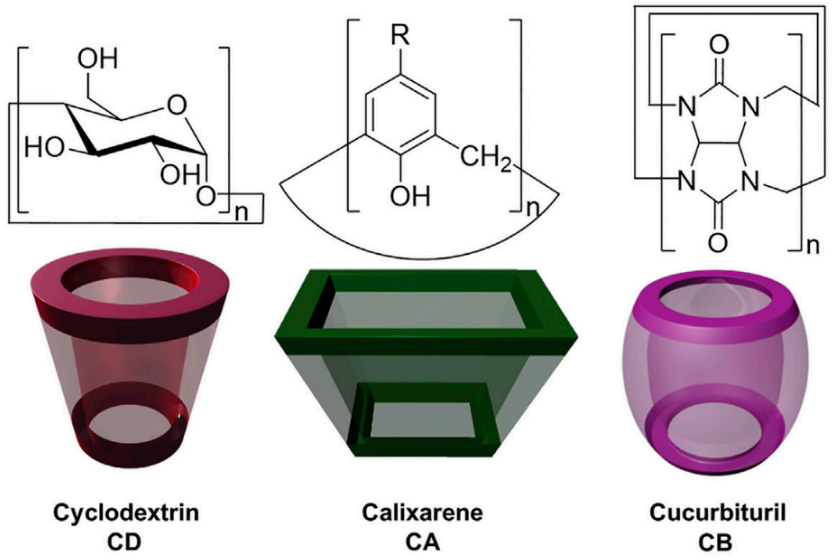

Figure 1.11. General structure and cartoon representation of cyclodextrin, calixarene, and cucurbituril.[26] Reused with permission, license number 5895100584896.

1.2.1.1 Ion-pairing

A subset of interactions that have seen similar applications to traditional host guest chemistry are ion pairs. Ion pairing refers to the association between oppositely charged ionic species in solution.[34] While ions expectedly dissociate in solution and interact at long distances, stronger associations may exist. Two ions of opposite charge can form an ion pair if they spend a greater amount of time together than the time for diffusion.[34] At which point, the ions will no longer dissociate to interact preferentially with other ions in solution. Similar to host-guest systems, a complementarity in electrostatic interactions is the driving force for a complex. Upon complexation the ion pair becomes an overall neutral species that may be extracted and isolated. Methylene blue (MB), a cationic dye, is a well-documented, redox active molecule that is commonly monitored for ion-paring complexation.

The Environmental Protection Agency (EPA) has published numerous acceptable methods for water quality testing; among them is Method 425.1, a quantification method for

surfactants by colorimetry.[35] Surfactants are recognized by their amphiphilic properties, with polar head groups, and long non-polar alkyl tails.[36] Their stability, and emulsification properties have made them popular throughout industry and personal care products.[36] However, their resistance to degradation and ubiquity has led to widespread pollution. As a result, the detection and quantification of surfactants in water bodies is a concern for environmental monitoring. Method 425.1 exploits the ion-pair that forms between MB and the anionic surfactants to quantify the pollutant. The method relies on the liquid-liquid extraction of the neutral ion pair for further spectroscopic quantification.

1.2.2 Resorcinarene Hosts

Resorcinarenes, belonging to the calix[4]arene family, are cone-shaped aromatic phenolic macrocycles (Figure 12).[26,37] The hosts were first reported in 1968, being synthesized by the acid-catalyzed condensation of resorcinol with an aldehyde.[26,38] The structure is maintained through H-bonding between adjacent resorcinol subunits. Again, the resorcinarenes benefit from an electron-rich, hydrophobic cavity and hydrophilic outer rims.[37] However, the core resorcinarene cavity is very shallow and can only accommodate small guests.[38] Interestingly, resorcinarene synthesis is simple and low-cost, allowing for a scaled synthesis for wider applications. Thus, a lot of work has gone into modifying these hosts to accommodate a wider array of guests. The three most common modifications to resorcinarenes are at the C-2 sites (R^1), the phenolic hydroxyl groups, and the lower rim methylene bridges (R^2) (Figure 12).[39] The recent advances in the modification of resorcinarenes makes them an excellent candidate for development of an electroactive HG complex. Literature has already demonstrated the encapsulation of ferrocene by resorcinarenes as well as the direct modification of resorcinarenes with a ferrocene probe.[40,41]

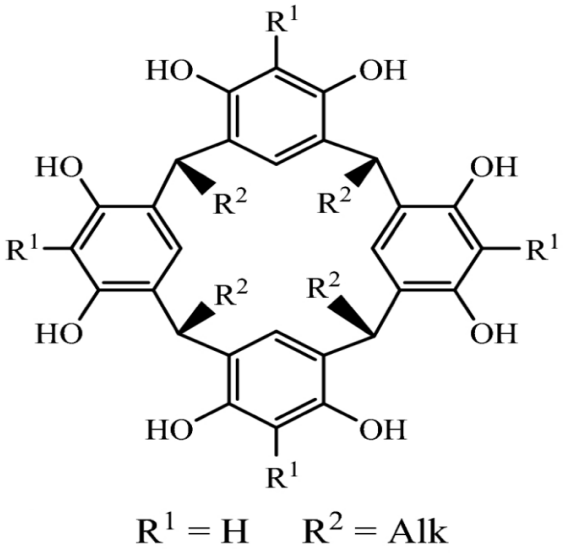

Figure 1.12. General resorcinarene structure.[39] Reproduced with permission, license number 5895091014380.

1.2.3 Modification of Resorcinarenes

The electron rich C-2 site on the resorcinol subunits are highly activated by the phenolic hydroxyl substituents, creating favorable conditions for electrophilic aromatic substitution.[37,39] The simplest and earliest of which is the bromination of the C-2 sites (**3**), with further linking of the resorcinol subunits by methylene (**4**) (Figure 13).[39,42,43] This modification locks the bowl shape cavity in place, alleviating the resorcinarene of its solvent dependent structural stability.

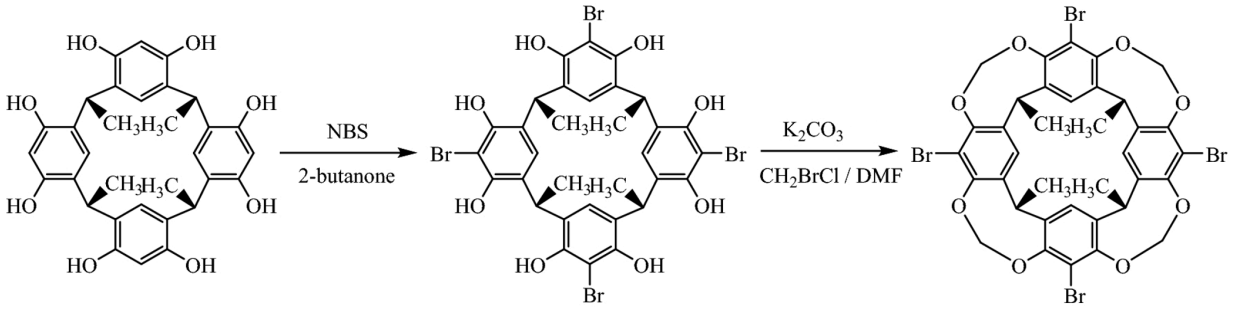

Figure 1.13. Bromination (3) on the C-2 positions and methylene linkage (4) of calix[4]resorcinarene (2).[39] Reproduced with permission, license number 5895091014380.

Functionalization of the resorcinarene at the C-2 position to form tetrabenzoxazine is also popular.[44,45] The Mannich condensation of the core resorcinarene with a 1° amine and excess formaldehyde produces a tetrabenzoxazine host in high yields (Figure 14).[39,46,47] The benzoxazine moieties are then cleaved in by refluxing with a mineral acid (HCl, HBr) in butan-1-ol to produce the unique N-alkyl ammonium resorcinarene halides (NARX) at yields up to 90%.[46] These unique hosts are deep cavity cavitands held together by a hydrogen bond belt between the halide ions and the ammonium groups (Figure 13). The cooperative use of the hydrogen and halogen bond in the NARX host is a different approach to impart specificity in a host.[48] Unlike the core resorcinarene or cavitands formed by bridging with methylene groups, the NARX possess a deeper, rigid cavity which may accommodate much larger electron-rich guests.[37,48] Exploiting the halogen bond, a charge transfer interaction between the polarized halogen and a Lewis base, allows for a new tool in the design of hosts with similar strength to the hydrogen bond.[49] The halogen bond strength rank orders from weakest to strongest, F << Cl << Br < I, given the reliance on anisotropic electron distribution for the electropositive σ hole on the halogen atom. The halide ions in the belt allow the NARX to participate in the formation of novel halogen bond assemblies.[37]

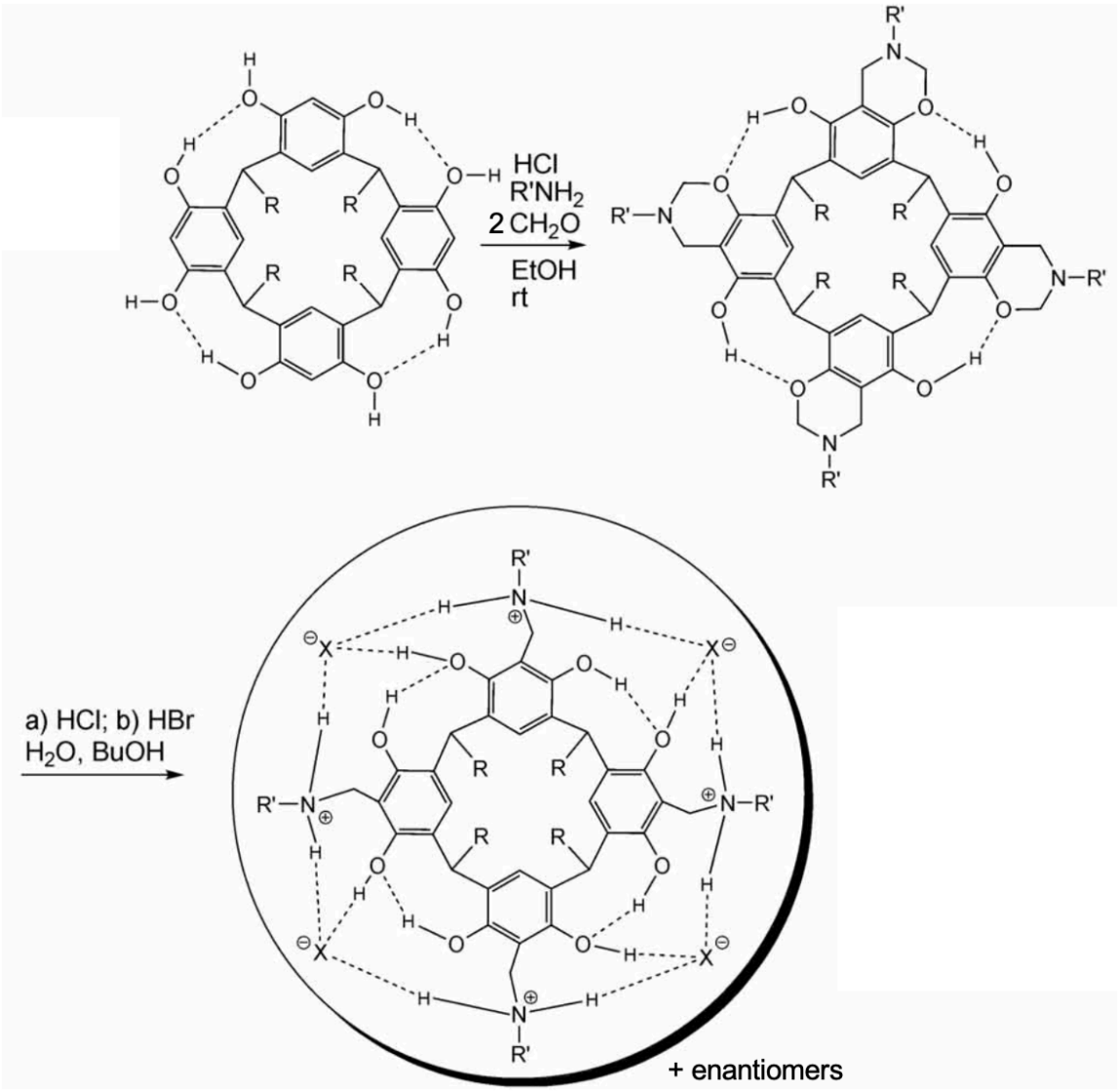

Figure 1.14. General Synthesis of the resorcinarene tetrabenzoxazines and -alkyl ammonium resorcinarene halides.[46] Reused under a creative commons license.

The halides in the belt of the NARX allow for further extension of the cavity and formation of unique supramolecular assemblies. Beyeh *et al.* demonstrated that the NARX host cavity was further extended the cavity in the presence of the halogen bond donor, bromotrichloromethane (CCl_3Br) (Figure 15). The bromine behaves as a good halogen bond donor given the inductive

effects of the chlorine atoms leading to a $CCl_3Br\ldots Br^-$ interaction, further stabilized by van der Waals between the CCl_3Br and NARX. The assembly was then capable of forming host-guest complexes with 1,4-Dioxane and butan-1-ol. The NARX also demonstrated the ability to form the first dimeric capsule constructed from only halogen bonding.[50] The capsule was formed between two NARX hosts, with iodine molecules as halogen bond donors ($Cl^-\ldots I—I\ldots Cl^-$) . The capsule captured 3 dioxane molecules in the cavity, fixed in the cavity through hydrogen bonding with the NARX ammonium groups.

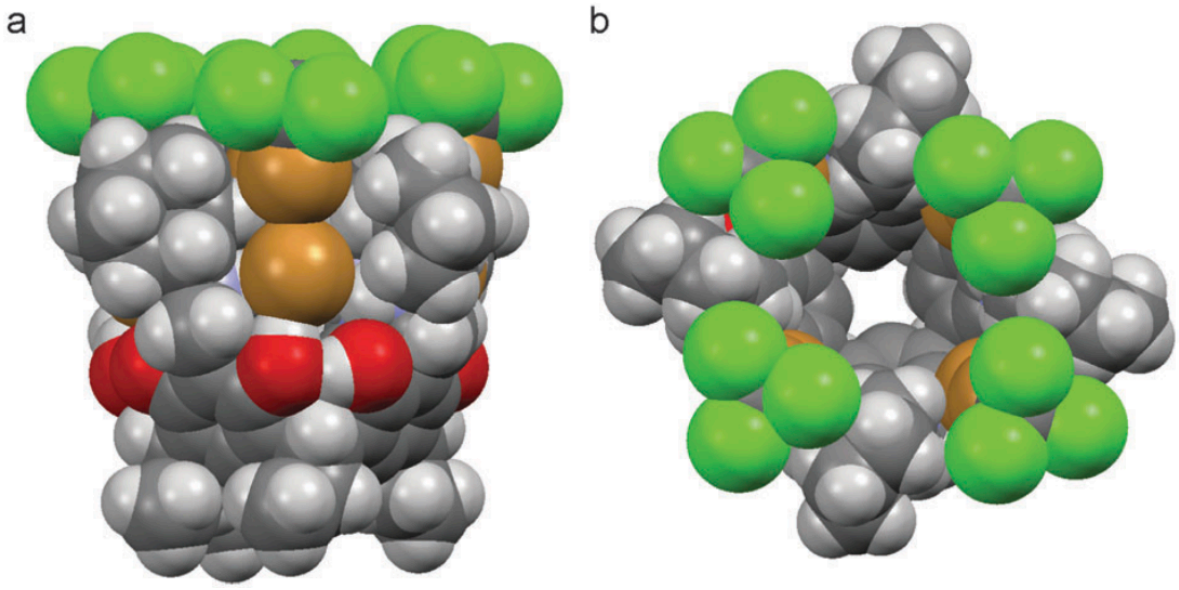

Figure 1.15. CPK representation of the NARX- CCl3Br assembly from a) side view and b) top view.[48] Reproduced with permission, license number 1539007.

The N-Alkyl ammonium resorcinarene chloride receptors ($NARCl_4$) are of particular interest given their water solubility and ion selectivity in complex media. The development of high-affinity hosts for anions in biological contexts has presented a significant challenge due to the competitive nature of the solvents.[50–52] The $NARCl_4$ were previously shown to be high-affinity receptors towards the biological anion pyrophosphate (PPi). PPi is of particular interest since it

can be used as for the diagnosis of various diseases, including vascular calcification. Twum *et al.* demonstrated that the $NARCl_4$ hosts had affinities as high as $10^7\ M^{-1}$ in pure water, and in biologically relevant buffer the hosts were specific to PPi over other phosphate anions.[53] However, to determine the extent of complexation, NMR spectroscopy, and isothermal calorimetry (ITC) were necessary. Therefore, in this thesis the NARX hosts demonstrate an opportunity for incorporation into an electrochemical sensor to impart sensitivity and selectivity. The simplicity and scalability of synthesis provides an advantage over traditional, complex electrode modifications.

1.3 Integration of Host-Guest or Ion-Pairing Systems and Electrochemical Sensing

With a better understanding of electroanalytical methods and host-guest chemistry, the benefits of joining the two disciplines are evident. The transition away from traditional lab-based methods towards in situ. sensing relies on the adoption of electrochemical sensors. From well-known glucometers, which continue to be improved upon and now offer continuous monitoring, to novel electrochemical sensors for chemical warfare agents, electrochemical sensing is preferred as a rapid, cost-effective, simple method.[54,55] While these sensing methods have gained popularity in literature, they all suffer from complex modifications that are necessary for imparting specificity to the sensor. As an alternative, recently, host-guest chemistry has been used in electrochemical sensing. The deterministic complexation and the simplicity of swapping between hosts for different applications presents the opportunity to develop a general sensing platform. A few approaches have been taken towards this goal. Here, the various methods of host-guest electrochemical sensing are covered, followed by examples of successful integration of host-guest chemistry into electrochemical sensor. This is necessary as in this thesis the goal is to work towards

generalizable host-guest electrochemical sensors by incorporating new NARX hosts into electrochemical sensors.

1.3.1 Electrochemical host guest and ion-pairing sensing methods.

The simplest form of host-guest sensing relies on redox mediators for signal transduction. Instead of worrying about designing an electroactive host or limiting sensing to electroactive guests, well-known redox mediators such as ferrocene may be used. The formation of a host-guest complex can instead impede the electron transfer reaction of the redox mediator at the electrode. One approach to this method included the synthesis of CB modified graphene sheets; the CBs were sensitive to the plasticizer pollutant di-(2-ethylhexyl)phthalate (DEHP).[56] Since neither the CB or DEHP were electroactive, $[FeCN_6]^{3-/4-}$ was instead used as a redox mediator. When the DEHP guest was added to solution, it would complex with the CB hosts on the electrode surface. As a result, the $[FeCN_6]^{3-/4-}$ electron transfer was impeded; the increase in impedance could be monitored via EIS. A growth in the resistance to charge transfer was evident in the Nyquist plot and was in turn used to quantify the concentration of DEHP guest (Figure 16). Another approach to this method was to fix the redox mediator to the surface. Qi *et al.* developed a competitive assay for the detection of three different drug candidates.[31] Here, ferrocenylalkylthiolates were fixed to a gold electrode surface for a redox signal. The introduction of CB hosts anodically shifted the ferrocene redox signal as they for a host-guest complex. However, since the drug candidate guests form higher affinity complexes with the CB, the CBs disassociate from the fixed ferrocene to complex with the drugs. Thus, the ferrocene redox signal experience a cathodic shift towards the original redox potential. With CV, the deconvolution of the anodic wave allowed for the quantification of drugs by comparing the ferrocene with and without complexed CB. Another approach that relies on redox mediators is the ion-pairing complexes previously mentioned. Specifcally, MB is a

common redox mediator that has been previously used for detection of DNA complexation.[57] MB has a clear reduction signal from the transformation to the leuco species. Alternatively, the MB signal can serve as an indicator for surfactant quantification post-extraction. Lopez *et al.* demonstrated that the MB signal was sufficient for the quantification of surfactants.[58] However, they only explore the quantification via ion-pairing for one class of surfactants and failed to optimize the sensor for environmentally relevant concentrations.

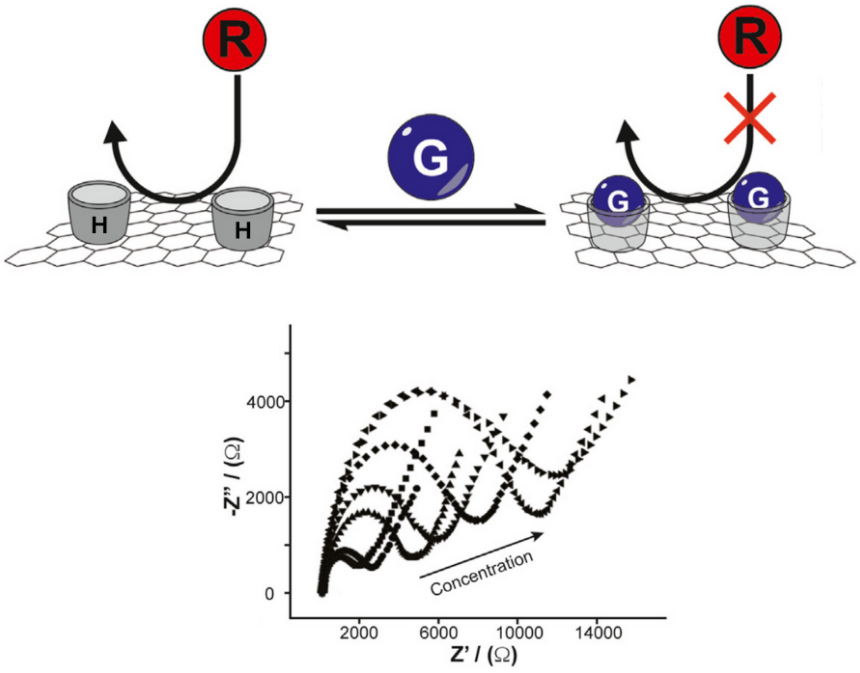

Figure 1.16. Schematic representation of redox mediated host-guest electrochemical sensing. Where host-guest complexation increasing impedance in Nyquist plot.[54] Reproduced with permission, license number 5895100153284.

The concentration of an electroactive guest near the surface by a host is a common method of detection. Similar to the previously described CB modified graphene sheets, the formation of a host-guest complex can instead increase the current response. By accumulating the guest at the surface, the increase in current response can be used to quantify the concentration of guest. Maity

et al. functionalized gold nanoparticles with pillar[6]arene hosts on the electrode surface.[59] The hosts were specific towards bisphenol A and demonstrated a nanomolar detection limit. Interestingly, they were able to use DPV, a pulse method, to achieve the low LOD. The benefit of this method of host-guest electrochemical sensing is the versatility of host functionalization. The ability to synthesize hosts independently in their preferred solvent prior to fixing onto the surface and measuring in the solvent of interest improves the applicability.

A final method of electrochemical detection of host guest complexation is the modulation of redox behaviour of an electroactive host. Upon guest binding, the redox signal of the host is either anodically or cathodically shifted, allowing for quantification of guest. There has also been attempts to develop bi-functional hosts, capable of binding redox mediators while encapsulating a guest (Figure 17).[60] Here in this thesis, the approach of a bifunctional host is attractive given the goal of developing a sensing platform. Resorcinarene hosts have been previously designed with ferrocene-modified rims, however, the electron transfer kinetics of the redox mediator are negatively impacted. Also, the modification with ferrocene limits the modification of the host towards guest specificity. Therefore, a host that can simultaneously interact with a redox mediator and a guest is an interesting approach to creating new electroactive supramolecular assemblies for electrochemical sensing.

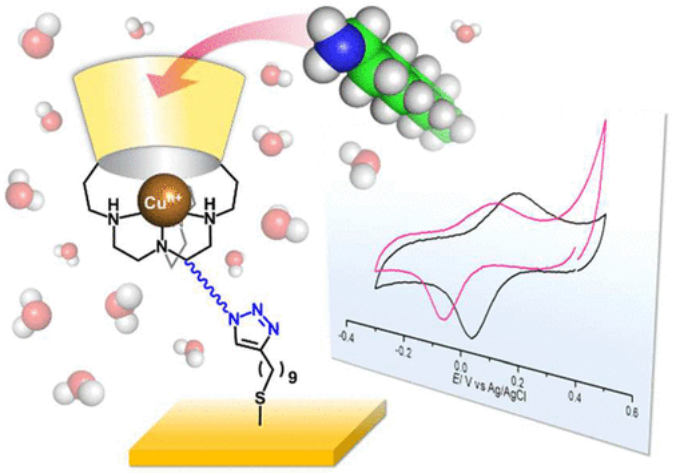

Figure 1.17. Schematic of bifunctional calix[6]arene host interacting with electroactive copper and non-electroactive guest. Where introduction of guest modulates assembly redox properties.[60] Reused under a creative commons lic*ense.*

1.4 Thesis Research

As demand for accesible analytical methods increase, there must be a transiton from cumberosme, expensive lab-based methods. Electrochemical sensors overcome the drawbacks of traditonal analytical methods, primairly they are cost-effective and simple to use. However, electrochemical sensors suffer from a lack of specificity without extensive, complicated modifications. To overcome the need for complex electrode modification, host-guest chemistry presents a unique opportunity. The development of novel resorcinarenes, the NARX hosts, have demonstrated high affinities for PPi in biological media, while being easily synthesized and scaled up. By incorporating the NARX hosts with electroanalytical methods such as EIS, or pulse voltammetry, new sensors can be developed to replace traditional analytical methods. Another inherent benefit of incorporating hosts into electrochemical sensors is the facile swapping of hosts to meet the application.

In this thesis, NARX hosts will be investigated for their ability to serve as electroactive hosts for quantification of guests, as well as bifunctional hosts, with capabilities to form assemblies with redox mediators and guest simutaneously. Host-guest complexation will be a driving principle throughout, with alternative ion-pairing complexes also being investigated as candidates for electrochemical quantification instead of traditional spectroscopic quantification in Chapter 4. It is expected that electroanalytical methods will corroborate traditional methods of monitoring host-guest complexation, thus supporting a transtion to electrochemical quantification. To this extent, the first objective is the electrochemical characterization of resorcinarene hosts in Chapter 2 and 3. The redox behaviour of host will inform the optimal electroanalytical methods for quantification. The second objective is to electrochemically and traditionally charaterize the host-guest interactions between the hosts and redox mediators in Chapter 2. This is necessary for the potential application of as bifunctional hosts for guest and redox mediator interactions. The third objective is to directly electrochemically quantify guests through the redox behaviour of hosts in Chapter 3. Finally, the last objective is to investigate alternative ion-pairing complexes and quantification of complexation via electrochemical means in Chapter 4. This will serve as further support for the transition to electroanalysis over traditional spectroscopic analysis by comparing the selectivity and sensitivity of either method.

1.5 References

(1) Diouf, A.; Moufid, M.; Bouyahya, D.; Österlund, L.; El Bari, N.; Bouchikhi, B. An Electrochemical Sensor Based on Chitosan Capped with Gold Nanoparticles Combined with a Voltammetric Electronic Tongue for Quantitative Aspirin Detection in Human Physiological Fluids and Tablets. *Materials Science and Engineering: C* **2020**, *110*, 110665. https://doi.org/10.1016/j.msec.2020.110665.

(2) Ali, M. Y.; Alam, A. U.; Howlader, M. M. R. Fabrication of Highly Sensitive Bisphenol A Electrochemical Sensor Amplified with Chemically Modified Multiwall Carbon Nanotubes and β-Cyclodextrin. *Sensors and Actuators B: Chemical* **2020**, *320*, 128319. https://doi.org/10.1016/j.snb.2020.128319.

(3) Rajendrachari, S.; Basavegowda, N.; Adimule, V. M.; Avar, B.; Somu, P.; R. M., S. K.; Baek, K.-H. Assessing the Food Quality Using Carbon Nanomaterial Based Electrodes by Voltammetric Techniques. *Biosensors* **2022**, *12* (12), 1173. https://doi.org/10.3390/bios12121173.

(4) Alam, A. U.; Clyne, D.; Jin, H.; Hu, N.-X.; Deen, M. J. Fully Integrated, Simple, and Low-Cost Electrochemical Sensor Array for in Situ Water Quality Monitoring. *ACS Sens.* **2020**, *5* (2), 412–422. https://doi.org/10.1021/acssensors.9b02095.

(5) Beyeh, N. K.; Pan, F.; Ras, R. H. A. N-Alkyl Ammonium Resorcinarene Chloride Receptors for Guest Binding in Aqueous Environment. *Asian Journal of Organic Chemistry* **2016**, *5* (8), 1027–1032. https://doi.org/10.1002/ajoc.201600187.

(6) Li, C.; Wu, Z.; Yang, H.; Deng, L.; Chen, X. Reduced Graphene Oxide-Cyclodextrin-Chitosan Electrochemical Sensor: Effective and Simultaneous Determination of *o*- and *p*-Nitrophenols. *Sensors and Actuators B: Chemical* **2017**, *251*, 446–454. https://doi.org/10.1016/j.snb.2017.05.059.

(7) Zhu, G.; Yi, Y.; Chen, J. Recent Advances for Cyclodextrin-Based Materials in Electrochemical Sensing. *TrAC Trends in Analytical Chemistry* **2016**, *80*, 232–241. https://doi.org/10.1016/j.trac.2016.03.022.

(8) Luo, H.; Chen, L.-X.; Ge, Q.-M.; Liu, M.; Tao, Z.; Zhou, Y.-H.; Cong, H. Applications of Macrocyclic Compounds for Electrochemical Sensors to Improve Selectivity and Sensitivity. *J Incl Phenom Macrocycl Chem* **2019**, *95* (3), 171–198. https://doi.org/10.1007/s10847-019-00934-6.

(9) del Pozo, M.; Mejías, J.; Hernández, P.; Quintana, C. Cucurbit[8]Uril-Based Electrochemical Sensors as Detectors in Flow Injection Analysis. Application to Dopamine Determination in Serum Samples. *Sensors and Actuators B: Chemical* **2014**, *193*, 62–69. https://doi.org/10.1016/j.snb.2013.11.074.

(10) Bard, A.; Faulkner, L. *Electrochemical Methods: Fundamentals and Applications*; Pearson, 2000.

(11) Elgrishi, N.; Rountree, K. J.; McCarthy, B. D.; Rountree, E. S.; Eisenhart, T. T.; Dempsey, J. L. A Practical Beginner's Guide to Cyclic Voltammetry. *J. Chem. Educ.* **2018**, *95* (2), 197–206. https://doi.org/10.1021/acs.jchemed.7b00361.

(12) Zabik, N. L.; Anwar, S.; Ziu, I.; Martic-Milne, S. Electrochemical Reactivity of Bulky-Phenols with Superoxide Anion Radical. *Electrochimica Acta* **2019**, *296*, 174–180. https://doi.org/10.1016/j.electacta.2018.11.051.

(13) Min, J.; Tu, J.; Xu, C.; Lukas, H.; Shin, S.; Yang, Y.; Solomon, S. A.; Mukasa, D.; Gao, W. Skin-Interfaced Wearable Sweat Sensors for Precision Medicine. *Chem. Rev.* **2023**, *123* (8), 5049–5138. https://doi.org/10.1021/acs.chemrev.2c00823.
(14) ELSAHWI, E. S. System and Method for Determining the Impedance Properties of a Load Using Load Analysis Signals. WO2021003577A1, January 14, 2021. https://patents.google.com/patent/WO2021003577A1/en (accessed 2024-05-09).
(15) Simões, F. R.; Xavier, M. G. 6 - Electrochemical Sensors. In *Nanoscience and its Applications*; Da Róz, A. L., Ferreira, M., de Lima Leite, F., Oliveira, O. N., Eds.; Micro and Nano Technologies; William Andrew Publishing, 2017; pp 155–178. https://doi.org/10.1016/B978-0-323-49780-0.00006-5.
(16) Dickinson, E. J. F.; Wain, A. J. The Butler-Volmer Equation in Electrochemical Theory: Origins, Value, and Practical Application. *Journal of Electroanalytical Chemistry* **2020**, *872*, 114145. https://doi.org/10.1016/j.jelechem.2020.114145.
(17) Department of Physics, Karnatak University Dharwad, India-580003; Mundinamani, S. P.; Rabinal, M. K. Cyclic Voltammetric Studies on the Role of Electrode, Electrode Surface Modification and Electrolyte Solution of an Electrochemical Cell. *IOSRJAC* **2014**, *7* (9), 45–52. https://doi.org/10.9790/5736-07924552.
(18) Mathad, A. S.; Seetharamappa, J.; Kalanur, S. S. β-Cyclodextrin Anchored Neem Carbon Dots for Enhanced Electrochemical Sensing Performance of an Anticancer Drug, Lapatinib via Host-Guest Inclusion. *Journal of Molecular Liquids* **2022**, *350*, 118582. https://doi.org/10.1016/j.molliq.2022.118582.
(19) Yilmaz, S.; Sadikoglu, M.; Saglikoglu, G.; Yagmur, S.; Askin, G. Determination of Ascorbic Acid in Tablet Dosage Forms and Some Fruit Juices by DPV. *International Journal of Electrochemical Science* **2008**, *3* (12), 1534–1542. https://doi.org/10.1016/S1452-3981(23)15537-4.
(20) Li, H.; Wei, D. Electrochemical Detection of Caffeine in Sports Drinks Based on Molecular Imprinting Technology. *Food Measure* **2024**. https://doi.org/10.1007/s11694-024-02427-8.
(21) Laschuk, N. O.; Easton, E. B.; Zenkina, O. V. Reducing the Resistance for the Use of Electrochemical Impedance Spectroscopy Analysis in Materials Chemistry. *RSC Adv* **2021**, *11* (45), 27925–27936. https://doi.org/10.1039/d1ra03785d.
(22) Lazanas, A. Ch.; Prodromidis, M. I. Electrochemical Impedance Spectroscopy─A Tutorial. *ACS Meas. Sci. Au* **2023**, *3* (3), 162–193. https://doi.org/10.1021/acsmeasuresciau.2c00070.
(23) Jin, X.; Nodehi, M.; Baghayeri, M.; Xu, Y.; Hua, Z.; Lei, Y.; Shao, M.; Makvandi, P. Development of an Impedimetric Sensor for Susceptible Detection of Melatonin at Picomolar Concentrations in Diverse Pharmaceutical and Human Specimens. *Environmental Research* **2023**, *238*, 117080. https://doi.org/10.1016/j.envres.2023.117080.
(24) Aguedo, J.; Lorencova, L.; Barath, M.; Farkas, P.; Tkac, J. Electrochemical Impedance Spectroscopy on 2D Nanomaterial MXene Modified Interfaces: Application as a Characterization and Transducing Tool. *Chemosensors* **2020**, *8* (4), 127. https://doi.org/10.3390/chemosensors8040127.
(25) Duan, Z.; Xu, F.; Huang, X.; Qian, Y.; Li, H.; Tian, W. Crown Ether-Based Supramolecular Polymers: From Synthesis to Self-Assembly. *Macromolecular Rapid Communications* **2022**, *43* (14), 2100775. https://doi.org/10.1002/marc.202100775.
(26) Yang, X.; Yuan, D.; Hou, J.; Sedgwick, A. C.; Xu, S.; James, T. D.; Wang, L. Organic/Inorganic Supramolecular Nano-Systems Based on Host/Guest Interactions.

Coordination Chemistry Reviews **2021**, *428*, 213609. https://doi.org/10.1016/j.ccr.2020.213609.
(27) Yoshio, M.; Noguchi, H. Crown Ethers for Chemical Analysis: A Review. *Analytical Letters* **1982**, *15* (15), 1197–1276. https://doi.org/10.1080/00032718208065134.
(28) Szejtli, J. Introduction and General Overview of Cyclodextrin Chemistry. *Chem. Rev.* **1998**, *98* (5), 1743–1754. https://doi.org/10.1021/cr970022c.
(29) I. Assaf, K.; M. Nau, W. Cucurbiturils: From Synthesis to High-Affinity Binding and Catalysis. *Chemical Society Reviews* **2015**, *44* (2), 394–418. https://doi.org/10.1039/C4CS00273C.
(30) Ong, W.; Kaifer, A. E. Unusual Electrochemical Properties of the Inclusion Complexes of Ferrocenium and Cobaltocenium with Cucurbit[7]Uril. *Organometallics* **2003**, *22* (21), 4181–4183. https://doi.org/10.1021/om030305x.
(31) Qi, L.; Wang, R.; Yu, H.-Z. Supramolecular Cucurbit[7]uril@Ferrocene Complexation on Surface: From Nanostructure Differentiation to Guest Quantitation. *Acc. Mater. Res.* **2023**, *4* (5), 457–466. https://doi.org/10.1021/accountsmr.3c00025.
(32) Ludwig, R. Calixarenes in Analytical and Separation Chemistry. *Fresenius J Anal Chem* **2000**, *367* (2), 103–128. https://doi.org/10.1007/s002160051611.
(33) S. K. Menon; M. Sewani. Chemical Modifications of Calixarenes and Their Analytical Applications. *Reviews in Analytical Chemistry* **2006**, *25* (1), 49–82. https://doi.org/10.1515/REVAC.2006.25.1.49.
(34) Marcus, Y.; Hefter, G. Ion Pairing. *Chem. Rev.* **2006**, *106* (11), 4585–4621. https://doi.org/10.1021/cr040087x.
(35) *Document Display | NEPIS | US EPA*. https://nepis.epa.gov/Exe/ZyNET.exe/30000Q10.TXT?ZyActionD=ZyDocument&Client=EPA&Index=1976+Thru+1980&Docs=&Query=&Time=&EndTime=&SearchMethod=1&TocRestrict=n&Toc=&TocEntry=&QField=&QFieldYear=&QFieldMonth=&QFieldDay=&IntQFieldOp=0&ExtQFieldOp=0&XmlQuery=&File=D%3A%5Czyfiles%5CIndex%20Data%5C76thru80%5CTxt%5C00000001%5C30000Q10.txt&User=ANONYMOUS&Password=anonymous&SortMethod=h%7C-&MaximumDocuments=1&FuzzyDegree=0&ImageQuality=r75g8/r75g8/x150y150g16/i425&Display=hpfr&DefSeekPage=x&SearchBack=ZyActionL&Back=ZyActionS&BackDesc=Results%20page&MaximumPages=1&ZyEntry=1&SeekPage=x&ZyPURL (accessed 2024-10-23).
(36) Shaban, S. M.; Kang, J.; Kim, D.-H. Surfactants: Recent Advances and Their Applications. *Composites Communications* **2020**, *22*, 100537. https://doi.org/10.1016/j.coco.2020.100537.
(37) Twum, K.; Rissanen, K.; Beyeh, N. K. Recent Advances in Halogen Bonded Assemblies with Resorcin[4]Arenes. *The Chemical Record* **2021**, *21* (2), 386–395. https://doi.org/10.1002/tcr.202000140.
(38) Wang, K.; Liu, Q.; Zhou, L.; Sun, H.; Yao, X.; Hu, X.-Y. State-of-the-Art and Recent Progress in Resorcinarene-Based Cavitand. *Chinese Chemical Letters* **2023**, *34* (10), 108559. https://doi.org/10.1016/j.cclet.2023.108559.
(39) Liu, J.-L.; Sun, M.; Shi, Y.-H.; Zhou, X.-M.; Zhang, P.-Z.; Jia, A.-Q.; Zhang, Q.-F. Functional Modification, Self-Assembly and Application of Calix[4]Resorcinarenes. *J Incl Phenom Macrocycl Chem* **2022**, *102* (3), 201–233. https://doi.org/10.1007/s10847-021-01119-w.

(40) Han, J.; Cai, Y. H.; Liu, L.; Yan, C. G.; Li, Q. Syntheses, Crystal Structures, and Electrochemical Properties of Multi-Ferrocenyl Resorcinarenes. *Tetrahedron* **2007**, *63* (10), 2275–2282. https://doi.org/10.1016/j.tet.2006.12.073.
(41) Philip, I. E.; Kaifer, A. E. Electrochemically Driven Formation of a Molecular Capsule around the Ferrocenium Ion. *J. Am. Chem. Soc.* **2002**, *124* (43), 12678–12679. https://doi.org/10.1021/ja028202d.
(42) Moran, J. R.; Karbach, S.; Cram, D. J. Cavitands: Synthetic Molecular Vessels. *J. Am. Chem. Soc.* **1982**, *104* (21), 5826–5828. https://doi.org/10.1021/ja00385a064.
(43) Cram, D. J.; Cram, J. M. *Container Molecules and Their Guests*; The Royal Society of Chemistry, 1997. https://doi.org/10.1039/9781847550620.
(44) Beyeh, N. K.; Rissanen, K. N-Alkyl Ammonium Resorcinarene Salts: A Versatile Family of Calixarene-Related Host Molecules. In *Calixarenes and Beyond*; Neri, P., Sessler, J. L., Wang, M.-X., Eds.; Springer International Publishing: Cham, 2016; pp 255–284. https://doi.org/10.1007/978-3-319-31867-7_11.
(45) McIldowie, M. J.; Mocerino, M.; Ogden, M. I. A Brief Review of C n -Symmetric Calixarenes and Resorcinarenes. *Supramolecular Chemistry* **2010**, *22* (1), 13–39. https://doi.org/10.1080/10610270902980663.
(46) Beyeh, N. K.; Cetina, M.; Löfman, M.; Luostarinen, M.; Shivanyuk, A.; Rissanen, K. Hydrogen Bond-Stabilised N-Alkylammonium Resorcinarene Halide Cavitands. *Supramol. Chem.* **2010**, *22* (11), 737–750. https://doi.org/10.1080/10610278.2010.506543.
(47) Beyeh, N. K.; Cetina, M.; Rissanen, K. Binding Modes of Nonspherical Anions to N-Alkylammonium Resorcinarenes in the Solid State. *Crystal Growth & Design* **2012**, *12* (10), 4919–4926. https://doi.org/10.1021/cg3008409.
(48) Beyeh, N. K.; Cetina, M.; Rissanen, K. Halogen Bonded Analogues of Deep Cavity Cavitands. *Chem. Commun.* **2014**, *50* (16), 1959–1961. https://doi.org/10.1039/C3CC49010F.
(49) Desiraju, G. R.; Ho, P. S.; Kloo, L.; Legon, A. C.; Marquardt, R.; Metrangolo, P.; Politzer, P.; Resnati, G.; Rissanen, K. Definition of the halogen bond (IUPAC Recommendations 2013). *Pure and Applied Chemistry* **2013**, *85* (8), 1711–1713. https://doi.org/10.1351/PAC-REC-12-05-10.
(50) Beyeh, N. K.; Pan, F.; Rissanen, K. A Halogen-Bonded Dimeric Resorcinarene Capsule. *Angewandte Chemie* **2015**, *127* (25), 7411–7415. https://doi.org/10.1002/ange.201501855.
(51) Ji, X.; Wu, R.-T.; Long, L.; Guo, C.; Khashab, N. M.; Huang, F.; Sessler, J. L. Physical Removal of Anions from Aqueous Media by Means of a Macrocycle-Containing Polymeric Network. *J Am Chem Soc* **2018**, *140* (8), 2777–2780. https://doi.org/10.1021/jacs.7b13656.
(52) Borissov, A.; Marques, I.; Lim, J. Y. C.; Félix, V.; Smith, M. D.; Beer, P. D. Anion Recognition in Water by Charge-Neutral Halogen and Chalcogen Bonding Foldamer Receptors. *J Am Chem Soc* **2019**, *141* (9), 4119–4129. https://doi.org/10.1021/jacs.9b00148.
(53) Twum, K.; Sadraei, S. I.; Feder, J.; Taimoory, S. M.; Rissanen, K.; Trant, J. F.; Beyeh, N. K. Sharing the Salt Bowl: Counterion Identity Drives N-Alkyl Resorcinarene Affinity for Pyrophosphate in Water. *Org. Chem. Front.* **2022**, *9* (5), 1267–1275. https://doi.org/10.1039/D1QO01877A.
(54) d'Astous, É. V.; Dauphin-Ducharme, P. Harnessing Host–Guest Chemistry for Electrochemical Sensing in Complex Matrices. *Chem. Eur. J.* **2022**, *34*, 101029. https://doi.org/10.1016/j.coelec.2022.101029.

(55) Singh, V. V.; Sharma, P. K.; Shrivastava, A.; Gutch, P. K.; Ganesan, K.; Boopathi, M. Electrochemical Sensing of Chemical Warfare Agent Based on Hybrid Material Silver-Aminosilane Graphene Oxide. *Electroanalysis* **2020**, *32* (8), 1671–1680. https://doi.org/10.1002/elan.202000014.
(56) Xiong, S.; Cheng, J.; He, L.; Wang, M.; Zhang, X.; Wu, Z. Detection of Di(2-Ethylhexyl)Phthalate through Graphene–β-Cyclodextrin Composites by Electrochemical Impedance Spectroscopy. *Anal. Methods* **2014**, *6* (6), 1736–1742. https://doi.org/10.1039/C3AY42039F.
(57) Jin, Y.; Yao, X.; Liu, Q.; Li, J. Hairpin DNA Probe Based Electrochemical Biosensor Using Methylene Blue as Hybridization Indicator. *Biosensors and Bioelectronics* **2007**, *22* (6), 1126–1130. https://doi.org/10.1016/j.bios.2006.04.011.
(58) González-López, A.; Costa-Rama, E.; Fernández-Abedul, M. T. Electrochemical Micropipette-Tip for Low-Cost Environmental Applications: Determination of Anionic Surfactants through Their Interaction with Methylene Blue. *Talanta* **2021**, *224*, 121732. https://doi.org/10.1016/j.talanta.2020.121732.
(59) Tan, X.; Yang, H.; Ran, X.; Li, Z.; Zhang, L.; Gao, W.; Zhou, X.; Du, G.; Yang, L. Pillar[6]Arene-Modified Gold Nanoparticles Grafted on Cellulose Nanocrystals for the Electrochemical Detection of Bisphenol A. *New J. Chem.* **2021**, *45* (31), 14126–14133. https://doi.org/10.1039/D1NJ02040D.
(60) De Leener, G.; Evoung-Evoung, F.; Lascaux, A.; Mertens, J.; Porras-Gutierrez, A. G.; Le Poul, N.; Lagrost, C.; Over, D.; Leroux, Y. R.; Reniers, F.; Hapiot, P.; Le Mest, Y.; Jabin, I.; Reinaud, O. Immobilization of Monolayers Incorporating Cu Funnel Complexes onto Gold Electrodes. Application to the Selective Electrochemical Recognition of Primary Alkylamines in Water. *J. Am. Chem. Soc.* **2016**, *138* (39), 12841–12853. https://doi.org/10.1021/jacs.6b05317.

Chapter 2 – The Differential Impact of Resorcinarenes on Ferrocene Redox Couple in Electroactive Host-Guest Systems

Abstract

As an alternative to complex labelling of resorcinarene hosts with redox-active probes, non-covalent complex formation offers a unique avenue towards the design of electro-active host-guest systems. Here, *N*-alkyl ammonium resorcinarene halides (NARX) hosts were evaluated with the well-known redox probe ferrocene (**Fc**). Specifically, the NARX hosts were designed based on the tuning of the resorcinarene upper rim to allow for hydrogen bonding, π- π stacking, ion and halogen binding interactions in organic and aqueous environments. The NARX host induced a significant anodic shift of **Fc** $E_{1/2}$; once formed, the **Fc**-NARX complex undergoes oxidation and reduction without **Fc** dissociation. Data indicates hydrophobic interactions stabilize **Fc** interactions with the resorcinarene upper rim, which is directly related to the structural functionalization of the resorcinarene. Thus, we provide evidence for a controlled and tunable redox host-guest system with well-defined redox properties, which may be used to inform functional sensors and devices.

Chapter Status:

This chapter has been accepted into the Canadian Journal of Chemistry. Quintero-Arias, C.; Osei, B. O.; Twum, K.; Lewis, T.; Steinkamp, B. A.; McCormick, T. M.; **Beyeh, N. K.;** Martic, S. *Canadian Journal of Chemistry*, **2024**, *accepted.*

Contributions:

In this chapter, I contributed to the experiment design and planning. I carried out the electrochemical methods, including CV, EIS, and chronoamperometry. Collaborators at Oakland U synthesized the host compounds and performed the NMR spectroscopy. Collaborators at Portland State completed the DFT simulations.

2.1 Introduction

Resorcinarenes, belonging to the calix[n]arene family, are cone-shaped aromatic phenolic macrocycles. In their simplest form, the core resorcinarene is characterized by a wide upper rim and narrow lower rim. The bowl shape (C4v) is stabilized through hydrogen bonding from neighbouring resorcinol groups.[1] Meanwhile host-guest binding is available through C-H... π and cation...π interactions with the four aromatic rings. This unique branch of hosts is especially attractive for their modifiability, stability, and scalability for production. The formation of host-guest systems has led to extensive utilization of resorcinarenes, with applications spanning sensors, materials, drug delivery, catalysis, and sequestration.[2–6]

Recently, a new class of resorcinarenes, *N*-alkyl ammonium resorcinarene halides (NARXs), have been developed to expand the host cavity depth to accommodate novel and larger guests.[1,7] An alternative to deep cavity cavitands, they are prepared via a Mannich condensation reaction with resorcinarenes, excess formaldehyde and primary amine; The resulting tetrabenzoxazine ring is opened through refluxing with mineral acids to form the NARXs.[1] These hosts contain a unique wide upper rim with cationic ammonium groups which hydrogen bond with anionic halogen counter ions to form a strong circular hydrogen bond seam. The unique properties granted by the modifications have allowed for the formation of HG complexes with electron-rich guests that were previously too large for traditional resorcinarenes such as dioxane, naphthalene, anthracene, and pyrene.[1,8,9] They also behave as Lewis bases, accepting halogen bonds with directional control due to the placement of the halides for hydrogen bonding with the ammonium groups.[1]

The lack of redox activity in traditional resorcinarene hosts limits their electrochemical applications. To render the resorcinarenes electrochemically active, they may be further modified

or complexed with a redox-active group.[10] Often, Ferrocene (**Fc**) is used in combination with traditionally non-electroactive compounds, as a mediator or label, to obtain electrochemical information which would be otherwise inaccessible. **Fc**, a thermally stable and well established redox active molecule, exhibits a reversible **Fc**/**Fc**$^+$ redox couple.[11] Modifying a traditionally electro-inactive host with **Fc** is of particular interest to impart an observable signal to monitor the formation of host-guest complexes. Indeed, the direct modification of the resorcinarene rims with **Fc** has resulted in redox-active **Fc**-modified resorcinarenes.[12] However, the attachment of the **Fc** label complicates the design of hosts, impedes host-guest binding, selectivity, and electrochemical reversibility, hence, resulting electroactive resorcinarenes display poorly defined redox couples. These challenges associated with direct covalent host modifications may be solved by creating a supramolecular system using **Fc** as a non-covalently bound redox probe (mediator) rather than a label. To achieve this type of macromolecular control, it is necessary to understand the fundamental intermolecular interactions between the host and **Fc**.

The non-covalent host-**Fc** complexation has been previously reported for cyclodextrin (CD) and cucurbituril (CB) hosts.[13–17] While the interaction between CD and **Fc** is well understood, host functionalization constraints have limited selectivity.[13] CB hosts have offered an avenue for improved host-guest affinity given the addition of ion-dipole interactions for discrimination between guests.[14–16] However, limited solubility and complicated modifications, leave room for an improved class of hosts such as resorcinarenes.[14] Using an analogue of the core resorcinarene (Host **1**, Figure 1) containing a pendant methyl or undecane alkyl substituent (at the lower rim), solution electrochemical studies in organic solvent showed that six hosts formed a capsule around **Fc** resulting in an irreversible redox signal.[18] The octaacid cavitand host, an analogue of host 1 with pendent carboxylic acids at the lower rim, resulted in a loss of **Fc** signal which was ascribed to the

slower electron transfer kinetics due to **Fc** encapsulation.[19] By using exclusively modification at the lower rim, the reversibility and redox-activity of host-**Fc** complexes may be lost. Alternatively, by structurally tunning the upper rim, the interactions with **Fc** may be well controlled promising improved binding affinity, solubility and electrochemical properties.[1]

However, up-to-date, reports on the non-covalent interactions between modified resorcinarenes (upper rim) and **Fc** are scarce. Specifically, the NARXs' ability to bind to unique guests offers an avenue for novel electrochemically active supramolecular systems, but there have been no reports of such hosts with **Fc**. To this extent, a NARX host (Host **2**) was screened for its ability to interact with and form a redox-active supramolecular system with **Fc** (Figure 1). We selected a well-studied, representative NARX host (Host **2**) to compare to a simple, core resorcinarene (Host **1**). **Fc** and the hosts were first characterized independently, then in complexation, by various methods, including electrochemistry, spectroscopy, and mass spectrometry.

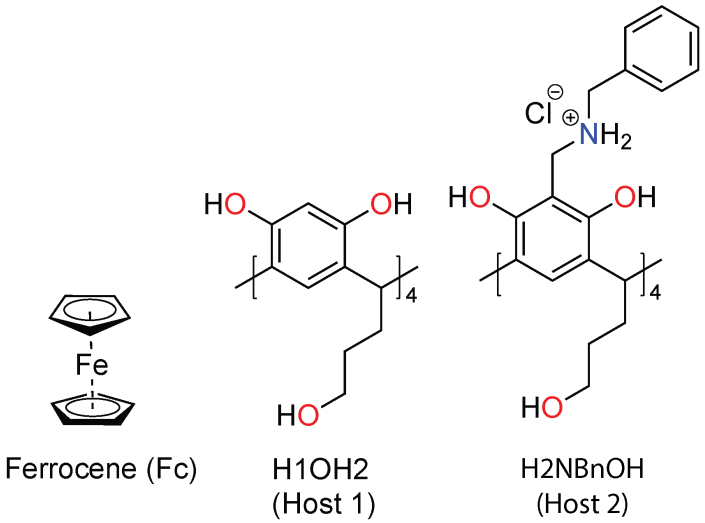

Figure 2.1. Chemical structures of Fc and the resorcinarene hosts.

2.2 Materials and Methods

2.2.1 Materials & Reagents

Electrochemical cells contained **Fc** (TCI America, USA), Tetrabutylammonium perchlorate (TBAP) (TCI America, USA), and MeOH (Fisher Scientific, USA). CHI104 Glassy carbon (GCE), CHI111 Ag wire reference electrode, and CHI115 platinum (Pt) counter electrodes were purchased from CH Instruments (USA). All electrochemical experiments were performed on the Autolab PGSTAT302N potentiostat, with the Nova software purchased from MetroOhm. All host compounds Host **1** (MW = 720.8 g/mol), Host **2** (MW = 1343.2 g/mol) were synthesized, purified and characterized as previously reported by the Beyeh Lab at Oakland University.[8,20,21]

2.2.2 Electrochemical Methods

Electrochemical measurements were carried out in a three-electrode, single-chamber cell with an Autolab potentiostat/galvanostat with a GCE, Ag wire reference electrode and a Pt wire counter electrode. The GCE surface was cleaned prior to each measurement. Briefly, the GCE surface was renewed via polishing on a polishing pad for 10 min in a solution of Alumina powder, followed by polishing on a clean polishing pad for 3 min, 8 min of sonication in an ethanol-activated carbon solution and finally 3 min sonication in ethanol.

The Nova 2.1 software by MetroOhm was used as the data collection interface on the potentiostat. Cyclic voltammograms were carried out in the -1.0 – 1.5 V potential range using multiple CVs (10 scans per CV), at a step of 0.00244 V, and varying scan rates between 0.1 - 1.0 V s^{-1}, unless otherwise specified. EIS measurements were carried out at respective oxidation potentials with an amplitude of 0.01 V. Each data point consists of three replicate measurements.

2.2.3 Ferrocene, host or host-ferrocene studies

Fc or host solution was prepared by weighing out the solid into the MeOH to make a 10 mM working solution. For CV measurement of **Fc**, a 3 mL sample solution (10 mM **Fc** with 100 mM TBAP in MeOH) was prepared and vortexed for 20 s. For CV measurement of a host, a 3 mL sample solution (10 mM host in 100 mM TBAP in MeOH)

was prepared and vortexed for 20 s. For CV measurement of the mixed host-**Fc** solutions, 10 mM **Fc** in 100 mM TBAP in MeOH was co-mixed with each host (10 mM). The final host:**Fc** molar ratio was 1:1, unless otherwise mentioned. The mixture was vortexed for 20 s then incubated at RT for 1 hr, unless otherwise mentioned, and subsequently measured.

2.2.4 Host displacement studies

A 3 mL sample solution (10 mM **Fc** with 100 mM TBAP in MeOH and 10 mM Host **1**) was prepared, vortexed for 20 s and incubated at RT for 1 hr. Next, Host **2** (10 mM) was added to the 3 mL sample solution and left to incubate for another 1 hr period at RT, then measured promptly by CV. Co-mixing experiments were also conducted. Two independent 3 mL solutions were prepared with 10 mM **Fc** with 100 mM TBAP in MeOH with either 10 mM of Host **1** or Host **2**. The solutions were vortexed for 20 s and incubated at RT for 1 hr. Next, in a new cell, 1.5 mL of each solution was added to create a co-mixed solution containing both host-guest complexes (10 mM **Fc**, 5mM Host **1** and Host **2**). After incubation at RT for 1 hr the solution was

measured by CV.

2.2.5 Electrospray Ionization Mass Spectrometry

An orbitrap Q-Exactive mass spectrometer (Thermo Fisher Scientific) equipped with an electrospray ionization (ESI) source was used to analyze all samples. Samples were analyzed in positive and negative modes with a sample flow rate of 10 μL/min. The capillary voltage was set

to 4.00 kV with a nitrogen sheath gas flow rate of 5 arbitrary units. The capillary temperature on the ESI source was set to 40 °C. The instrument resolving power was set to 17,500. Spectra were captured with an acquisition time of 1 minute over the mass range of m/z 150-2000 or 500-2000. The spectra were analyzed, and elemental composition was predicted using the ThermoScientific Freestyle 1.3 software.

2.2.6 UV-Vis spectroscopy

Solution UV–vis spectroscopy was performed on a BioTek Cytation 5 UV/Vis spectrometer in quartz cuvettes with the analyte dissolved in MeOH. 500 μL of the respective solution was pipetted into the cuvette after electrochemical measurements were performed.

2.2.7 NMR spectroscopy

NMR spectra were recorded on a Bruker Avance DRX 400 spectrometer at Oakland University. All signals are given as δ values in ppm using residual solvent signals as the internal standard. For sample preparation, stock solutions of the macrocyclic hosts (10 mM) and **Fc** (10 mM) were prepared in CD3OD. For the pure hosts and **Fc**, 250 μL of the stock solution was measured into the NMR tube and diluted with 250 μL of CD3OD. For a 1:1 mixture, 250 μL of macrocyclic host and 250 μL of **Fc** were measured into an NMR sample tube.

2.2.8 DFT

All calculations were completed with the Gaussian09 software pack.[22] Geometry optimizations were carried out at the B3LYP level of theory, optimized structures were determined for both the individual host molecules and the host and guest molecules. For the host only optimizations, basis sets of 6-311+g(d) for Host **1** and 6-311g for Host **2** were used. **Fc** was optimized at 6-311+g(d) and LANL2DZ for Fe. For the combination of the host and guest, the basis sets were 6-311g for Host **1** and 6-31g for Host **2** with LANL2DZ used for Fe throughout. Optimizations were

confirmed to be at the local minimum energy state through a frequency calculation using the same functional and basis sets. Single point energy calculations were completed with B3LYP and 6-311+g(d) (LANL2DZ for Fe) for all optimized structures. Images of the optimized structures were generated using Mercury.[23]

2.2.9 ATR-FTIR

A ThermoFisher Scientific (Waltham, MA, USA) Nicolet 300 FTIR spectrometer with a diamond ATR attachment was used for all the collected ATR-FTIR spectra. The Host spectra were collected as powders, while the **Fc** and Host 2-**Fc** spectra were collected from rinsed, dried crystal samples. All spectra were collected from 32 scans between 4000 and 600 cm^{-1} at a resolution of 2 cm^{-1}.

2.3 Results and Discussion

2.3.1 Host Electrochemical Studies

The solution electrochemical properties of **Fc** were investigated by cyclic voltammetry (CV), and a characteristic reversible redox signal was observed (Figure S1). The anodic peak was representative of the oxidation of **Fc** to ferrocenium (**Fc** → $\mathbf{Fc}^+ + e^-$), while the cathodic peak was due to the reduction of ferrocenium back to **Fc** ($\mathbf{Fc}^+ + e^-$ → **Fc**). At a scan rate of 200 mV s^{-1}, **Fc** was characterized by an E_{pa} of 307 ± 27 mV, E_{pc} of -27 ± 21 mV, $E_{1/2}$ of 140 ± 6 mV and a ΔE of 334 ± 47 mV (Table 1).

Table 1. Electrochemical parameters extracted from CVs for **Fc**, and mixtures of each host with **Fc** (1:1 eq. [**Fc**] = 10 mM; [host] = 10 mM; GCE as WE, Pt as CE and Ag+/Ag RE, MeOH, 100 mM TBAP).

	Fc	**Host 1 – Fc**	**Host 2 - Fc**
Scan Rate (mV s^{-1})	200	200	200
E_{pa} (mV)	307 ± 27	376 ± 6	509 ± 31
E_{pc} (mV)	-27 ± 21	3 ± 57	209 ± 25
i_{pa} (µA)	293 ± 9	282 ± 49	339 ± 2
i_{pc} (µA)	-304 ± 11	-229 ± 25	-323 ± 2
i_{pa}/i_{pc}	1.06 ± 0.01	1.23 ± 0.08	1.05 ± 0.04
ΔE_p (mV)	334 ± 47	373 ± 25	300 ± 5
$E_{1/2}$ (mV)	140 ± 6	187 ± 32	360 ± 11

Next, the electrochemical solution behavior of hosts was characterized. The presence of a host-related redox signal may introduce a confounding variable to the voltammogram; thus, preventing the isolation of mediator-related signals for monitoring complexation. Host **1** was characterized by the prominent irreversible oxidation peak at 1100 mV in CV (Figure 2 A). However, the anodic current dramatically decreased with each consecutive scan. Based on the CV data and the presence of 1,3-dihydroxybenzene groups in Host **1**, the irreversible oxidation of a phenol moiety is likely and commonly seen with other phenolic compounds.[24] The decrease in the current maximum with continuous CV scanning may suggest that the host is being irreversibly oxidized to a redox-inactive species or fouling the electrode surface.

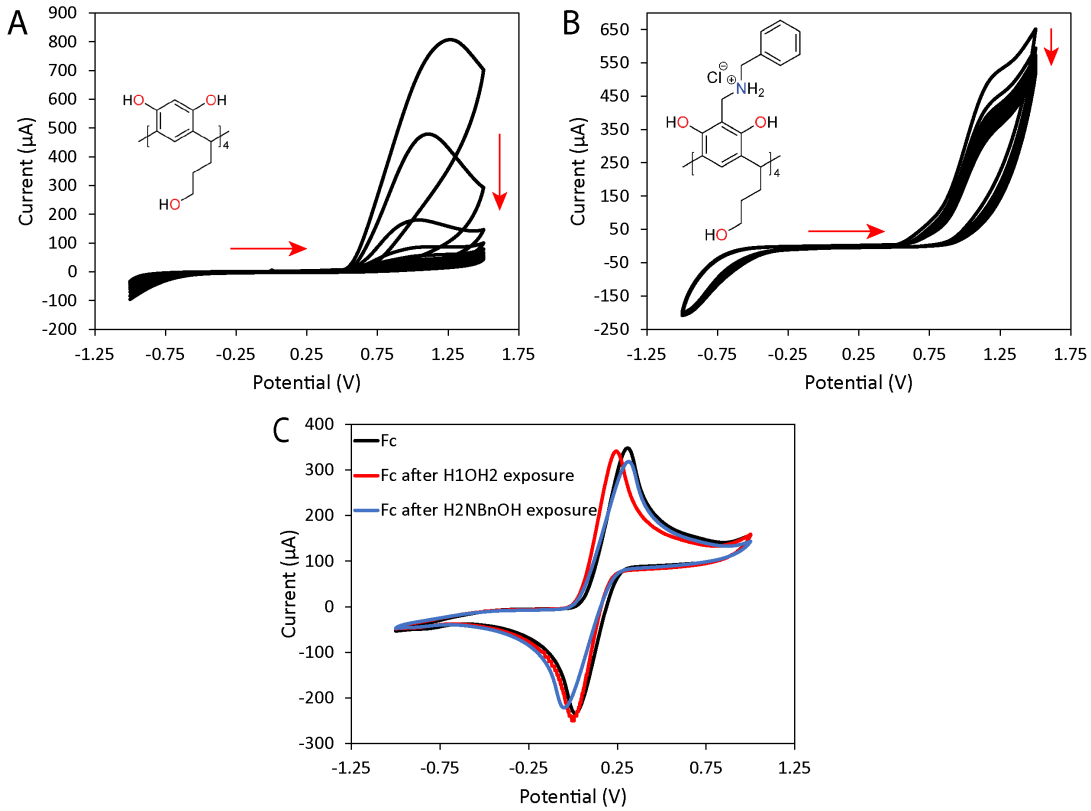

Figure 2.2. A) CVs of Host **1** B) Host **2** (10 mM, 10 scans), red arrows illustrate direction of the forward scan and change in current between subsequent scans. (C) CVs of **Fc** using bare GCE before and after exposure to host solutions (GCE as WE, MeOH, [**Fc**] = 10 mM, [host] = 10 mM, [TBAP] = 100 mM), Ag wire as RE, and Pt as CE).

Fouling occurs as a layer of the fouling agent accumulates on the surface of the electrode due to favorable non-covalent interactions between the surface and the fouling agent. As the fouling agent accumulates, this passivates the electrode surface reducing the transfer of electrons and decreasing the current maxima. To test for electrode fouling, after exposure to Host **1** (CV measurement), the working electrode was used to measure a **Fc** standard solution. The CVs of **Fc** were similar for the clean GCE (i_{pa}/ i_{pc} = 1.06) and the GCE after Host **1** exposure (i_{pa} / i_{pc} = 1.07), indicating no fouling and that the original decrease in current for Host **1** was due to host oxidation

into non-electroactive species (Figure 2C). The oxidation signal likely involves the two hydroxyl groups from the resorcinol moiety since phenols may undergo electrochemical oxidation at positive potentials greater than 1000 mV.[24] Therefore, Host **1** exhibited an irreversible oxidation at approximately 1100 mV, which did not overlap with the redox signal of **Fc**.

Host **2** was stable under electrochemical conditions as evidenced by the minimal change in subsequent CV scans (Figure 2B). The irreversible redox potential at 1100 mV was ascribed to the oxidation of a phenol group. Notably, no evidence of side reactions or electrode fouling were observed. The **Fc** CVs were similar for the clean GCE ($i_{pa}/ i_{pc} = 1.06$) and the GCE used after Host **2** ($i_{pa}/i_{pc} = 1.08$) proving the electrode surface was not fouled (Figure 2C). Therefore, Host **2** demonstrated ideal, improved characteristics for use with a **Fc** redox mediator compared to the core resorcinarene. Host **2** did not foul the electrode surface, oxidize to a side-product, or produces a confounding signal that overlapped with **Fc**. Alternatively, Host **1** was oxidized to a non-electroactive side product. Data clearly demonstrates that diverse modifications of the host upper rim may have a dramatic influence on the host electrochemical properties.

2.3.2 Host-Ferrocene Electrochemical Studies

With a better understanding of **Fc** and the hosts independent behavior, the interactions between **Fc** and hosts can be monitored. Free **Fc** in solution was characterized by an $E_{1/2} = 140 \pm 6$ mV (scan rate = 200 mV s^{-1}). Based on host studies, the potentials of **Fc** and host are not likely to overlap significantly; ideally, electrochemical trends related to **Fc** and hosts can be independently assessed. Herein, the host-guest complexation between hosts and **Fc** was characterized. It is anticipated that the modifications of Host **2**'s upper rim will improve affinity for **Fc**, inducing a greater shift in $E_{1/2}$.

The electrochemical behavior of Host **1** and **Fc** was investigated in solution. The Host **1**-**Fc** co-mixture (1:1 eq.) was characterized by an $E_{1/2}$ = 187 ± 32 mV, slightly anodically shifted compared to the free **Fc** (Figure 3A). Alongside **Fc**'s redox signal was a significant anodic current in the positive potential range associated with the host. Interestingly, extended cycling (50+ scans) revealed a degradation of the host signal and fouling of the electrode surface; electrochemical impedance spectroscopy (EIS) revealed a significant increase in the resistance to charge transfer (4.3×10^3 Ω). Whilst free **Fc** maintained a current signal limited by the mass transport (Figure 3B). To further understand the current behaviour of **Fc** and its relationship with the host the Cottrell equation was applied.

$$i_0(t) = \frac{nFAC_0\sqrt{D}}{\sqrt{\pi t}},$$

where $i_0(t)$ is the current, n is the number of electrons, F is the faraday constant, C_0 is the initial concentration of ferrocene, A is the area of the electrode, D is ferrocene's diffusion coefficient, and t is time. Derived from Fick's second law of diffusion under the assumptions of planar electrode, one dimensional diffusion for a quiescent solution, the Cottrell equation can be simplified to [25]:

$$i_0(t) = \frac{k}{\sqrt{t}},$$

in this form of the equation k represent the constant terms and a relationship between $i_0(t)$ and √t is revealed. The Host **1**-**Fc** co-mixture exhibited similar diffusion controlled current behaviour as the free **Fc**. The linear behaviour supports the weak, insignificant interaction between the core resorcinarene and **Fc** (Figure 3C).[25] Similar trends were observed for co-mixtures measured after 1 h or 24 h, indicating that the host 1 – **Fc** interactions form within 60 min (Figure S2).

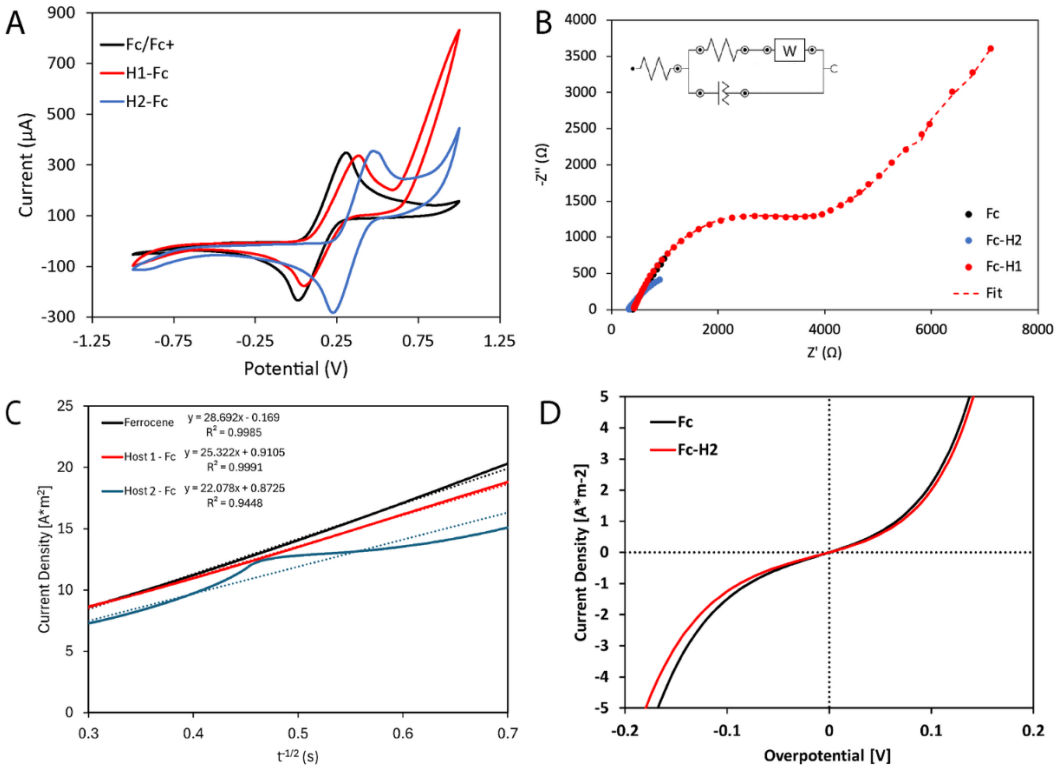

Figure 2.3. A) CVs of free **Fc** and **Fc**- Host complexes (1:1 eq., [host] = 10 mM; [**Fc**] = 10 mM, MeOH, [TBAP] = 100 mM). B) Nyquist plots of Free **Fc** and **Fc**- Host complexes after 50 CV scans (inset, equivalent circuit model for data fitting). (C) Cottrell plots of Free **Fc** and **Fc**- Host complexes (D) Butler-Volmer plots of Free **Fc** and **Fc**- Host **2** complex after 50 CV scans (GCE as WE, Ag wire as RE and Pt as CE).

Unlike Host **1**, Figure 3A demonstrates a dramatic anodic shift in peak potentials for Host **2-Fc**, characterized by $E_{1/2}$ = 360 ± 11 mV. Notably, the **Fc**/**Fc**$^+$ redox couple reversibility was maintained and remained like that of free **Fc**. Additionally, this complex was stable during CV cycling and did not induce electrode fouling, EIS demonstrated that oxidation of Host **2-Fc** remained facile and reached the mass transport limited current (Figure 3B). Butler-Volmer analysis after repeated cycling supported a facile, diffusion-limited current, since the exchange current density of Host **2** - **Fc** (j_0 = 0.23) and free **Fc** (j_0 = 0.26) were not significantly different (Figure

3D). Interestingly, the Cottrell plot of the comixture deviated from linearity, suggesting that the redox event was associated with a secondary process such as association with the host (Figure 3C). Therefore, electrochemical data provided strong evidence of an interaction between Host **2** and **Fc** with a greater affinity than Host **1**.

The shift in the $E_{1/2}$ of **Fc**/**Fc**$^{+}$ to a more positive value may be ascribed to the host-**Fc** interactions, and potentially formation of a highly stable supramolecular system. The Host **2**-**Fc** complex may be stabilized through hydrophobic non-covalent interactions. Host **2** hosts have been shown to interact with one another through π. . . π interactions of the benzyl groups which may also facilitate an interaction with **Fc** cyclopentadienyl (Cp) rings.[26] The increase in the peak currents of the Host **2**-**Fc** mixture compared to free **Fc** demonstrate an increased kinetic controlled current region, supporting electron transfer facilitation by host interactions (D value 1.59 ± 0.05 10-5 cm2 s^{-1} vs free **Fc** D value of 1.185 ± 0.047 * 10-5 cm2 s^{-1}). Previously, **Fc** was incorporated into a host-guest system with graphene oxide (GO) by intercalation into the GO sheets.[27] The strong π. . . π interactions between the layered graphene and the **Fc** molecules were credited for the stabilization of the complex and demonstrated similar modulation of current behaviour.

Various co-mixtures of **Fc** and Host **2** (10:1, 2:1, 1:1, and 0.5:1, host:**Fc** eq.) were compared to determine the coordination ratio of the complex formed (Figure 4 A, B, S3). Siu et al. previously exploited the Nernstian dependence of the redox shift to determine the stoichiometry of a redox active supramolecular complex; Host2-**Fc** also demonstrated a 1:1 stoichiometric relationship by the slope approaching the theoretical 59 mV dec^{-1} (Figure 4A).[28] Of note is the presence of two E_{pa} peaks (major and minor) when using the 2:1 and 1:1 ratio indicating two distinct populations of bound **Fc** (Figure 4A). This may indicate the presence of two kinds of **Fc** environments when

interacting with host 2 and has been previously observed for **Fc**-labeled resorcinarenes with a unique **Fc** group on both sides of the host.[12]

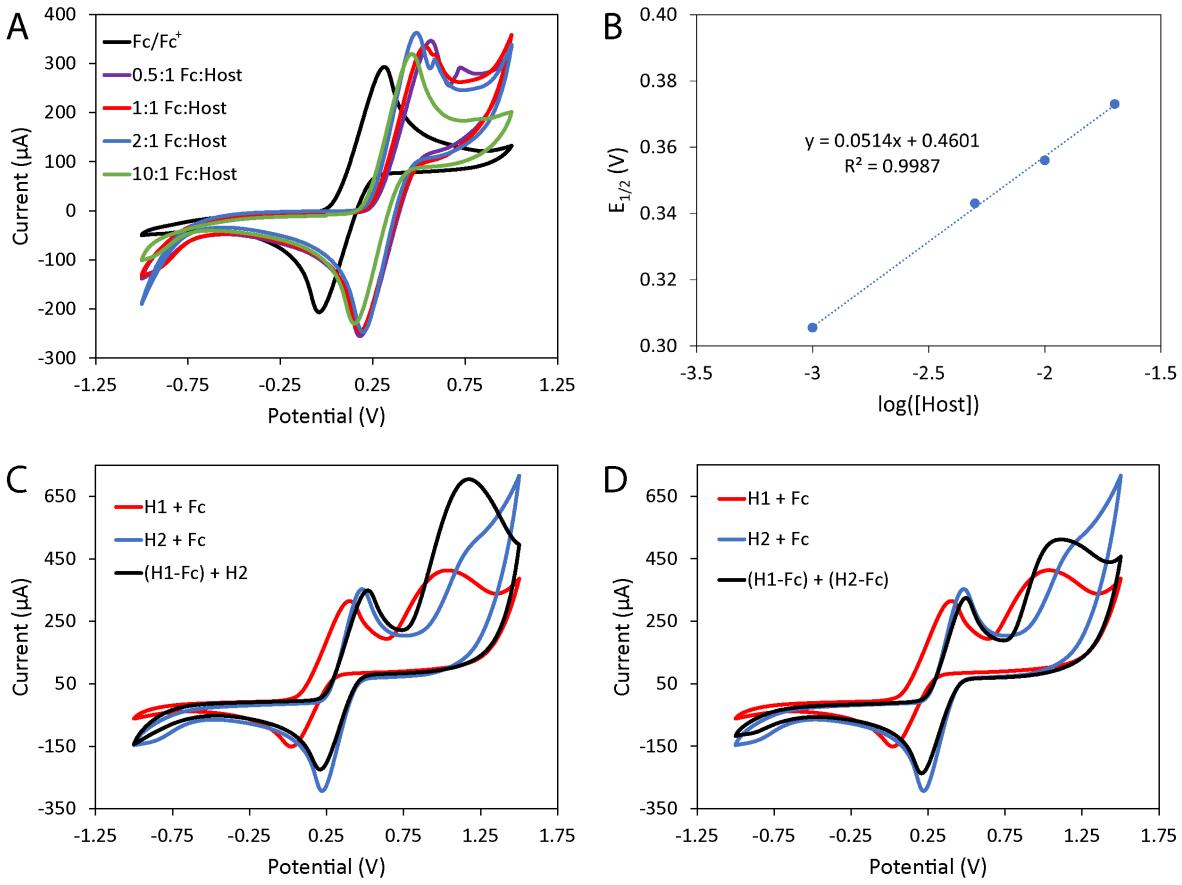

Figure 2.4. A) Cyclic voltammograms of various ratios of Host to **Fc** taken on a bare glassy carbon electrode in MeOH with TBAP (100 mM) vs Ag wire reference and Pt counter electrode. Measurements were taken after 1 h of incubation. 1:1 ratio of **Fc** to Host **2** (10 mM), (blue) 2:1 ratio of **Fc** (10 mM) to Host **2** (5 mM), (green) 10:1 ratio of **Fc** (10 mM) to Host **2** (1 mM). B) Half wave potentials ($E_{1/2}$) of **Fc**-host complexes at various concentrations of the host. C) Cyclic voltammogram of Host **1**-**Fc** after 1 h of incubation with Host **2**; D) Cyclic voltammogram of Host **1**-**Fc** comixed with Host **2**-**Fc** after 1 h of incubation together; (C & D) cyclic voltammogram of Host **1**-**Fc** after 1 h of incubation, (Blue) cyclic voltammogram of Host **2**-**Fc** after 1 h of incubation.

To further compare the hosts' affinity for **Fc**, competition and displacement measurements were conducted (Figure 4C, D). It was expected that Host **2** would outcompete Host **1** for **Fc**. When the Host **2** was added to a mixture of Host **1**-**Fc**, the resulting CV was similar to that of Host **2**-**Fc** mixture only, and no evidence of Host **1**-**Fc** complex was observed. In fact, there was a peak that was previously associated with free Host **1** at approximately 1100 mV that appeared upon the addition of Host **2**. The free and displaced Host **1** was evident upon continuous CV cycling which showed the dramatic decrease in E_{pa} of the Host **1** signal. Therefore, it was likely that Host **2** displaced Host **1** for **Fc**.

The mechanism dictating the electron transfer of the Host **2**-**Fc** complex can be understood based on the host-guest complex redox behavior. To investigate the mechanism, CV experiments were conducted at various scan rates. At 1000 mV s^{-1} the voltammograms remained unchanged and maintained reversibility (Figure S4). Thus, even at the shortest time scale available, the electron transfer process for the **Fc** $\rightleftharpoons$ $\mathbf{Fc}^{+}$ + e^{-} redox couple occurred while complexed with Host **2**. Commonly, electroactive hosts must undergo a complex dissociation prior to an electron transfer reaction (Scheme 1A).[29] At shorter time scales, and faster scan rates, there is insufficient time for the complex to dissociate and produce sufficient guest for electron transfer. As a result, the voltammogram is distorted and the redox signal reversibility is lost due to the limiting rate of the preceding chemical reaction; also known as a chemical-electrochemical (CE) mechanism.[29] *Matsue et al.* demonstrated that the β-CD-**Fc**COO- complex underwent a CE mechanism when the anodic voltametric peak flattened at fast scan rates (above 100 V s^{-1}), as the complex dissociation process became too slow to provide enough free ferrocenecarboxylate to sustain the fast-paced electrochemical oxidation.[29] CD and CB host-guest complexes have also exhibited a dissociation

preceding the electron transfer step, as in Pathway A, as for several **Fc** derivatives, reduced viologens and cobaltocene (Scheme 1).[30–32]

The electron transfer reaction may occur via direct oxidation through a different mechanism (Pathway B). In Pathway B, the electron transfer reaction is the only step, so the observed current must approach the mass transport limited value at sufficiently positive polarization. Here the guest can be directly oxidized while interacting with the host and the possibility exists that host-$\mathbf{Fc}^+$ is formed (Scheme 1). Similarly, to the current findings $\mathbf{Fc}^+$ formed a highly stable complex with CB[7] that underwent electron transfer through pathway B. The CV remained undistorted and fully reversible up to 2 V s^{-1}.[33]

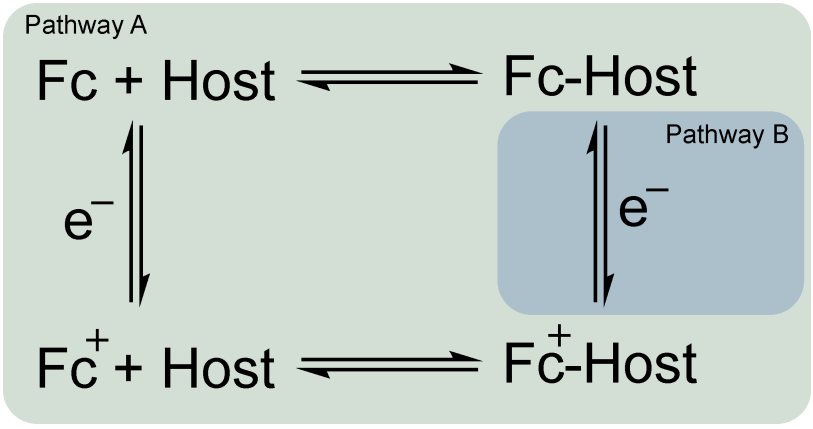

Scheme 2.1 Demonstrates two potential mechanisms for the electron transfer reaction of an electroactive guest in the presence of a host. (A) a chemical-electrochemical mechanism whereby the guest must first dissociate from the host to undergo an electron transfer. (B) a potential mechanism where the guest may be oxidized directly while interacting with the host.

In conclusion, $E_{1/2}$ and current parameters were measured which may be associated with host-guest interactions and complexation. Host **2** demonstrated significantly improved characteristics ($E_{1/2}$, i_{pa}/i_{pc}, ΔEp) compared to the core resorcinarene while maintaining complex stability and unique redox mechanisms. Although electrochemical measurements indicated an

interaction between hosts and **Fc**, to gain insight into the mode of interaction, non-electrochemical measurements were carried out. Thus, allowing for the identification of intermolecular interactions between host and **Fc** that gave rise to electrochemical trends observed.

2.3.3 Non-electrochemical characterization of Ferrocene and host interactions and complexation

The interactions between **Fc** and hosts were next characterized by non-electrochemical means, such as electrospray ionization - mass spectrometry (ESI-MS), NMR, and Density Functional Theory (DFT); to gain further insight into the intermolecular interactions that contributed to electrochemical findings.

ESI-MS, was used to characterize **Fc**, hosts, and their respective complexes. In the positive ion mode, the **Fc** mass spectrum revealed a peak at m/z 186.01, associated with the ferricenium cation (Figure S5). The MS spectra for Host **1**, and Host **2** hosts demonstrated peaks at m/z 721.3262 [Host **1** + H]$^{+}$, and 599.3128 [Host **2** - 4HCl + 2H]$^{2+}$ respectively (Figure 5). Interestingly, analysis of Host **2** with **Fc** did not yield any peaks associated with Host-**Fc** complexes under the same conditions. However, upon incubation of Host **1** with **Fc**, a peak at m/z 906.3318 appeared, suggesting a 1:1 interaction. The lack of MS peaks for **Fc** complexes with Host **2** may be due to complex instability in the gas phase or the specific solvent used for MS measurements.

^{1}H NMR spectroscopy was used for screening the interaction between **Fc** and the hosts (Figure 5C, S6, 7). Guest complexation in the resorcinarene cavity is typically indicated by shielding and broadening of the guests' ^{1}H NMR signals through the anisotropic effect from the aromatic internal cavity.[20] No significant changes were observed from the ^{1}H NMR of Host **1**-**Fc** (Figure S6) thus indicating that any interaction between the species is outside the cavity or a gas

phase phenomena in ESI-MS. Shielding of the **Fc** peaks was not observed for either of the hosts indicating that interactions, if any, did not involve the hydrophobic internal cavity. However, this shielding of the guest signal is not observed if the interaction is outside the internal cavity of the resorcinarene. In fact, there was a clear downfield movement of the methylene protons (0.04 ppm) closest to the N^+. . . Cl^-. . . N^+ salt bridge for Host **2** when **Fc** was co-present in a 1:1 eq mixture (Figure 5C, S7). Though the **Fc** is not in the internal cavity, the interaction with Host **2** is exo- with the flexible methylene protons readjusting to facilitate the interaction, thus, corroborating the electrochemical findings. Hence, unlike traditional host-guest complexes, the **Fc** is not encapsulated into the resorcinarene cavity.

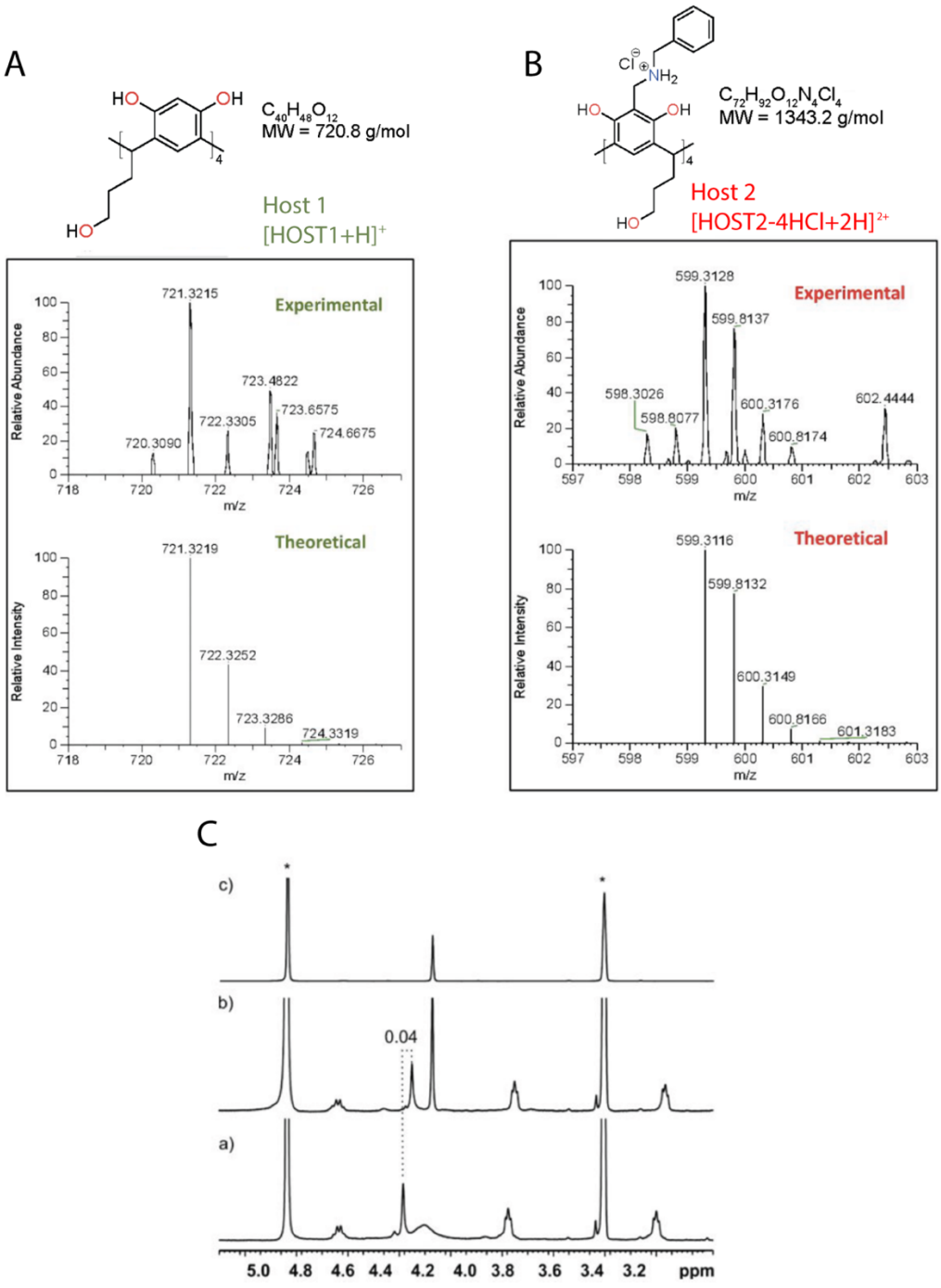

Figure 2.5. Positive mode ESI-MS spectra of experimental and theoretical spectra of A) Host **1** B) Host **2**, C) ^{1}H NMR (CD3OD, at 298 K) showing (a) Host **2** (1 mM), b) an equimolar mixture of **Fc** and Host **2**, and (c) pure **Fc** Star (*) represents CD3OD signal used as calibrant.

The interactions of hosts with **Fc** were also evaluated by ATR-FTIR. Initially, the crystallized **Fc** exhibited characteristic peaks associated with the sp2 C due to cyclopentadienyl rings. At a lower wavenumber, a strong sharp C-H bending at 812 cm^{-1} was observed alongside strong C=C stretching and bending at 1630 and 999 cm^{-1} respectively (Figure S8). The results were in line with previously reported FTIR spectra of **Fc**.[34] Individual analysis of the hosts also revealed unique peaks, both associated with their common core resorcinol, as well as the unique NARX decorations. The resorcinol core was identified by a broad O-H stretch at 3310 cm^{-1}, as well as a strong aromatic C=C stretch at 1600 cm^{-1}. While the lower alkyl chain was identified by a C-H stretch at 2860 cm^{-1} (Figure S8). Host **2** exhibited a sharp peak N-H stretching at 2980 cm^{-1}. The C=C stretching peak at 1600 cm^{-1} was also a higher intensity, likely due to the benzyl substituents. Thus, the unique wavenumbers associated with hosts and **Fc** could be individually tracked allowing for a direct measure of their complex formation, upon their co-crystallization.

The co-crystallized Host **2**-**Fc** complex was analyzed by FTIR and indicated the presence of characteristic peaks associated with both Host **2** and **Fc** (812, 999, 1630, 2980, and 3320 cm^{-1}) (Figure S8). Therefore, Host **2** and **Fc** were both present upon crystallization of the complex supporting an interaction between the two. Furthermore, the lack of Host **2** peak shifts also supports the lack of traditional encapsulation. Instead, the Host **2** peak at 1600 cm^{-1} was significantly reduced post-crystallization with **Fc**. The decreased intensity may indicate the interaction between the **Fc** with the upper-rim benzyl substituents of Host **2**.

At high concentrations of Host **2** (10 mM) self-association via π. . . π interactions was observed in the UV Vis spectrum (lambda = 473 nm) (Figure S9). Previous host-guest studies have cited shifts as small as 4 nm as significant and indicative of complexation.[35] The electronic transitions for the host include a major peak at 501 nm and a shoulder at 473 nm. However, for

host-**Fc** complex, the spectrum contains two absorbance bands at similar intensities. Assuming the absorbance is associated with the self-assembly of the host at high concentrations, the change in absorbance upon the addition of **Fc** may indicate that **Fc** disrupts the intermolecular host-host interactions.

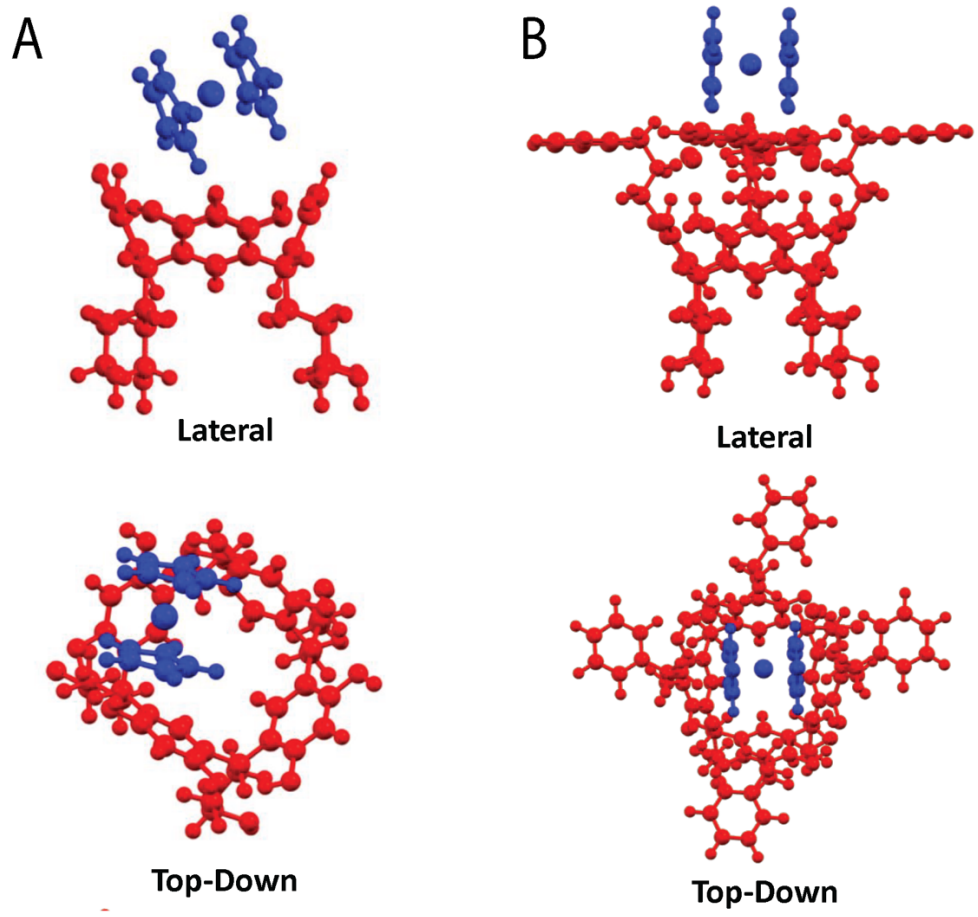

Figure 2.6. A, B) DFT simulations of the Host **1**-**Fc**, and Host **2**-**Fc** complexes respectively: lateral view of the complex and top-down view of the complex.

DFT-based computations were carried out to investigate theoretical binding interactions between the host and guests (Figure 6, S10). The calculations further support Host **2** interacting with **Fc** more favorably than Host **1**. The calculations relied on the energy of the molecules to determine whether favorable interactions or a complex may form, where the energy of the hosts

and free **Fc** were determined from single-point energy calculations carried out on the optimized structures. The sum of these separate total energies was compared to the energy taken from a single-point energy calculation of an optimized structure of **Fc** interacting with the host. Upon complexation with **Fc**, it is expected that the energy will decrease if there is a stabilization of the molecules upon the formation of a host-guest complex. The calculations suggest that Host **2** has the most stabilization with an energy decrease of 2.88 kcal/mol when interacting with **Fc** as opposed to Host **1** with showed a significant energy increase of 490 kcal/mol. These calculations support Host **2**'s higher binding affinity for **Fc** than Host **1**, which is in line with electrochemical and NMR data. The chemical structure of Host **2** in MeOH was found to take on an "open flower" confirmation with high stability.[26] From the NMR data, Host **2**-**Fc** interactions were ascribed to host methylene spacers with Cp rings, which is also reflected in the DFT calculations (Figure 6B). Therefore, results support that the careful modification of NARX hosts were energetically favourable for **Fc** interaction compared to the core resorcinarene.

2.4 Conclusion

Altogether, the electrochemical, spectroscopic and computational data demonstrated that the novel NARX resorcinarenes interact with **Fc**, leading to redox active and stable complexes. Traditional resorcinarenes have a shallow solvent-dependent cavity that cannot hold large guests. However, Host **2** has been modified with an extended, deep cavity. The cavity was made permanent through the addition of ammonium groups and halides to form a strong, stable cation-anion hydrogen bond around the host. The -CH2 groups connecting to the benzyl substituent are flexible and allow the benzyl groups to swing outwards, away from the resorcinarene core. This confirmation also allows for the -CH2 group to interact with the phenyl rings from the core resorcinarene through intramolecular -CH. . . π interactions, further stabilizing the orientation.[26]

Host **2** could associate with **Fc** preferentially over the core resorcinarene which was ascribed to the structural moieties of Host **2**. The Host **2**-**Fc** demonstrated a characteristic, reversible, one-electron oxidation whilst forming a stable complex that maintained the redox couple electron transfer kinetics. Traditional methods for monitoring the formation of host-guest complexes supported the formation of an exo-interaction between Host **2** and **Fc**.

Therefore, a fundamental understanding of the interactions between the NARX hosts and **Fc** was gained and proven to improve upon the core resorcinarene's affinity and complex stability. Unlike other traditional host-guest monitoring methods, the sensitive electrochemical methods offer unique means of evaluation of intermolecular interactions which may be elusive by other techniques. The work expands our understanding of host-guest interactions allowing the design of new electroactive supramolecular systems. By demonstrating the formation of a stable NARX-**Fc** noncovalent system, there is strong support for development of novel electrochemical sensors that incorporate this unique branch of hosts. Given the sensitivity, selectivity and scalability of the NARX hosts, its incorporation into electroactive systems greatly widens the library of guests for detection in complex media. Further work is necessary to understand the complex behavior of the NARX interactions with **Fc** to elucidate the mechanism of complexation and the applications in resorcinarene-redox mediated electrochemical sensors.

2.5 References

(1) Twum, K.; Rissanen, K.; Beyeh, N. K. Recent Advances in Halogen Bonded Assemblies with Resorcin[4]Arenes. *Chem. Rec.* **2021**, *21* (2), 386–395. https://doi.org/10.1002/tcr.202000140.

(2) Karle, A.; Twum, K.; Sabbagh, N.; Haddad, A.; Taimoory, S. M.; Szczęśniak, M. M.; Trivedi, E.; Trant, J. F.; Beyeh, N. K. Naphthalene-Functionalized Resorcinarene as Selective, Fluorescent Self-Quenching Sensor for Kynurenic Acid. *Analyst* **2022**, *147* (10), 2264–2271. https://doi.org/10.1039/D1AN02224E.

(3) Yan, X.; Peng, H.; Xiang, Y.; Wang, J.; Yu, L.; Tao, Y.; Li, H.; Huang, W.; Chen, R. Recent Advances on Host–Guest Material Systems toward Organic Room Temperature Phosphorescence. *Small* **2022**, *18* (1), 2104073. https://doi.org/10.1002/smll.202104073.

(4) Wankar, J.; Kotla, N. G.; Gera, S.; Rasala, S.; Pandit, A.; Rochev, Y. A. Recent Advances in Host–Guest Self-Assembled Cyclodextrin Carriers: Implications for Responsive Drug Delivery and Biomedical Engineering. *Adv Funct Mater* **2020**, *30* (44), 1909049. https://doi.org/10.1002/adfm.201909049.

(5) Zhao, L.; Cai, J.; Li, Y.; Wei, J.; Duan, C. A Host–Guest Approach to Combining Enzymatic and Artificial Catalysis for Catalyzing Biomimetic Monooxygenation. *Nat. Commun.* **2020**, *11* (1), 2903. https://doi.org/10.1038/s41467-020-16714-7.

(6) Deng, C.-L.; Murkli, S. L.; Isaacs, L. D. Supramolecular Hosts as in Vivo Sequestration Agents for Pharmaceuticals and Toxins. *Chem. Soc. Rev.* **2020**, *49* (21), 7516–7532. https://doi.org/10.1039/D0CS00454E.

(7) Beyeh, N. K.; Cetina, M.; Löfman, M.; Luostarinen, M.; Shivanyuk, A.; Rissanen, K. Hydrogen Bond-Stabilised N-Alkylammonium Resorcinarene Halide Cavitands. *Supramol Chem* **2010**, *22* (11), 737–750. https://doi.org/10.1080/10610278.2010.506543.

(8) Twum, K.; Sadraei, S. I.; Feder, J.; Taimoory, S. M.; Rissanen, K.; Trant, J. F.; Beyeh, N. K. Sharing the Salt Bowl: Counterion Identity Drives N-Alkyl Resorcinarene Affinity for Pyrophosphate in Water. *Org. Chem. Front.* **2022**, *9* (5), 1267–1275. https://doi.org/10.1039/D1QO01877A.

(9) Beyeh, N. K.; Cetina, M.; Rissanen, K. Halogen Bonded Analogues of Deep Cavity Cavitands. *Chem. Commun.* **2014**, *50* (16), 1959–1961. https://doi.org/10.1039/C3CC49010F.

(10) d'Astous, É. V.; Dauphin-Ducharme, P. Harnessing Host–Guest Chemistry for Electrochemical Sensing in Complex Matrices. *Curr. Opin. Electrochem.* **2022**, *34*, 101029. https://doi.org/10.1016/j.coelec.2022.101029.

(11) Astruc, D. Why Is Ferrocene so Exceptional? *Eur J Inorg Chem* **2017**, *2017* (1), 6–29. https://doi.org/10.1002/ejic.201600983.

(12) Han, J.; Cai, Y. H.; Liu, L.; Yan, C. G.; Li, Q. Syntheses, Crystal Structures, and Electrochemical Properties of Multi-Ferrocenyl Resorcinarenes. *Tetrahedron* **2007**, *63* (10), 2275–2282. https://doi.org/10.1016/j.tet.2006.12.073.

(13) Schmidt, B. V. K. J.; Barner-Kowollik, C. Dynamic Macromolecular Material Design—The Versatility of Cyclodextrin-Based Host–Guest Chemistry. *Angew Chem Int Ed* **2017**, *56* (29), 8350–8369. https://doi.org/10.1002/anie.201612150.
(14) Kim, K.; Selvapalam, N.; Oh, D. H. Cucurbiturils–a New Family of Host Molecules. *Journaltitle Incl. Phenom. Macrocycl. Chem.* **2004**, *50* (1), 31–36. https://doi.org/10.1007/s10847-003-8835-7.
(15) Droguett, K.; Quintero, G. E.; Santos, J. G.; Aliaga, M. E. Advancement in Supramolecular Control of Organic Reactivity Induced by Cucurbit[n]Urils. *Journaltitle Incl. Phenom. Macrocycl. Chem.* **2023**, *103* (1), 1–20. https://doi.org/10.1007/s10847-022-01172-z.
(16) Jeon, W. S.; Moon, K.; Park, S. H.; Chun, H.; Ko, Y. H.; Lee, J. Y.; Lee, E. S.; Samal, S.; Selvapalam, N.; Rekharsky, M. V.; Sindelar, V.; Sobransingh, D.; Inoue, Y.; Kaifer, A. E.; Kim, K. Complexation of Ferrocene Derivatives by the Cucurbit[7]Uril Host: A Comparative Study of the Cucurbituril and Cyclodextrin Host Families. *Journaltitle Am. Chem. Soc.* **2005**, *127* (37), 12984–12989. https://doi.org/10.1021/ja052912c.
(17) Qi, L.; Wang, R.; Yu, H.-Z. Supramolecular Cucurbit[7]uril@Ferrocene Complexation on Surface: From Nanostructure Differentiation to Guest Quantitation. *Acc. Mater. Res.* **2023**, *4* (5), 457–466. https://doi.org/10.1021/accountsmr.3c00025.
(18) Philip, I. E.; Kaifer, A. E. Electrochemically Driven Formation of a Molecular Capsule around the Ferrocenium Ion. *Journaltitle Am. Chem. Soc.* **2002**, *124* (43), 12678–12679. https://doi.org/10.1021/ja028202d.
(19) Podkoscielny, D.; Philip, I.; Gibb, C. L. D.; Gibb, B. C.; Kaifer, A. E. Encapsulation of Ferrocene and Peripheral Electrostatic Attachment of Viologens to Dimeric Molecular Capsules Formed by an Octaacid, Deep-Cavity Cavitand. *Chem. Weinh. Bergstr. Ger.* **2008**, *14* (15), 4704–4710. https://doi.org/10.1002/chem.200701961.
(20) Twum, K.; Bhattacharjee, A.; Laryea, E. T.; Esposto, J.; Omolloh, G.; Mortensen, S.; Jaradi, M.; Stock, N. L.; Schileru, N.; Elias, B.; Pszenica, E.; McCormick, T. M.; Martic, S.; Beyeh, N. K. Functionalized Resorcinarenes Effectively Disrupt the Aggregation of αA66-80 Crystallin Peptide Related to Cataracts. *RSC Med. Chem.* **2021**, *12* (12), 2022–2030. https://doi.org/10.1039/D1MD00294E.
(21) Hoegberg, A. G. S. Cyclooligomeric Phenol-Aldehyde Condensation Products. 2. Stereoselective Synthesis and DNMR Study of Two 1,8,15,22-Tetraphenyl[14]Metacyclophan-3,5,10,12,17,19,24,26-Octols. *Journaltitle Am. Chem. Soc.* **1980**, *102* (19), 6046–6050. https://doi.org/10.1021/ja00539a012.
(22) Frisch, M. J.; Trucks, G. W.; Schlegel, H. B.; Scuseria, G. E.; Robb, M. A.; Cheeseman, J. R.; Scalmani, G.; Barone, V.; Petersson, G. A.; Nakatsuji, H.; Li, X.; Caricato, M.; Marenich, A. V.; Bloino, J.; Janesko, B. G.; Gomperts, R.; Mennucci, B.; Hratchian, H. P.; Ortiz, J. V.; Izmaylov, A. F.; Sonnenberg, J. L.; Williams-Young, D.; Ding, F.; Lipparini, F.; Egidi, F.; Goings, J.; Peng, B.; Petrone, A.; Henderson, T.; Ranasinghe, D.; Zakrzewski, V. G.; Gao, J.; Rega, N.; Zheng, G.; Liang, W.; Hada, M.; Ehara, M.; Toyota, K.; Fukuda, R.; Hasegawa, J.; Ishida, M.; Nakajima, T.; Honda, Y.; Kitao, O.; Nakai, H.; Vreven, T.;

Throssell, K.; Montgomery, J. A., Jr.; Peralta, J. E.; Ogliaro, F.; Bearpark, M. J.; Heyd, J. J.; Brothers, E. N.; Kudin, K. N.; Staroverov, V. N.; Keith, T. A.; Kobayashi, R.; Normand, J.; Raghavachari, K.; Rendell, A. P.; Burant, J. C.; Iyengar, S. S.; Tomasi, J.; Cossi, M.; Millam, J. M.; Klene, M.; Adamo, C.; Cammi, R.; Ochterski, J. W.; Martin, R. L.; Morokuma, K.; Farkas, O.; Foresman, J. B.; Fox, D. J. Gaussian˜16 Revision C.01, 2016.

(23) Macrae, C. F.; Sovago, I.; Cottrell, S. J.; Galek, P. T. A.; McCabe, P.; Pidcock, E.; Platings, M.; Shields, G. P.; Stevens, J. S.; Towler, M.; Wood, P. A. Mercury 4.0: From Visualization to Analysis, Design and Prediction. *Journaltitle Appl. Crystallogr.* **2020**, *53* (1), 226–235. https://doi.org/10.1107/S1600576719014092.

(24) Zabik, N. L.; Anwar, S.; Ziu, I.; Martic-Milne, S. Electrochemical Reactivity of Bulky-Phenols with Superoxide Anion Radical. *Electrochimica Acta* **2019**, *296*, 174–180. https://doi.org/10.1016/j.electacta.2018.11.051.

(25) Bard, A.; Faulkner, L. *Electrochemical Methods: Fundamentals and Applications*; Pearson, 2000.

(26) Pan, F.; Beyeh, N. K.; Ras, R. H. A.; Rissanen, K. Guest-Induced Folding of the N-Benzyl Substituents in an Ammonium Resorcinarene Chloride and the Formation of a Halogen-Bonded Dimer of Capsules. *Cryst. Growth Des.* **2016**, *16* (12), 6729–6733. https://doi.org/10.1021/acs.cgd.6b01454.

(27) Gao, Y.; Hu, G.; Zhang, W.; Ma, D.; Bao, X. π–π Interaction Intercalation of Layered Carbon Materials with Metallocene. *Dalton Trans.* **2011**, *40* (17), 4542–4547. https://doi.org/10.1039/C0DT01392G.

(28) Siu, J. C.; Sauer, G. S.; Saha, A.; Macey, R. L.; Fu, N.; Chauviré, T.; Lancaster, K. M.; Lin, S. Electrochemical Azidooxygenation of Alkenes Mediated by a TEMPO–N3 Charge-Transfer Complex. *J. Am. Chem. Soc.* **2018**, *140* (39), 12511–12520. https://doi.org/doi.org/10.1021/jacs.8b06744.

(29) Matsue, T.; Evans, D. H.; Osa, T.; Kobayashi, N. Electron-Transfer Reactions Associated with Host-Guest Complexation. Oxidation of Ferrocenecarboxylic Acid in the Presence of .Beta.-Cyclodextrin. *Journaltitle Am. Chem. Soc.* **1985**, *107* (12), 3411–3417. https://doi.org/10.1021/ja00298a003.

(30) Isnin, R.; Salam, C.; Kaifer, A. E. Bimodal Cyclodextrin Complexation of Ferrocene Derivatives Containing N-Alkyl Chains of Varying Length. *Journaltitle Org. Chem.* **1991**, *56* (1), 35–41. https://doi.org/10.1021/jo00001a009.

(31) Mirzoian, A.; Kaifer, A. E. Reactive Pseudorotaxanes: Inclusion Complexation of Reduced Viologens by the Hosts β-Cyclodextrin and Heptakis(2,6-Di-o-Methyl)-β-Cyclodextrin. *Chem Eur J* **1997**, *3* (7), 1052–1058. https://doi.org/10.1002/chem.19970030711.

(32) Wang, Y.; Mendoza, S.; Kaifer, A. E. Electrochemical Reduction of Cobaltocenium in the Presence of β-Cyclodextrin. *Inorg. Chem.* **1998**, *37* (2), 317–320. https://doi.org/10.1021/ic970702y.

(33) Ong, W.; Kaifer, A. E. Unusual Electrochemical Properties of the Inclusion Complexes of Ferrocenium and Cobaltocenium with Cucurbit[7]Uril. *Organometallics* **2003**, *22* (21), 4181–4183. https://doi.org/10.1021/om030305x.
(34) Guan, L.; Shi, Z.; Gu, Z. Ferrocene-Filled Single-Walled Carbon Nanotubes. *Carbon* **2005**, *43* (13), 2780–2785. https://doi.org/10.1016/j.carbon.2005.05.025.
(35) Johnson, A. M.; Moshe, O.; Gamboa, A. S.; Langloss, B. W.; Limtiaco, J. F. K.; Larive, C. K.; Hooley, R. J. Synthesis and Properties of Metal–Ligand Complexes with Endohedral Amine Functionality. *Inorg. Chem.* **2011**, *50* (19), 9430–9442. https://doi.org/10.1021/ic201092s.

2.6 Appendix A: Chapter 2 Supporting Information

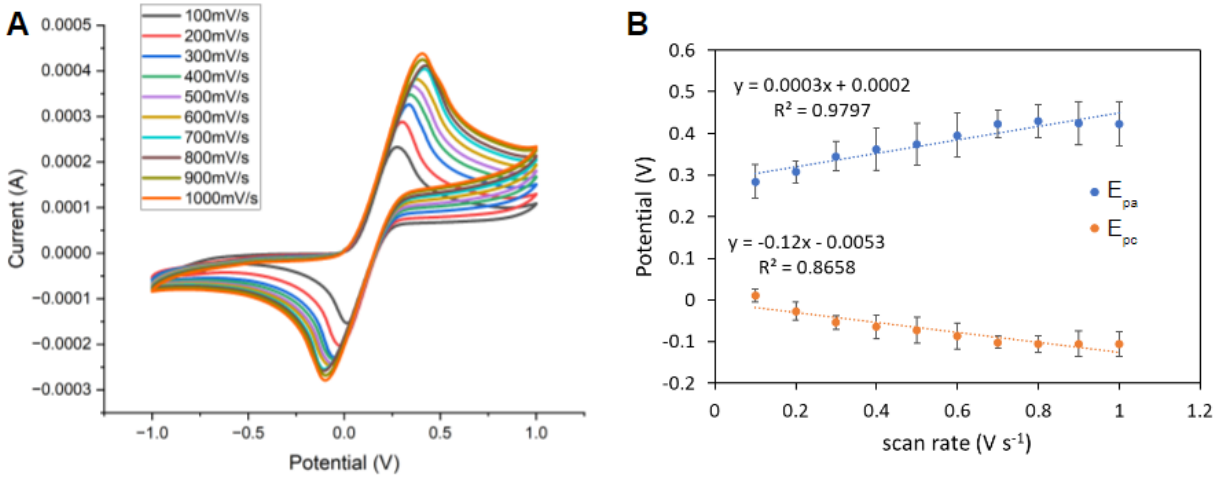

Figure S1. (A) Cyclic voltammograms in a solution of 10 mM Ferrocene at various scan rates 0.1 to 1 V s^{-1}; (B) linear correlation of the peak current on the square root of the scan rate. All measurements taken on a GCE in MeOH with 100 mM TBAP vs Ag wire reference and Pt counter electrode.

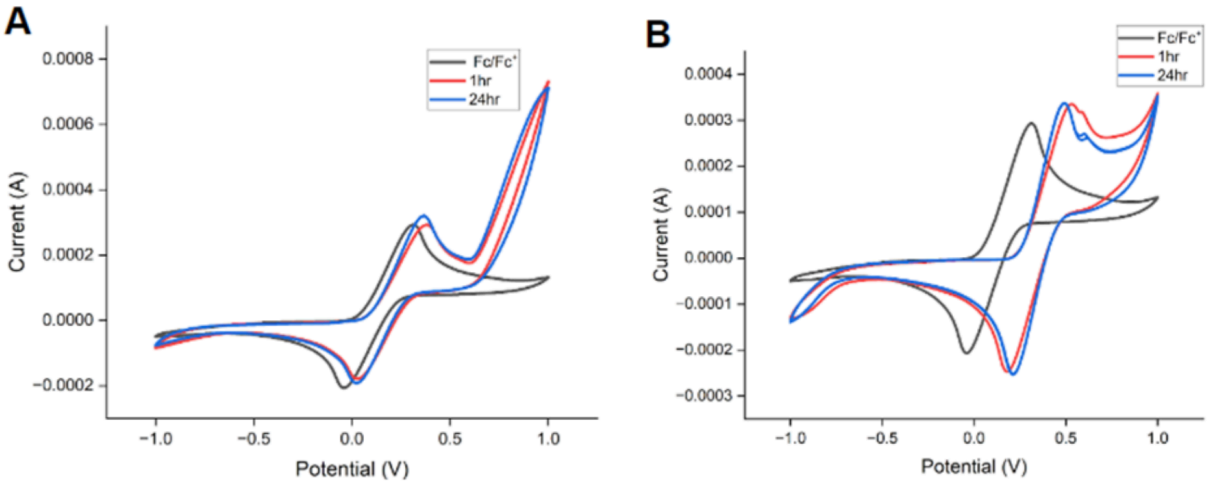

Figure S2. Cyclic voltammograms of (A) H1OH2-ferrocene and (B) H2NBnOH-ferrocene taken on a bare glassy carbon electrode in MeOH with TBAP (100 mM) vs Ag wire reference and Pt counter electrode. Measurements were taken after 1 h and 24 h of incubation.

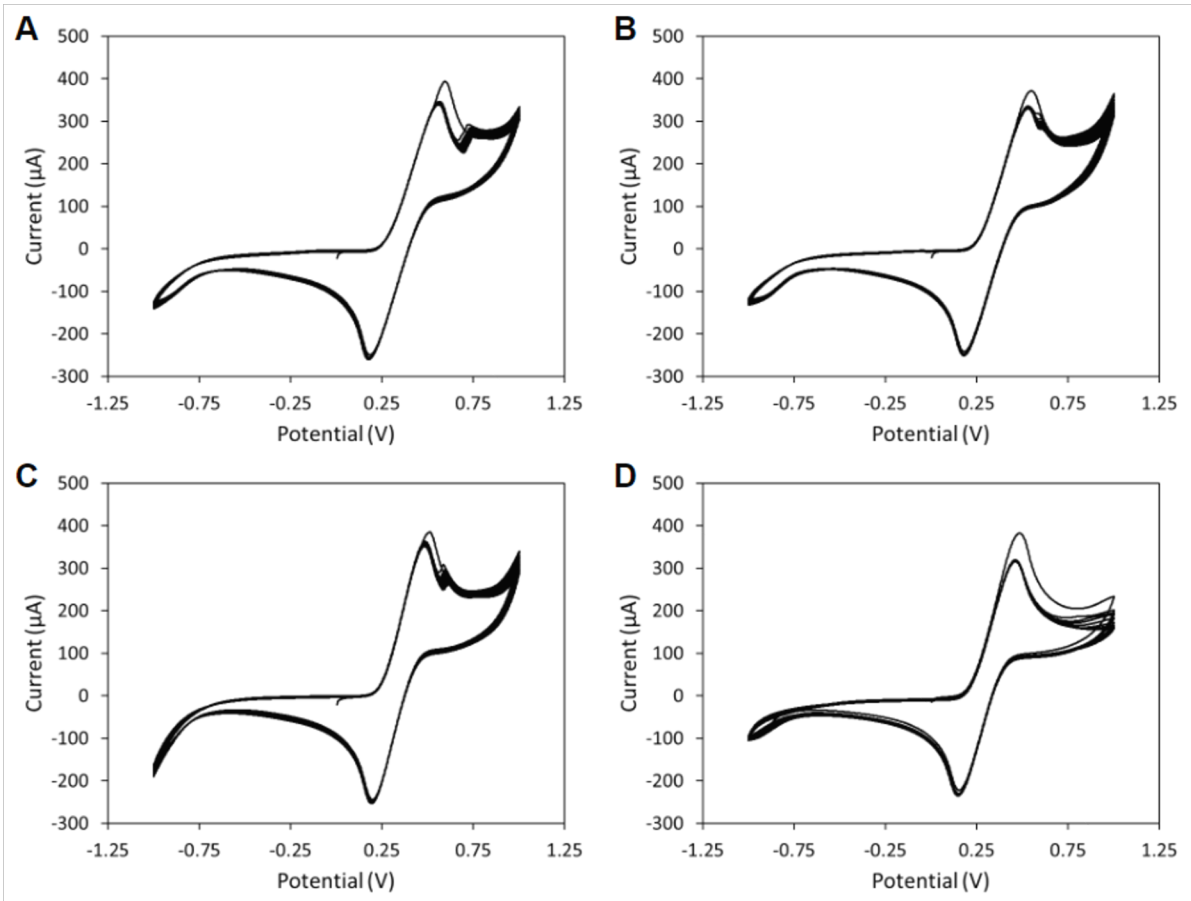

Figure S3. Cyclic voltammogram of various ratios of Host 2-Fc complex where Fc concentration was maintained throughout at 10 mM, taken on a bare glassy carbon electrode in MeOH with TBAP (100 mM) vs Ag wire reference and Pt counter electrode. (A) 0.5:1 Fc:Host, (B) 1:1, (C) 2:1, (D) 10:1.

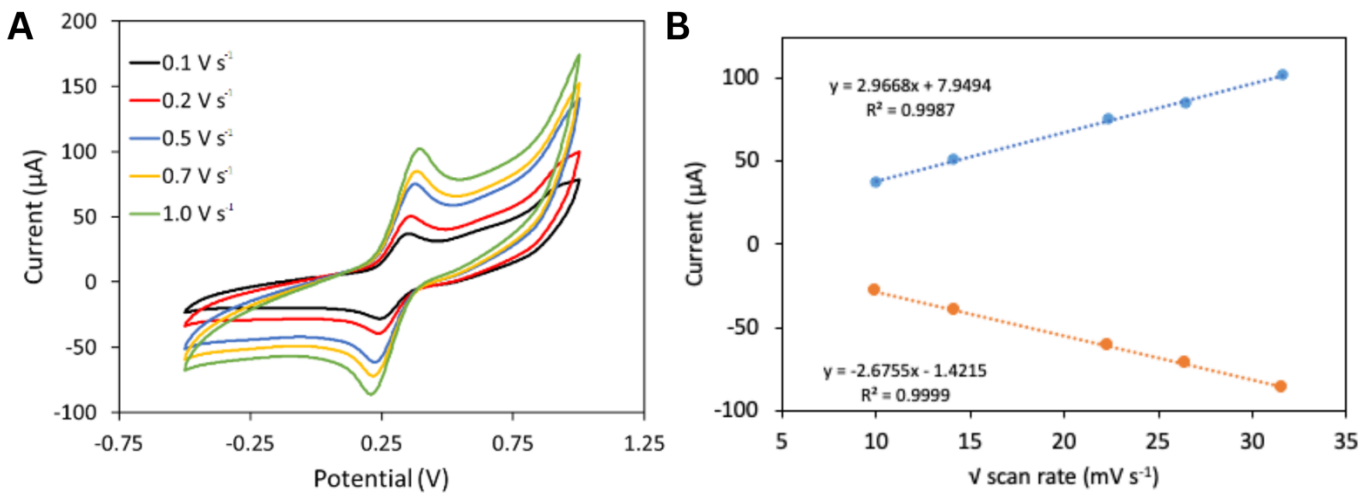

Figure S4. (A) CV responses of 1 mM H3NBnOH-Fc complex at various scan rates ranging from 0.1 - 1.0 V s^{-1}. (B) linear correlation of the peak current on the square root of the scan rate. All measurements taken on a GCE in MeOH with 100 mM TBAP vs Ag wire reference and Pt counter electrode.

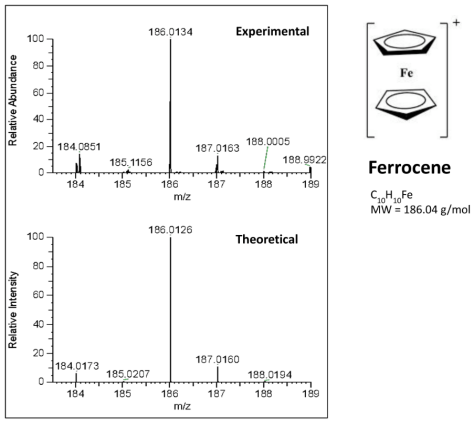

Figure S5. Positive mode ESI-MS partial spectrum of Ferrocene.

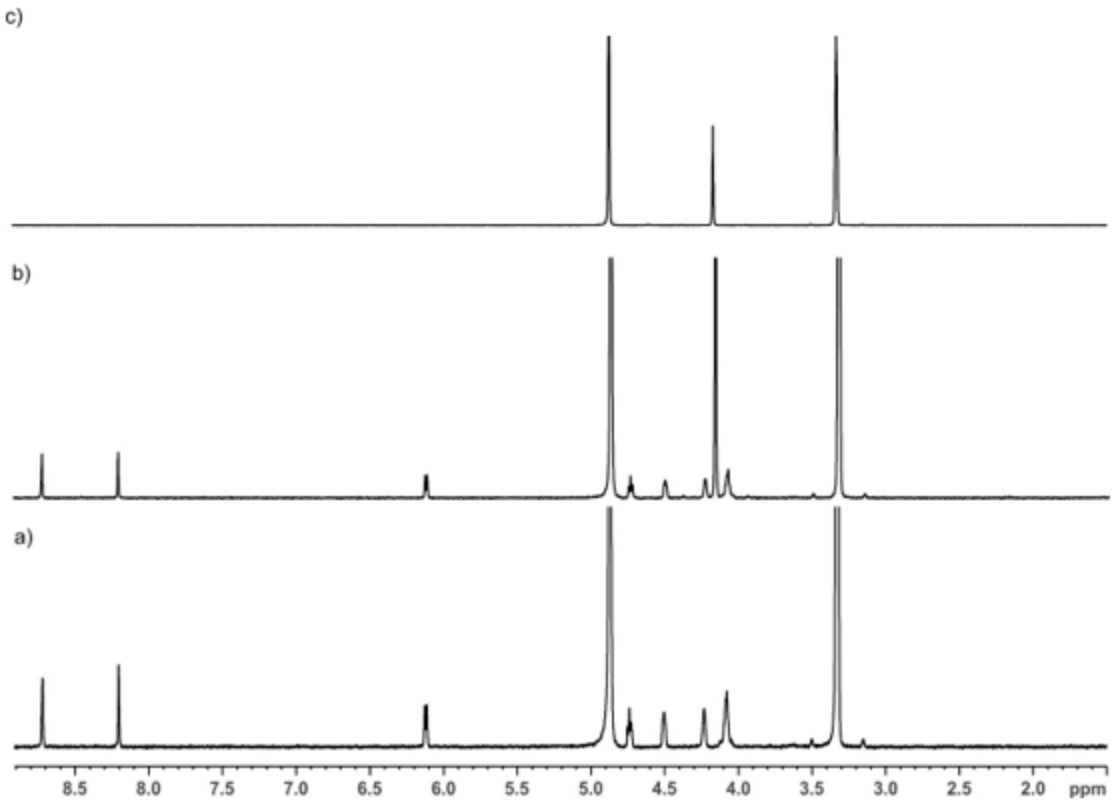

Figure S6. ^{1}H NMR (CD_3OD, at 298 K) showing (a) host **1** (1 mM), b) an equimolar mixture of ferrocene and host **1**, and (c) pure ferrocene

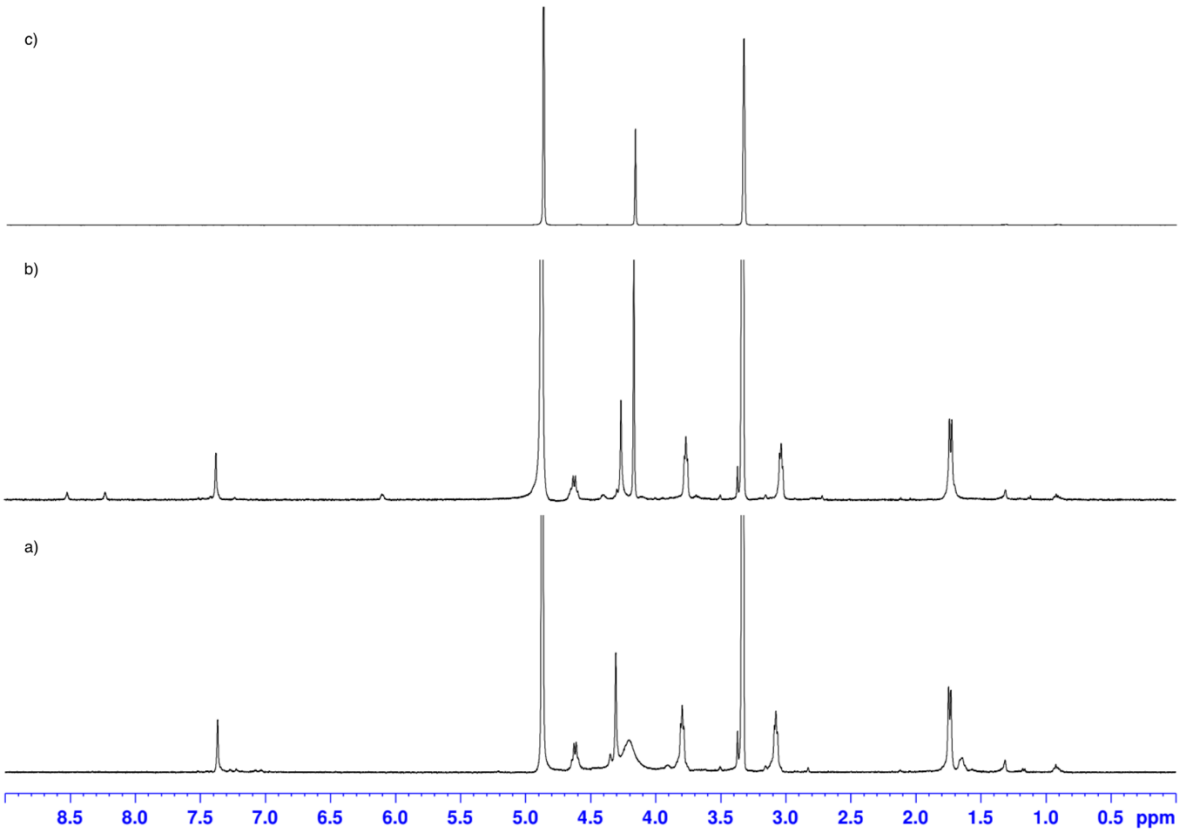

Figure S7. ^{1}H NMR (CD_3OD, at 298 K) showing (a) host **2** (1 mM), b) an equimolar mixture of ferrocene and host **2**, and (c) pure ferrocene

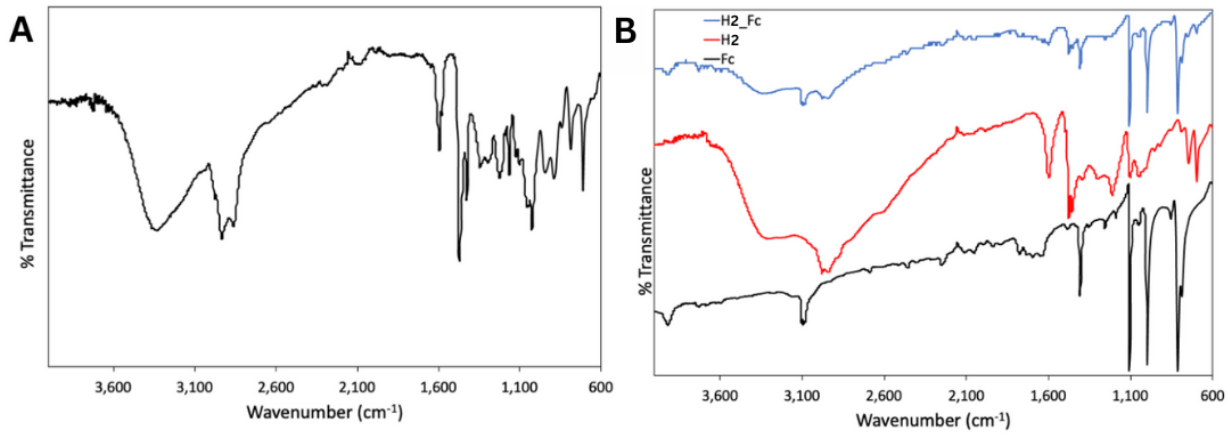

Figure S8. ATR-FTIR spectra collected between 4000 – 600 cm^{-1} of (A) Host 1, (B) Host 2, Fc, and Host 2 – Fc (1:1 equiv.).

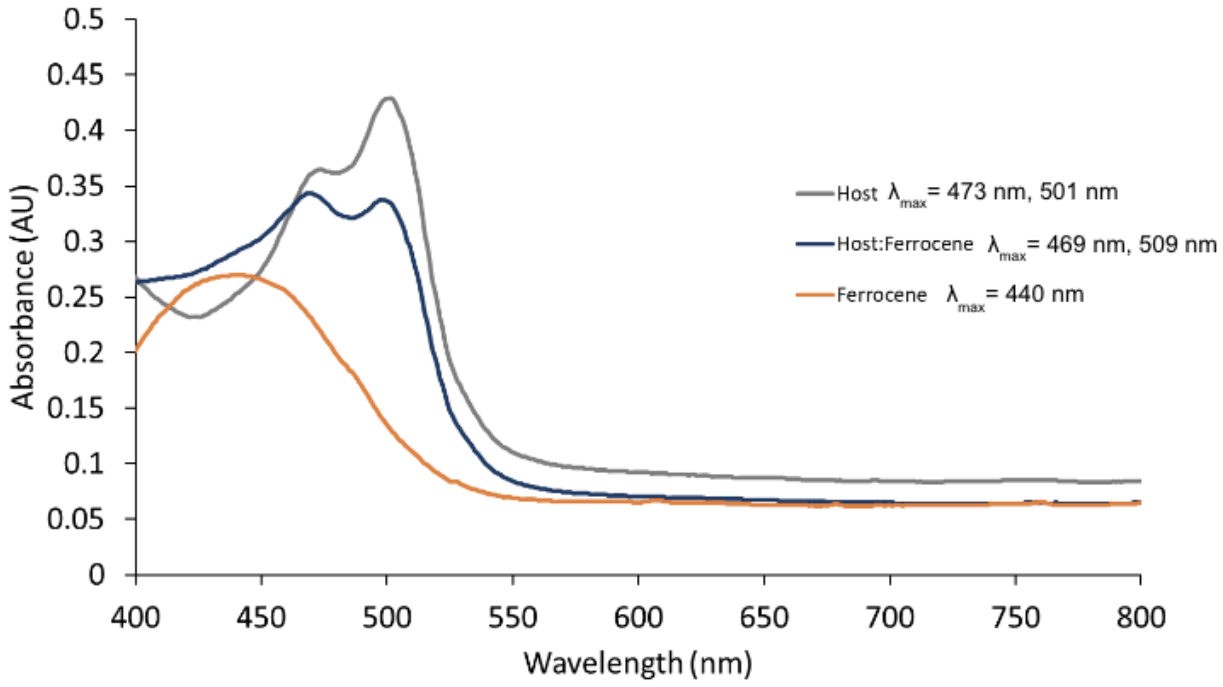

Figure S9 UV-Vis changes of Host 2 (10 mM) upon titrating equimolar Fc and incubating at RT for 1 h.

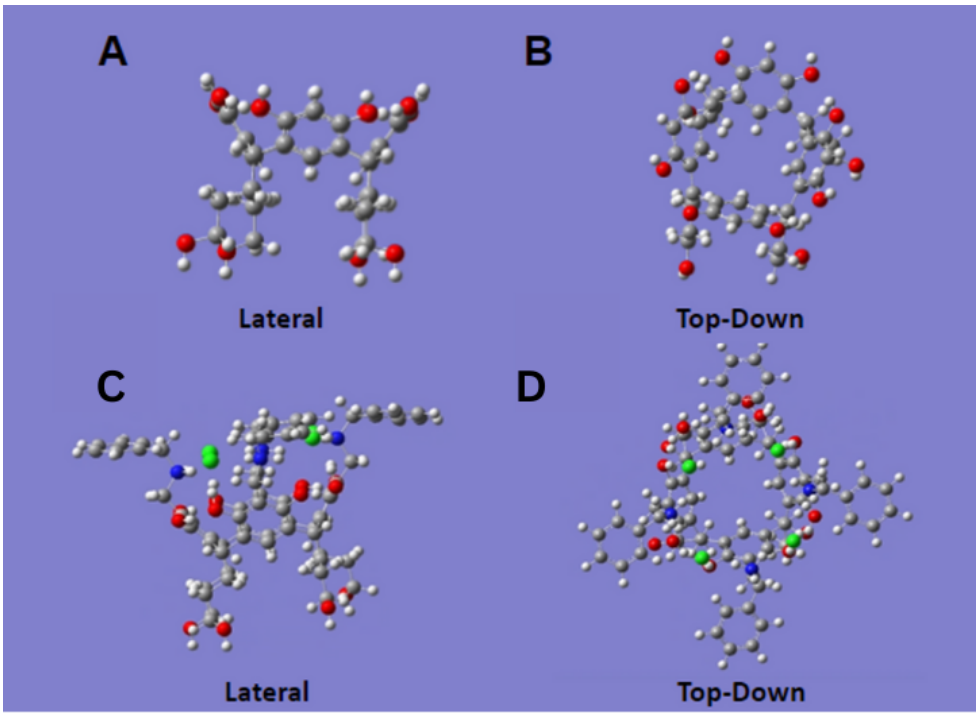

Figure S10. Schematic of the H1OH2 host molecule: (A) lateral view of host (B) top-down view of host. H2NBnOH host molecule: (C) lateral view of host (D) top-down view of host. Red represents oxygen, white represents hydrogen, grey represents carbon, blue represents nitrogen, green represents chlorine.

Chapter 3 – Electrochemical detection of adenosine monophosphate by N-alkyl resorcinarene recognition

Abstract

Recent advancements in the synthesis of resorcin[4]arenes has led to the development of anion receptors, previously a significant supramolecular challenge. The N-Alkyl ammonium resorcinarene chloride receptors, $NARX_4$, have demonstrated sensitivity and selectivity to adenosine monophosphate (AMP) over its di-, and triphosphate variants. Dysregulation of AMP has been associated with various neurodegenerative diseases, thus serving as a potential biomarker and guest of interest. Electrochemical sensors offer a unique, facile, cost-effective diagnostic method, opposed to complex traditional methods of monitoring host-guest complexation. Here, a representative NARX host was compared to an unmodified resorcinarene host for its ability to selectively and sensitively form complexes with AMP. In this chapter, the AMP interactions with the host were successfully measured by electrochemical methods.

Contributions:

In this chapter, I contributed to the experiment design and planning. I also carried out the electrochemical and spectroscopic methods.

3.1 Introduction

The development of synthetic receptors for the recognition of anions has been of specific interest, given their relevance in biological, environmental, and industrial applications.[1–4] The selective detection of phosphate anions has attracted attention due to their various roles in biological systems, from energy storage to signal transduction.[2] Adenosine-5'-monophosphate (AMP), the parent compound of adenosine di- and tri-phosphate (ADP, ATP), plays a crucial role as a coenzyme and in cellular metabolism. Beyond its functional purposes, AMP dysregulation may indicate greater health concerns. AMP-activated protein kinases (AMPK), are cellular energy sensors that rely on AMP for activation to stimulate glucose uptake and lipid oxidation.[5] Abnormal AMPK activation and adenosine metabolism have been linked to neurodegenerative disease. Alzheimer's, Amyotrophic lateral sclerosis, and Parkinson's disease have all demonstrated dysregulation in AMPK.[5] As such, accurate monitoring of AMP may serve as a potential diagnostic tool for various diseases. However, the selective detection of phosphate anions has proven difficult due to competitive environments and high solvation energies complicating the design of receptors.

To that extent, various approaches have been taken towards the development of phosphate anion chemosensors. A majority of chemosensors rely on metal complexes for detection via optical methods.[1,6–10] More recently, receptors exploiting halogen bonding (XB) donors have shown promising results for phosphate anion detection.[11] While AMP sensors have been previously reported, novel XB donor receptors demonstrate the rare capability to favour AMP over ADP or ATP.[1] A new class of resorcinarenes, N-alkyl ammonium resorcinarene halide salts ($NARX_4$), have been developed to expand the host cavity depth to accommodate novel and larger guests.[12] This host commonly contains a unique wide upper rim containing cationic ammonium groups which hydrogen bond with anionic halogen counter ions to form a strong hydrogen bond seam. The

unique properties granted by the modifications have allowed for the formation of host-guest complexes with electron-rich guests that were previously too large for traditional resorcinarenes, namely dioxane, naphthalene, anthracene and pyrene.[1,12,13]

A NAR(Cl)$_4$ receptor has previously been demonstrated to recognize phosphate anions in aqueous environments with up to 10^7 M^{-1} affinity.[13] The increase in entropy by chloride ion displacement, size-charge complementarity, and chelating behaviour, has allowed for a selective and sensitive receptor to be developed. As such, there is a potential to exploit the affinity of the NARX receptors to AMP for sensor design. However, currently host-AMP complexation is monitored via traditional methods; namely, isothermal calorimetry, and ^{1}H, ^{31}P NMR. While sensitive and discriminatory, traditional methods suffer from high operational costs and rely on trained personnel, electrochemical methods offer a novel method for detecting complexation.

The facile detection of AMP has been of interest since specific electrochemical sensors have been previously reported. However, the existing sensors have relied on the extensive modification of electrodes for detection. Specifically, *Shen et al*. reported an aptamer-modified AMP sensor that relied on modulation in surface charges upon complexation with AMP.[14] The aptamers used were highly specific to AMP and did not bind to analogous monophosphate interferers. Despite the specificity and sensitivity, the sensor was highly dependent on the solution's ionic strength. At a common electrolyte concentration of 100 mM NaCl, the sensor's signal was lost. Whereas resorcinarenes have demonstrated strong binding at similar concentrations of electrolyte. Thus, new resorcinarene hosts may offer a more robust alternative to AMP detection in an electrochemical environment. Currently, there are no electrochemical sensors that can directly detect the presence of AMP by oxidation of a host. Unlike other electrochemical host-based sensors which may require redox labeling of the host, the resorcinarenes hosts here are

inherently redox-active and serve as a recognition probe as well as a transducer. To this extent, a NARX host was screened for its ability to form a redox-active host-guest complex with AMP. We selected a NARX host that was previously reported to be sensitive and specific to AMP and a core resorcinarene without upper rim modification to serve as a reference (Figure 1). AMP and the hosts were first characterized independently in the electrochemical system to achieve this goal. It is anticipated that the hosts will produce an electrochemical signal that is modulated upon the formation of a host-guest complex with AMP.

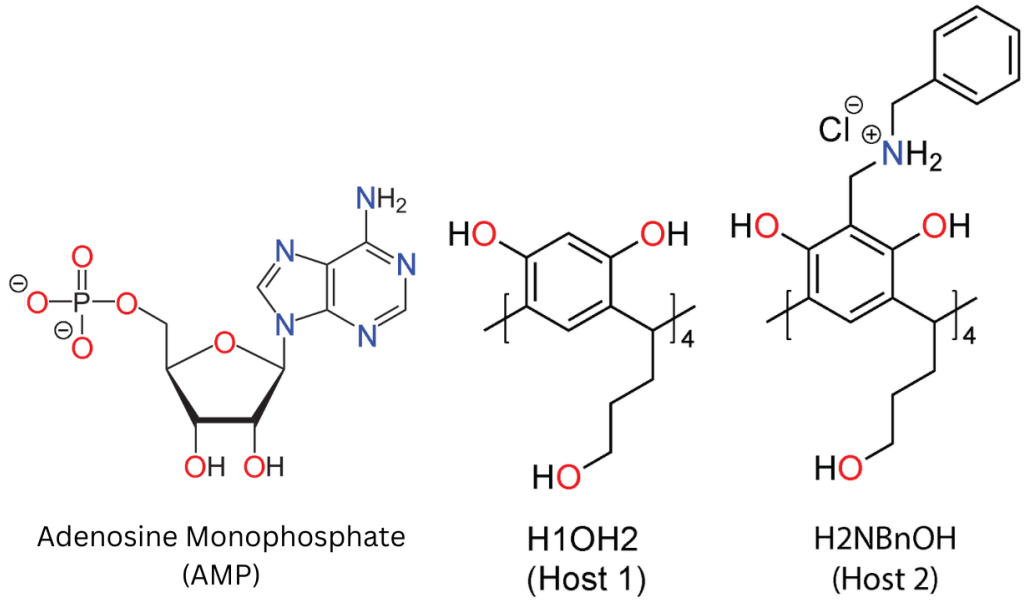

Figure 3.1. Chemical structures of Fc, AMP, and the resorcinarene hosts.

3.2 Experimental Section

3.2.1 Materials & Reagents

Electrochemical cells contained Adenosine 5–monophosphate (AMP) (Thermoscientific, Canada), Tetrabutylammonium perchlorate (TBAP) (TCI America, USA), and methanol (Fisher Scientific, USA). CHI104 Glassy carbon (GCE), CHI111 Ag wire reference electrode, and CHI115 platinum (Pt) counter electrodes were purchased from CH Instruments (USA). All electrochemical experiments were performed on the Autolab PGSTAT302N potentiostat, with the Nova software

purchased from MetroOhm. All host compounds H1OH2 (MW = 720.8 g/mol), H2NBnOH (MW = 1343.2 g/mol) were synthesized, purified and characterized as previously reported by the Beyeh Lab at Oakland University.[2,13,14]

3.2.2 Electrochemical methods

Electrochemical measurements were carried out in a three-electrode, single-chamber cell with an Autolab potentiostat/galvanostat. All cells contained 3 mL of solution (with 100 mM TBAP in methanol), GCE, an Ag wire reference electrode and a Pt wire counter electrode. The GCE had a geometrical surface area of 7.07 mm^2. The GCE surface was cleaned prior to each measurement. Briefly, the GCE surface was renewed via polishing on a polishing pad for 10 min in a solution of Alumina powder, followed by polishing on a clean polishing pad for 3 min, 8 min of sonication in ethanol, activated carbon solution and finally 3 min sonication in ethanol.

The Nova 2.1 software by MetroOhm was used as the data collection interface on the potentiostat. Square Wave Voltammetry (SWV) was carried out in the -1.0 - 1.5 V potential range, positive scan direction. Each data point consists of three replicate measurements.

3.2.3 AMP, host or host-AMP studies

For SWV measurements of AMP and hosts (1 mM), a 3 mL sample solution (as described above) was prepared in methanol and vortexed for 20 s.

For SWV measurements of the mixed host-AMP solutions, 18.75µL of AMP (40 mM) was titrated into a prepared host solution, vortexed for 20s, incubated at room temperature for 1 h and measured. AMP was titrated in and measured after each addition until AMP concentration reached 2 mM, the electrode was cleaned in between measurements. The final host:AMP molar ratio was 2:1 after all the additions of AMP.

3.2.4 UV-Vis spectroscopy

Solution UV–vis spectroscopy was performed on a BioTek Cytation 5 UV-Vis spectrometer in quartz cuvettes with the analyte dissolved in methanol. 500 μL of the respective solution was pipetted into the cuvette after electrochemical measurements were performed.

3.3 Results & Discussion

In chapter 2, Host-Fc complexation was demonstrated and was initially used for competitive binding to AMP. However, the Fc-based redox signal in the complex with the host did not change regardless of AMP addition. Hence, AMP could not be measured electrochemically by competitive assay. Herein, a direct measurement of AMP was tested with the hosts (in the absence of Fc) by electrochemical means.

The solution electrochemical properties of the resorcinarene hosts and AMP were first characterized individually by SWV a pulse voltammetric method. While the hosts share a basic resorcinarene core, the diversity in upper rim decorations was anticipated to create unique interactions between the hosts and AMP. AMP was characterized by a previously reported oxidation peak at 1.4 V.[15] Concerns of oxidation producing a free radical moiety at the amino group on the adenosine were suggested to induce dimerization and electrode fouling; thus hindering direct electrochemical detection of AMP. Here, AMP did not produce a significant electrochemical until 6 mM (Figure 2 A). To improve detection, and understand the mechanism of interaction, the behaviour of each host was independently investigated with SWV in the positive direction. As a consequence of the scan direction, only the oxidation signal of any redox-active groups is observed.

3.3.1 Electrochemical Host Studies

Host 1 was characterized by two prominent oxidation peaks, -0.05 ± 0.02 and 0.63 ± 0.03 V, that decreased in current maxima with consecutive scanning (Figure 2 A, S1A). Previous work with the host revealed the 1,3-dihydroxybenzene phenolic moieties on the resorcinol core are susceptible to irreversible oxidation leading to some electrode fouling with extended cycling.[16] The oxidation peak at -0.05 V likely represents a small number of ionized hydroxyl groups known as phenolates.[16] A previous report on the electrochemical reactivity of phenolic compounds demonstrates the tandem presence of phenol and phenolate peaks in cyclic voltammograms. They suggest that phenolate may undergo a single electron oxidation to a phenoxy radical. The inherent instability and reactivity of the radical product may explain the transient nature of the peak. Furthermore, the resorcinarene core shape is maintained by hydrogen bonding of adjacent resorcinol groups between $-O^{-}...HO-$; oxidation of the phenolate moiety supports host decomposition and subsequent fouling of the electrode surface. Organic acid addition induced a significant anodic shift of the -0.05 V oxidation peak towards the 0.64 V the 0.64 V oxidation peak was unchanged, again supporting the phenolate identity of the -0.05 V peak.

The SWV of Host 2 revealed two oxidation peaks at 0.18 ± 0.03 and 0.88 ± 0.01 V (Figure 2 A, S1B). Interestingly Host 2 did not exhibit a significant loss of current maxima with consecutive scanning. Previous studies demonstrated the remarkable stability of the host despite continuous electrochemical scanning. Therefore, the small decrease in current maxima can be attributed to the decrease in Host 2 concentration due to the single-direction scanning. Like previous hosts, the peaks can be attributed to the oxidation of the behaviour of the core resorcinol. The folding of Host 2 in MeOH was found to take on an “open flower” confirmation with high stability.[17] Host 2 has been modified with an extended, deep cavity made permanent through the

addition of ammonium groups and halides to form a strong, stable cation-anion seam around the host. The -CH_2 groups connecting to the benzyl substituent are flexible and allow the benzyl groups to swing outwards, away from the resorcinarene core. This confirmation also allows for the -CH_2 group to interact with the phenyl rings from the core resorcinarene through intramolecular -CH…π interactions, further stabilizing the orientation. Also, the orientation of the benzyl groups allows for intermolecular π…π interactions to stabilize multiple resorcinarenes.[17] At high concentrations of host 2 (10 mM) the self-association via π…π interactions was observed in the UV Vis spectrum (lambda = 473 nm) (Figure S2). The stability of host 2's confirmation demonstrates the functional groups most likely to be involved in the oxidation are the hydroxyl groups on the resorcinol. The slight positive shift and decreased current maxima compared to Host 1 may be attributed to the increased "difficulty" of oxidation due to steric hindrance.[18]

In conclusion, both the hosts demonstrated electrochemical activity when scanned in the anodic direction with SWV. Host 1 and host 2 both demonstrated signals associated with the oxidation of phenol and phenolate groups. However, host 2's current maxima were lower, likely due to steric hindrance and stability imparted by the modification to the upper rim. Therefore, the hosts exhibit electrochemical signals that may be exploited to monitor the formation of a host-guest complex.

3.3.2 Electrochemical Host-AMP Studies

With a better understanding of AMP and the host's independent behaviour the interactions between AMP and hosts could be monitored. Attempts to directly detect AMP's electrochemical signal were futile, with signals only beginning to appear at significant concentrations, thus supporting the need for a host-guest complex detection.

Host 1-AMP. Herein the electrochemical behavior of host 1 upon the titration of AMP was investigated. Upon AMP titration the two Host 1 oxidation peaks demonstrated opposite behavior (Figure 2B). The phenolate peak increased while the phenol peaks decreased linearly in response to AMP addition. The current begins to plateau (24 μA) after an equivalent of AMP is titrated into Host 1, suggesting a 1:1 complexation and calculated limit of detection (LOD) of 600 μM of AMP (Figure 2D). As expected, the free AMP peaks are never observed, even in titrations past the apparent saturation of the host (Figure 2A).

Given the simplicity of Host 1, extensive work has been conducted to understand the mechanisms dictating its binding to guests. *Aoyama et al*. demonstrated that a similarly decorated resorcinarene bound well to many alcohol and sugar compounds.[19] While non-specific, the host demonstrates a strong binding to specific hydroxyl-containing compounds with desirable orientations. The resorcinarene demonstrated the importance of the hydroxyl groups for host-guest complexation, as a modification to remove the host -OH groups prevented any complexation. Therefore, hydrogen bonding is crucial for recognition and complexation between Host 1 and a guest. Most importantly, they discovered that the resorcinarene bound strongly to a ribose sugar, the same sugar found in AMP. Further work by the same group demonstrated affinity of the host for sugars is dependent on the sugar's inherent traits.[20] Primarily, they propose that the cis conformation of OH groups, and greater lipophilicity improved the strength of the interaction between host and guest. Despite a hydrophilic phosphate group on the AMP, the cis-hydroxyl groups on the ribose sugar maximize the proximity to form hydrogen bonds. Further work by *Kobayashi et al*. sought to quantify the extent of binding between the host and guests.[21] They proposed that hydrogen bonding was not the sole contributor to complexation. NMR results demonstrated that hydrogen bonding works in tandem with CH-π to significantly enhance binding

affinity. They determined that the host did discriminate between guests, and it was more selective than previously reported. The binding affinity was distinct for varying lengths of aliphatic chains and stereoisomers. The aromatic rings of the host's resorcinol core interact with aliphatic groups to improve solubility and binding affinity. Most recently, Cho *et al*. demonstrated complex formation between AMP and a triazolium-based host. They proposed their host forms cation-π bonds between the adenine and their host.[22]

Therefore, host 1 is likely forming a complex with the ribose sugar or adenosine group of AMP. Hydrogen bonding between the ribose sugar or cation-π bonds with the adenosine is likely responsible for the interactions. This lack of specificity would support the large deviation in current between measurements. While host 1 demonstrates an interaction that can be monitored electrochemically, the lack of guest specificity limits its sensor applications. Therefore, the NARX host 2 offers a unique opportunity to maintain electrochemical activity whilst gaining a high degree of selectivity from the upper rim modifications.

Host 2-AMP. The NARX host, Host 2, was investigated similarly for electrochemical signal transduction of host-guest complexation. The Host demonstrated a significant increase in the current maxima at 0.2 V as AMP was titrated into solution (Figure 2C). The current increase became insignificant and plateaus (32 μA) after an equimolar amount of AMP was present, suggesting a 1:1 complex and a LOD of 240 μM (Figure 2D). However, the phenol peak seen in common with host 1 did not decrease to the same extent. Therefore, the interaction between host 2 and AMP is different from the core resorcinarene.

Host 2 demonstrates improved characteristics for electrochemical detection of host-guest complexation with AMP. The improvement in selectivity, sensitivity and stability can be attributed to the upper rim decorations stabilizing AMP upon complexation. Host 2 has been previously

reported to bind well to phosphate-containing compounds, including AMP. Previous NMR spectroscopy demonstrated the greatest field changes for AMP compared to ADP, ATP, pyrophosphate, and a phosphate ion. The phosphate group can displace the chloride counter ions in host 2 to better accommodate the guest.[13] The interaction also blocks a significant portion of the host from solvent, thus limiting interference from competing analytes. Furthermore, previous electrochemical characterization of host 2 demonstrated remarkable stability of the host upon continuous electrochemical cycling. Host 2 takes on an open-flower conformation in methanol where the -CH_2 groups connecting to the benzyl substituents can swing outwards, away from the resorcinarene core.[13] This conformation allows a host network to form through intramolecular -CH…π and π…π interactions, further stabilizing the host. Therefore, host 2 provides ideal characteristics for electrochemical host-guest complexation detection.

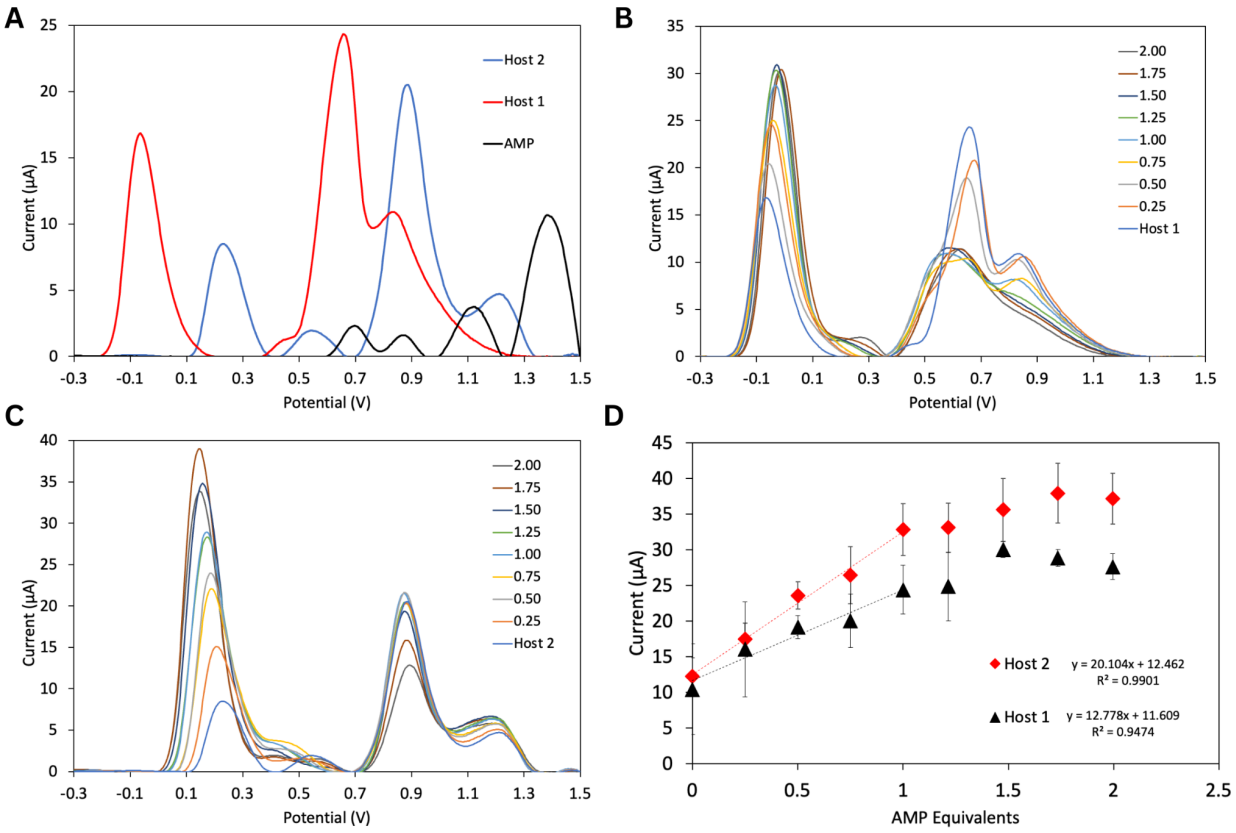

Figure 3.2. SWVs of A) Host 1, Host 2 (1 mM), and AMP (6 mM), B) Host 1 and C) Host 2 with various AMP equivalents (1st scan). D) Current maxima of the hosts after various additions of AMP, demonstrating the increase in current and saturation. (Glassy carbon electrode as working electrode, methanol, TBAP (100 mM) vs Ag wire reference and Pt counter electrode).

3.3.2 UV-Vis analysis of Host 2-AMP

Traditionally, host-guest complexation is monitored and confirmed via UV-Vis analysis, however, the method lacks the sensitivity of electrochemical methods.[23] Here, there was a 3 nm redshift upon titration of AMP into the Host 2 solution (Figure 3). Often, less than 5 nm redshifts are indicative of complexation. Pursell *et al.* demonstrated the complexation between iodine and cucurbituril induced a single nanometer redshift in the UV spectra.[23] Therefore, the UV-Vis results support the electrochemical detection of complexation.

The lack of sensitivity in the UV method demonstrates the importance of alternative electrochemical methods. Given the sensitivity to the local host environment of the electrochemical method, there is a significant increase in current post-complexation. While the UV method is sensitive to changes in the structure that alter the electronic transitions, the complex formed here is non-covalent and established by weak interactions. The same weak interactions can greatly alter the complexes' diffusion and redox behaviour.

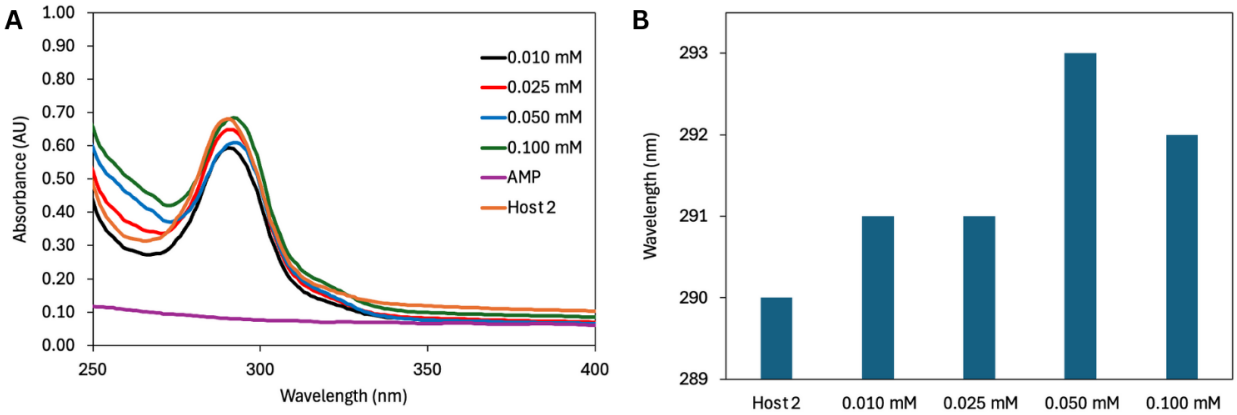

Figure 3.3. A) UV-Vis absorption spectra of various AMP titrations with AMP (0.010 – 0.100 mM), Host 2 (0.100 mM), and Host 2 (0.100 mM) controls (N = 1). B) Associated maximum absorption wavelengths.

3.4 Conclusion

Data supports that voltammetric methods can quantify the concentration of AMP bound to resorcinarene hosts. While the unmodified resorcinarene host signal was also modulated upon AMP titration, the modification of the upper rim for the NARX host imparted a significantly greater selectivity and specificity towards the AMP guest, while also improving the electrochemical sensitivity. The negatively charged phosphate group, along with the size complementarity of the AMP allows for a high affinity with the NARX host, as the halides are displaced in favour of the guest. The formation of the NARX-AMP complex was monitored by the

modulation of the phenolate peak at 0.2 V, as the current increased linearly until a 1:1 equivalent was titrated, supporting previous studies reporting an equimolar complex.

Therefore, a novel host-guest electrochemical AMP sensing method was described and may be used to replace alternative, cumbersome, lab-based methods of monitoring complexation. Interestingly, the unique branch of hosts does not require a traditional redox mediator and can instead directly transduce a representative signal. Future work requires further NMR and DFT studies to support the electrochemical findings. While electrochemical results suggest complex formation NMR and DFT will provide structural information to understand where the NARX host interacts with the AMP. The methods will also reveal the strength of the interaction through binding energies. Specifically, to determine the mechanism of interaction and associated energy. Nonetheless, in its current state, the electrochemical method serves as a preliminary method for AMP detection, before more complicated methods.

3.5 References

(1) Twum, K.; Sadraei, S. I.; Feder, J.; Taimoory, S. M.; Rissanen, K.; Trant, J. F.; Beyeh, N. K. Sharing the Salt Bowl: Counterion Identity Drives N-Alkyl Resorcinarene Affinity for Pyrophosphate in Water. *Org. Chem. Front.* **2022**, *9* (5), 1267–1275. https://doi.org/10.1039/D1QO01877A.

(2) Hargrove, A. E.; Nieto, S.; Zhang, T.; Sessler, J. L.; Anslyn, E. V. Artificial Receptors for the Recognition of Phosphorylated Molecules. *Chem. Rev.* **2011**, *111* (11), 6603–6782. https://doi.org/10.1021/cr100242s.

(3) Yang, X.; Wu, X.; Hao, H.; He, Z. Mechanisms and Assessment of Water Eutrophication. *J. Zhejiang Univ. Sci. B* **2008**, *9* (3), 197–209. https://doi.org/10.1631/jzus.B0710626.

(4) Fulmali, A.; Bharate, S. S. Phosphate Moiety in FDA-Approved Pharmaceutical Salts and Prodrugs. *Drug Dev. Res.* **2022**, *83* (5), 1059–1074. https://doi.org/10.1002/ddr.21953.

(5) Chang, C.-P.; Wu, K.-C.; Lin, C.-Y.; Chern, Y. Emerging Roles of Dysregulated Adenosine Homeostasis in Brain Disorders with a Specific Focus on Neurodegenerative Diseases. *J. Biomed. Sci.* **2021**, *28* (1), 70. https://doi.org/10.1186/s12929-021-00766-y.

(6) Li, S.-H.; Yu, C.-W.; Yuan, W.-T.; Xu, J.-G. A Lanthanide Hybrid Cluster as a Selective Optical Chemosensor for Phosphate-Containing Anions in Aqueous Solution. *Anal. Sci. Int. J. Jpn. Soc. Anal. Chem.* **2004**, *20* (10), 1375–1377. https://doi.org/10.2116/analsci.20.1375.

(7) Gao, J.; Riis-Johannessen, T.; Scopelliti, R.; Qian, X.; Severin, K. A Fluorescent Sensor for Pyrophosphate Based on a Pd(II) Complex. *Dalton Trans.* **2010**, *39* (30), 7114–7118. https://doi.org/10.1039/C0DT00434K.

(8) Wang, W.; Zhao, H.; Zhao, B.; Liu, H.; Liu, Q.; Gao, Y. Highly Selective Recognition of Pyrophosphate by a Novel Coumarin-Iron (III) Complex and the Application in Living Cells. *Chemosensors* **2021**, *9* (3), 48. https://doi.org/10.3390/chemosensors9030048.

(9) Qiang, J.; Chang, C.; Zhu, Z.; Wei, T.; Yu, W.; Wang, F.; Yin, J.; Wang, Y.; Zhang, W.; Xie, J.; Chen, X. A Dinuclear-Copper(II) Complex-Based Sensor for Pyrophosphate and Its Applications to Detecting Pyrophosphatase Activity and Monitoring Polymerase Chain Reaction. *Sens. Actuators B Chem.* **2016**, *233*, 591–598. https://doi.org/10.1016/j.snb.2016.04.082.

(10) Liu, J.-X.; Ding, S.-N. Monitoring Pyrophosphate Anions via Cobalt(II)-Modulated Fluorescence of Cadmium Sulfide Quantum Dots. *Anal. Methods* **2016**, *8* (10), 2170–2175. https://doi.org/10.1039/C5AY03116H.

(11) Mondal, S.; Ghosh, T. K.; Chowdhury, B.; Ghosh, P. Supramolecular Self-Assembly Driven Selective Sensing of Phosphates. *Inorg. Chem.* **2019**, *58* (23), 15993–16003. https://doi.org/10.1021/acs.inorgchem.9b02483.

(12) Twum, K.; Rissanen, K.; Beyeh, N. K. Recent Advances in Halogen Bonded Assemblies with Resorcin[4]Arenes. *Chem. Rec.* **2021**, *21* (2), 386–395. https://doi.org/10.1002/tcr.202000140.

(13) Beyeh, N. K.; Díez, I.; Taimoory, S. M.; Meister, D.; Feig, A. I.; Trant, J. F.; Ras, R. H. A.; Rissanen, K. High-Affinity and Selective Detection of Pyrophosphate in Water by a Resorcinarene Salt Receptor. *Chem. Sci.* **2018**, *9* (5), 1358–1367. https://doi.org/10.1039/C7SC05167K.

(14) Shen, L.; Chen, Z.; Li, Y.; Jing, P.; Xie, S.; He, S.; He, P.; Shao, Y. A Chronocoulometric Aptamer Sensor for Adenosine Monophosphate. *Chem. Commun.* **2007**, No. 21, 2169–2171. https://doi.org/10.1039/B618909A.

(15) Goyal, R. N.; Sangal, A. Electrochemical Oxidation of Adenosine Monophosphate at a Pyrolytic Graphite Electrode. *J. Electroanal. Chem.* **2003**, *557*, 147–155. https://doi.org/10.1016/S0022-0728(03)00367-X.
(16) Zabik, N. L.; Anwar, S.; Ziu, I.; Martic-Milne, S. Electrochemical Reactivity of Bulky-Phenols with Superoxide Anion Radical. *Electrochimica Acta* **2019**, *296*, 174–180. https://doi.org/10.1016/j.electacta.2018.11.051.
(17) Pan, F.; Beyeh, N. K.; Ras, R. H. A.; Rissanen, K. Guest-Induced Folding of the N-Benzyl Substituents in an Ammonium Resorcinarene Chloride and the Formation of a Halogen-Bonded Dimer of Capsules. *Cryst. Growth Des.* **2016**, *16* (12), 6729–6733. https://doi.org/10.1021/acs.cgd.6b01454.
(18) Schwan, S.; Schröder, D.; Wegner, H. A.; Janek, J.; Mollenhauer, D. Substituent Pattern Effects on the Redox Potentials of Quinone-Based Active Materials for Aqueous Redox Flow Batteries. *Chemsuschem* **2020**, *13* (20), 5480–5488. https://doi.org/10.1002/cssc.202000454.
(19) Aoyama, Yasuhiro.; Tanaka, Yasutaka.; Toi, Hiroo.; Ogoshi, Hisanobu. Polar Host-Guest Interaction. Binding of Nonionic Polar Compounds with a Resorcinol-Aldehyde Cyclooligomer as a Lipophilic Polar Host. *J. Am. Chem. Soc.* **1988**, *110* (2), 634–635. https://doi.org/10.1021/ja00210a073.
(20) Aoyama, Y.; Tanaka, Y.; Sugahara, S. Molecular Recognition. 5. Molecular Recognition of Sugars via Hydrogen-Bonding Interaction with a Synthetic Polyhydroxy Macrocycle. *J. Am. Chem. Soc.* **1989**, *111* (14), 5397–5404. https://doi.org/10.1021/ja00196a052.
(21) Kobayashi, K.; Asakawa, Y.; Kikuchi, Y.; Toi, H.; Aoyama, Y. CH-.Pi. Interaction as an Important Driving Force of Host-Guest Complexation in Apolar Organic Media. Binding of Monools and Acetylated Compounds to Resorcinol Cyclic Tetramer as Studied by Proton NMR and Circular Dichroism Spectroscopy. *J. Am. Chem. Soc.* **1993**, *115* (7), 2648–2654. https://doi.org/10.1021/ja00060a013.
(22) Cho, J.; Kim, S. Selective Sensing of Adenosine Monophosphate (AMP) by a Calix[6]Triazolium-Based Colorimetric Sensing Ensemble. *RSC Adv. 12* (51), 32784–32789. https://doi.org/10.1039/d2ra05987h.
(23) Pursell, J. L.; Pursell, C. J. Host–Guest Inclusion Complexation of α-Cyclodextrin and Triiodide Examined Using UV–Vis Spectrophotometry. *J. Phys. Chem. A* **2016**, *120* (13), 2144–2149. https://doi.org/10.1021/acs.jpca.6b00982.

Chapter 4 – Electrochemical Detection of Anionic Surfactants in Peterborough Ontario. Improving Upon Existing EPA Methods

Abstract

Surfactants have become ubiquitous across industrial processes and consumer goods due to their utility and convenience. The ever-growing demand has led to a significant growth in the surfactant market over the last decade. However, concerns have been raised regarding their environmental and biological toxicity. Despite concerns, current methods of detection are insufficient due to a lack of sensitivity or high operating costs. Electrochemical sensing has gained popularity for various analytes given high sensitivity, cost effectiveness, and unique *in situ.* operation. Here, an electrochemical method is proposed as a tandem step to existing methods for anionic surfactant detection. Results demonstrate a robust detection method with greater sensitivity for detection than traditional spectroscopic methods. The electrochemical method was applied to real water samples by testing River water in Peterborough, Ontario, a city with a legacy in manufacturing and topography favorable to waterway surfactant accumulation. Therefore, the proof of concept provides strong evidence for a novel and simple detection method for in situ. analysis of surfactant pollutants and may replace traditional spectroscopic methods.

Contributions:

In this chapter, I contributed to the experiment design and planning. I also carried out the electrochemical and spectroscopic methods. I collected and prepared river water samples as well.

4.1 Introduction

Surfactants have been touted as miracles of modern chemistry, however, the continued increase in production has raised concerns over their persistence and environmental toxicity. The unique amphiphilicity of surfactants allows for them to interact with polar solvents via a hydrophilic head group and nonpolar solvents via a hydrophobic tail.[1] This property allows for reduced surface tension and stabilization of foams and emulsifications. Thus, there is a significant demand for surfactants across industrial and consumer applications, including pharmaceuticals, agriculture, industrial laundering, petroleum recovery, and personal care products.[2–7] In approximately 25 years, the global production of surfactants has increased from 7 million tonnes to 15 million tonnes; with a market estimated to grow to a $52 billion valuation by 2028.[8–11] A vast majority of the market is comprised of anionic surfactants, negatively charged head groups, primarily sodium dodecyl sulfate (SDS) and linear alkylbenzene sulfonate (LAS); perfluorinated alkyl substances (PFAS) are similar anionic surfactants that have gained notoriety for their toxicity and persistence due to the bond strength of their fluorinated tail.[12] Despite the abundance of surfactants, their environmental toxicity is often overlooked.

Due to the ubiquity of surfactants in consumer products, they are often discharged into the environment. It is estimated that over half of all manufactured surfactants enter the environment. Recently, the Environmental Protection Agency (EPA) updated legal, enforceable limits on the concentration of various PFAS in drinking water, where the highest concentration is only 10 ppt.[13] Despite the recent action taken by the EPA, the Environmental Working Group (EWG) has reported firefighting activities, especially at military bases, have contaminated surrounding water with ppm concentrations of PFAS.[14] These organic pollutants are of primary concern, especially due to their ability to evade common water treatment methods.[15] While secondary treatment

methods may degrade the surfactants, recent evidence suggests that degradation products may be more toxic than the initial surfactant.[10,11] As a result, surfactants wind up in drinking water as toxic threats to humans and the environment. Synthetic phosphate-containing surfactants are the primary source of phosphate in aquatic systems, leading to eutrophication and its cascading effects.[9,16,17] Furthermore, chronic exposure to specific surfactants has been linked to various health effects on development, immunotoxicity, hepatotoxicity, and cancers.[18] As such, developing accessible and effective environmental monitoring methods for surfactants is crucial.

Currently, the EPA method 425.1, a colorimetric method, is employed for the detection and quantification of Methylene Blue Activated Substances (MBAS). Methylene Blue (MB) is a cationic dye that reacts with anionic surfactants, MBAS, to form an ion pair. The ion pair can be extracted via liquid-liquid extraction to determine the concentration of MBAS by spectroscopy of the aqueous or organic phase (Figure 1). While the method is well documented and widely accepted, replacing spectroscopy with an electrochemical sensor to measure the aqueous phase post-extraction offers a unique opportunity for *in situ*. detection and quantification. Currently, there are existing reports of electrochemical sensors for the detection of anionic surfactants. However, they rely on the complex modification of the electrode surface.[19] Instead, various sample preparation and filtration methods have been developed for the analysis of surfactant samples in water, thus overcoming the issue of interference during traditional electrochemical sensing. This was previously demonstrated in a micropipette tip-based sensor.[15] Here, Lopez *et al.* demonstrated that a carbon ink electrode was capable of electrochemically detecting a decreased concentration in MB after liquid-liquid extraction with SDS, a common surfactant.[15] However, they limited their electroanalysis to cyclic voltammetry and linear sweep voltammetry, both of which hindered the limit of detection. The work demonstrated a proof of concept for a surfactant sensor, yet did not

detect PFAS, a surfactant of concern, in real water samples. Given the well-defined redox behaviour of MB, the detection and quantification of MBAS may be completed via electrochemical means.

Electrochemical sensing of MBAS can greatly benefit cities such as Peterborough Ontario, where its topography and history create an increased risk for surfactant accumulation. The city of Peterborough runs along the Otonabee River, and its topography was formed during the Wisconsin glaciation by the receding of glaciers over 10,000 years ago.[20] Currently, the southern and downtown areas of the city overlay the bottom of the historical glacial lake. Due to this flat topography, the areas are prone to flooding as the surrounding Peterborough drumlin drains into the area. Along with the city's strong history of manufacturing, and growing population, there is concern over legacy and new MBAS concentrations in the Otonabee River.[21] A novel, sensitive, electrochemical sensing method would allow for reactive and proactive monitoring.

Ideally, electrochemical sensors offer a means for cost-effective, rapid, *in situ.* environmental monitoring, decreasing the barrier for the most vulnerable populations affected by the manufacturing and pollution of MBAS. Here, we propose a modification of EPA method 425.1 to incorporate electrochemical quantification of MBAS. Various MBAS with different hydrophilic head groups and hydrophobic tail lengths were quantified with the proposed electrochemical method. After a simple electrochemical pretreatment of the electrode, results demonstrated a significantly improved sensitivity and equal response to the tested MBAS with the electrochemical method. The method was further validated by quantification of surfactants in the Otonabee River, a local waterway running alongside an urban area with industrial and residential activity.

4.2 Materials and Methods

4.2.1 Materials and Reagents

As electrodes, CHI104 Glassy carbon (GCE), CHI111 Ag wire reference electrode, and CHI115 platinum (Pt) counter electrodes were purchased from CH Instruments (USA). All electrochemical experiments were performed on the Autolab PGSTAT302N potentiostat, with the Nova software purchased from MetroOhm. Acidic solutions of different concentrations of surfactants were prepared according to previous optimization of MB redox behavior in reverse osmosis (RO) water, in 0.1 M phosphate buffer (0.1 M NaH_2HPO_4 (VWR Chemicals) and 0.1 M Na_2HPO_4 (Westlab)) at pH 6.0 (Adjusted with 1M HCl (VWR Chemicals)).[22] River water samples were filtered five times through 0.45 μm nylon syringe filters prior to the addition of phosphate buffer. Surfactants tested include, sodium dodecyl sulfate (SDS) (BioRad), nonafluoro-1-butanesulfonic acid (PFNA) (TCI America), Perfluoropentanoic acid (PFC5) (Thermoscientific), and perfluorooctanoic acid (PFC8) (Sigma Aldrich). Also, chloroform (Sigma-Aldrich) and methylene blue (Sigma Aldrich) were used during surfactant extractions.

4.2.2 Surfactant extraction of the ion pair formed with MB

Extraction of anionic surfactants from aqueous samples was performed by modification of a previously described Environmental protection agency (EPA) standard method.[15,23] To 3 mL of aqueous sample, 100 μM MB (as a solid) was added and well mixed and sonicated to ensure full dissolution of MB. For the liquid-liquid extraction, 3 mL of chloroform was mixed with aqueous sample containing MB. Samples were then vortexed for 30 s and left to stand for phase separation. Then the aqueous phase was separated and measured electrochemically for surfactant quantification.

4.2.3 Electrochemical measurements

All electrochemical measurements were carried out on the aqueous phase from the extraction in a three-electrode, single-chamber cell with an Autolab potentiostat/galvanostat with a GC working electrode, Ag wire reference electrode and a Pt wire counter electrode. The GC surface was cleaned and pre-treated prior to each measurement. Briefly, the GC surface was renewed via polishing on a polishing pad for 6 min in Alumina powder slurries (1 μm, 0.3 μm, 0.05 μm), followed by polishing on a clean polishing pad for 3 min, 8 min of sonication in an activated carbon solution and finally 3 min sonication in RO water. Pretreatment of the surface consisted of a chronoamperometric step of 1.7 V for 120 s. The Nova 2.1 software by MetroOhm was used as the data collection interface on the potentiostat. Differential pulse voltammetry (DPV) was carried out in the -0.5 - 0.6 V potential range (cathodic sweep), at a step of -0.005 V, modulation amplitude of 0.025 V, and modulation time of 0.05 s. Each data point consists of three replicate measurements.

4.2.4 UV-vis Spectroscopy

Solution UV–vis spectroscopy was performed on a BioTek Cytation 5 UV/Vis spectrometer in 96-well plates. 50 μL of the aqueous phase from samples was diluted with 50 μL of phosphate buffer. Spectral scanning was conducted between 450-700 nm at a 1 nm step.

4.3 Results and Discussion

The MBAS compounds of interest include perfluorinated alkyls with various ionic head groups such as carboxylic acid. In this study, several representative MBAS were tested including, PFNA, PFC8, PFC5, alongside the well-known surfactant, SDS (Scheme 1). The SDS was chosen due to its prevalence in an aqueous environment, with sulfates being the most common MBAS. The

perfluorinated MBAS, such as PFNA, PFC8, and PFC5 were chosen due to their legacy persistence, and structural diversity due to alkyl chain length and polar group moiety.

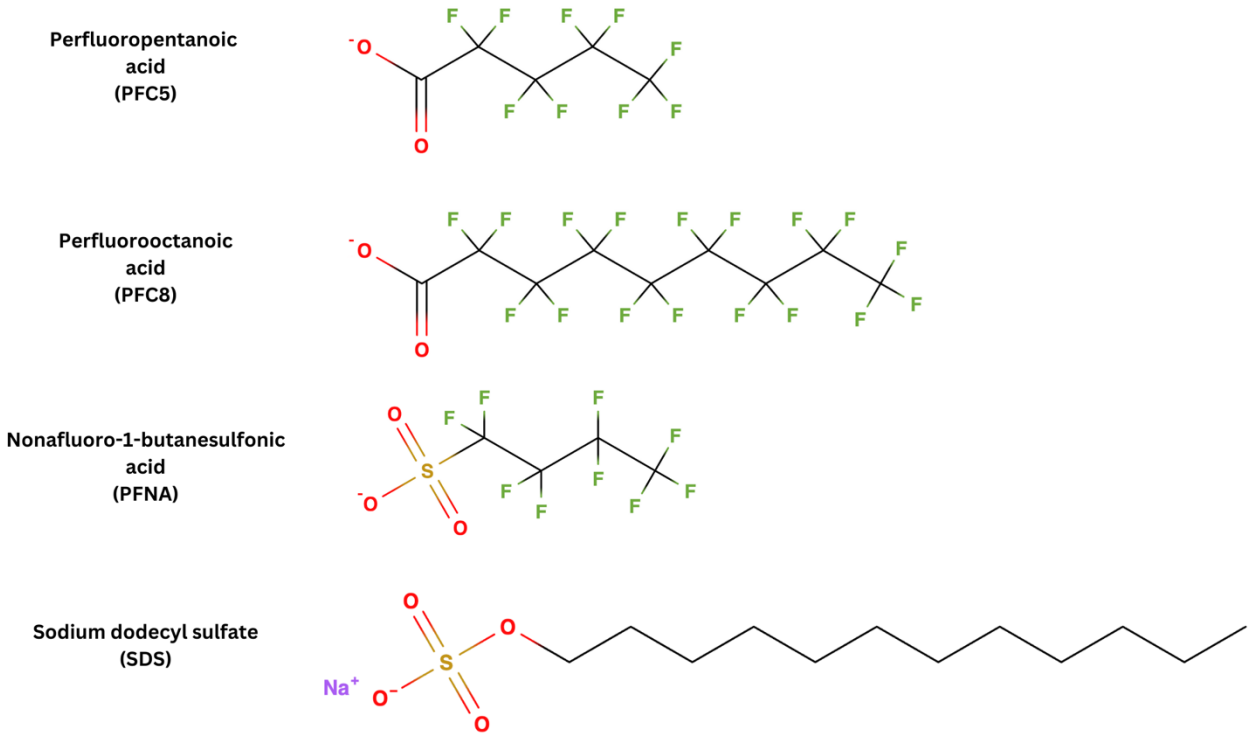

Scheme 1. Various MBAS (PFC5, PFC8, PFNA, SDS) chosen as representative anionic surfactants for quantification.

4.3.1 Characterization of methylene blue-surfactant ion pair

The MB-surfactant ion pairs were extracted from the aqueous phase to an organic chloroform phase, as shown for MB-SDS extractions in Figure 2A. The resulting aqueous phase was then measured electrochemically, and the MB was used to quantify the surfactant concentration in the initial water sample. The redox behaviour of MB has been well-documented

and optimized in aqueous media.[22,24] Hence, the reduction of MB was monitored by DPV in 0.1 M phosphate buffer solution, pH 6.0.

As expected, the reduction of MB to the leuco- form is apparent by the cathodic current peak at -0.29 V (Figure 2B). The PFNA concentration dependent studies were performed within the environmentally relevant concentration range of 0 - 3 μM. A chronoamperometric electrode pretreatment of 1.7 V for 120 s was used to optimize the sensitivity, which resulted in the LOD of 4.1 x 10^{-7} M with an R^2 of 0.98 and relative standard deviations (RSD) ranging from 0.8 - 5%, compared to the unmodified electrode (3.0 x 10^{-6} M) (Figure 2C). The current electrochemical sensor exhibited improved LOD compared to other similar unmodified sensors.[15]

Therefore, the electrochemical method can detect and quantify MBAS at reported concentrations of concern. The Environmental Working Group (EWG) maintains a database of total reported PFAS concentrations.[14] Various sites have reported micromolar concentrations of PFAS, significantly higher than levels deemed dangerous by the EPA. It is important to recognize that the sensor can detect total MBAS concentrations, where PFAS is one of the many detected substances. Therefore, without modification, the developed sensor can detect environmentally relevant concentrations of pollutants. Achieving such sensitivity without modification is important to the sensor's applicability at scale.

To investigate the robustness of the MB redox behavior river water samples were spiked with 2 μM of various MBAS. The ratio of current signal ratio (i_0/i) was used to differentiate the current maxima between the background and spiked samples. Like the traditional EPA method 425.1, the electrochemical signal was representative of total MBAS concentrations; Sulfonic and carboxylic acid head groups with varying alkyl chain lengths elicited similar MB reduction signals (Figure 2D). An ANOVA test indicated that the electrochemical sensor is a universal sensor for

MBAS which is on par with traditional spectroscopic assay (Figure 2C). Importantly, the total MBAS concentration could be accurately determined in the complex river water media. Between all the tested MBAS, the existence of background compounds and potential interferents did not prevent detection and quantification, demonstrating the reliability of the method for real use case scenarios.

Next, the performance of the electrochemical sensor was compared to the EPA UV-vis spectroscopy method (Figure S1). Within the tested concentration range, the resulting UV-vis calibration curve shows a lack of sensitivity and linearity compared to the electrochemical method (Figure 2E). Hence, the traditional spectroscopic method for MBAS based on MB detection was insensitive in the environmentally relevant calibration range. The spectroscopic method failed to distinguish between nanomolar concentration differences, unlike the electrochemical method. While UV-Vis is not compatible at low concentrations, the diffusion-limited current exhibited by the reduction in the electrochemical method results in a high sensitivity to changes in analyte concentration. Therefore, the proposed electrochemical sensor outperformed the traditional spectroscopic method and may serve as an improved alternative for *in situ* detection and quantification of MBAS. To further validate the method and explore its applicability, we investigated the MBAS concentrations of a local waterway as described below.

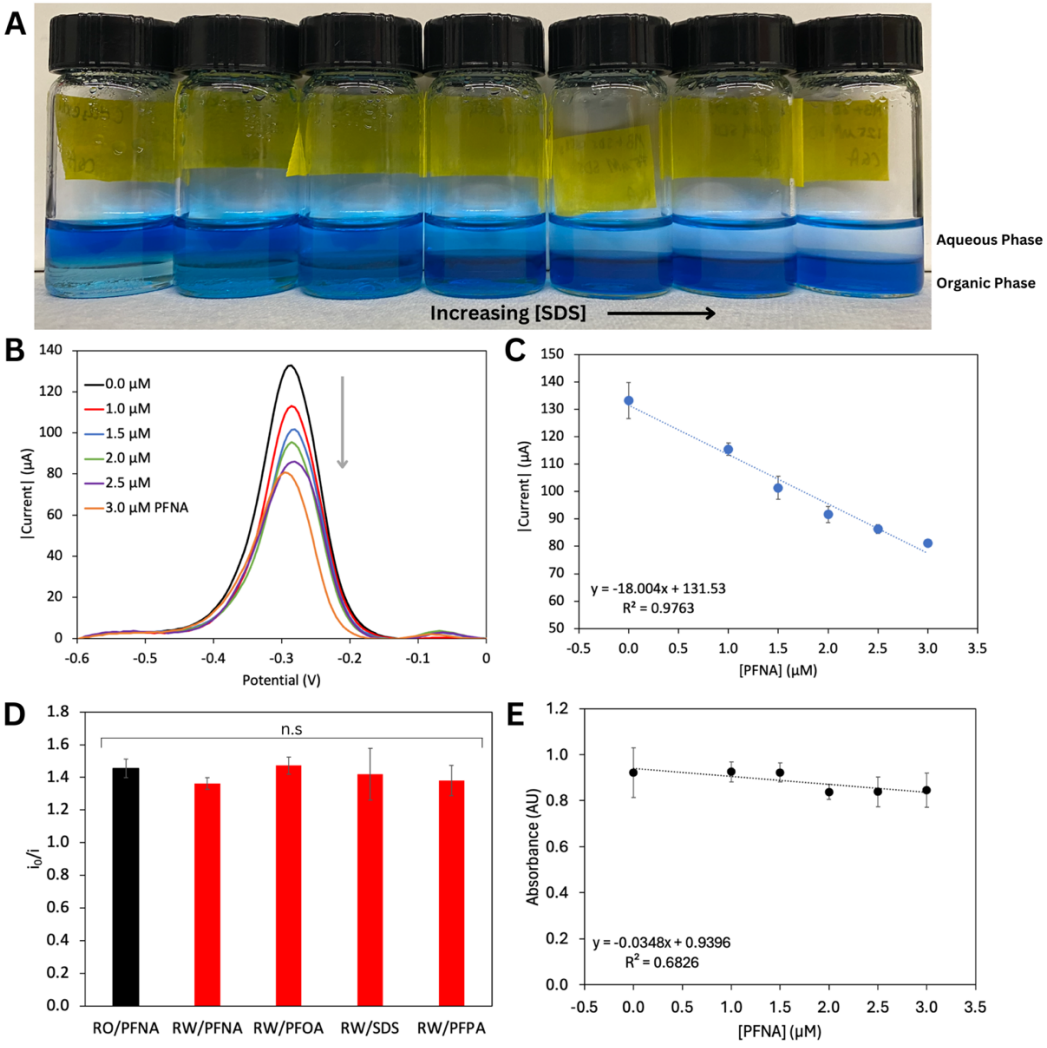

Figure 4.1. A) Picture of 20 mL vials with increasing concentrations of SDS (0, 10, 25, 50, 75, 100, 125 µM). B) Absolute current of MB aqueous phase post extraction with various PFNA concentrations (0 - 3 µM), cathodic sweep recorded by DPV with GC working electrode, Pt counter electrode, and Ag wire reference electrode. C) Absolute current maxima of MB from DPVs. D) The current ratios for spiked river water (RW) samples with various MBAS compared to standard (PFNA) prepared in RO ([MBAS] = 2 µM). E) UV-vis calibration curve of aqueous MB aqueous phase post extraction with various MBAS concentrations (0 - 3 µM) measured with (λ Abs = 610 nm). All samples were measured in triplicates.

4.3.2 Application to Otonabee River sample analysis

The US EPA has set guidelines for the maximum concentrations of various surfactant pollutants for biological and environmental toxicity.[24] Further work by the EWG has focused on compiling reported toxic surfactant concentrations in various sites across the United States.[14] While this is a well-established practice in the United States, countries such as Canada have fallen behind in regulation and environmental monitoring. Currently, Health Canada has set out "non-enforceable" guidelines for the maximum concentrations of various surfactant classes.[25] While these guidelines are above the levels of concern reported by the US EPA, they can only be improved through informed environmental monitoring.[25] Cities such as Peterborough Ontario serve as ideal models for monitoring of anionic surfactants due to the topography and legacy industrial manufacturing. Given the persistence of anionic surfactants like PFAS and the release of consumer surfactants from the growing population, the Otonabee River is vulnerable to the accumulation of these pollutants. Connecting Lake Huron and Lake Ontario, the Otonabee river sits along a portion of the Trent-Severn Waterway. Four locations were sampled along the Otonabee River at various public locks during the Spring of 2024 (Figure 3A). The river water samples were subjected to the prior electrochemical method for MBAS detection and quantification.

The analysis of Otonabee River samples revealed localized, elevated concentrations of MBAS. Interestingly, upstream of the downtown and southern areas of the city contained the highest concentrations. The highest determined concentrations were around the university, where a concentration of 2.9 ± 0.1 μM of MBAS was detected, with concentrations decreasing in the downtown area to 1.6 ± 0.4 μM (Figure 3B). The southernmost sampling location, Lansdowne, revealed a negligible concentration of MBAS.

Measured concentrations of MBAS are likely dependent on the time of sampling and may vary from day to day. The city of Peterborough has advisories against swimming for 48 hours after a rainstorm due to drainage into the Otonabee River, compromising water quality.[26] This may correlate to elevated MBAS levels as well. Furthermore, while water treatment facilities struggle to completely remove MBAS from water, effluent is expected to lower concentrations. Given the water treatment facility in Peterborough is close to the Lansdowne sampling location, it likely explains the negligible concentrations of MBAS. Nonetheless, the electrochemical method was capable of detecting and quantifying MBAS in various regions of the Otonabee River.

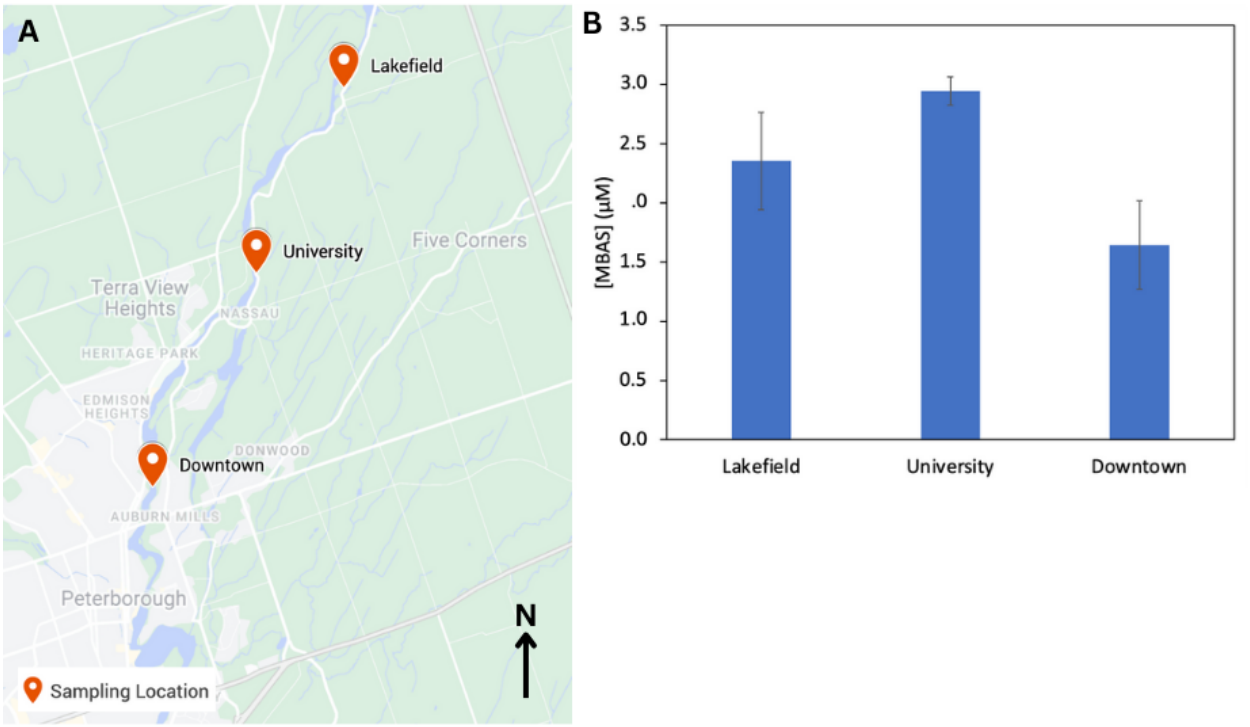

Figure 4.2. A) sampling locations across the Trent-Severn waterway. B) reported concentrations of MBAS determined from the sampling locations (N = 3).

4.4 Conclusion

Altogether, a modification of the existing EPA method 425.1 to replace spectroscopic quantification with an electrochemical method is possible. Electrochemical data demonstrated that via a simple chronoamperometric electrode pretreatment, an electroanalytical method is more precise and sensitive than the current method. The reduction of MB at -0.29 V requires a low overpotential and is highly reproducible. With low RSD and high linearity, the calibration within the environmentally relevant range of 0 - 3 μM was successfully achieved. MB is an effective probe for various surfactant classes and in the presence of more complex media, it was still capable of determining the total MBAS concentration. A real use case of the method was demonstrated by the detection and quantification of MBAS in the Otonabee River, running along the city of Peterborough. Legacy manufacturing and population growth created a study area of interest and results demonstrated elevated concentrations of MBAS in localized areas. The current MBAS liquid-liquid extraction is well accepted by the scientific community and the addition of an electrochemical quantification is a simple adjustment that will allow for facile, *in situ*. monitoring.

Existing policy on the environmental limits of various surfactant classes in Canada is lagging. To write informed policy, effective, and consistent environmental monitoring must first be achieved. By incorporating a simple electrochemical detection step, we can move towards cost-effective, rapid, real-time monitoring. While this study serves as strong support and a proof of concept for the amendment of MBAS quantification, future research must investigate interferences and corroboration with confirmatory methods such as liquid chromatography.

4.5 References

(1) Shaban, S. M.; Kang, J.; Kim, D.-H. Surfactants: Recent Advances and Their Applications. *Compos. Commun.* **2020**, *22*, 100537. https://doi.org/10.1016/j.coco.2020.100537.

(2) Masjedi, M.; Montahaei, T. An Illustrated Review on Nonionic Surfactant Vesicles (Niosomes) as an Approach in Modern Drug Delivery: Fabrication, Characterization, Pharmaceutical, and Cosmetic Applications. *J. Drug Deliv. Sci. Technol.* **2021**, *61*, 102234. https://doi.org/10.1016/j.jddst.2020.102234.

(3) Liao, Y.; Li, Z.; Zhou, Q.; Sheng, M.; Qu, Q.; Shi, Y.; Yang, J.; Lv, L.; Dai, X.; Shi, X. Saponin Surfactants Used in Drug Delivery Systems: A New Application for Natural Medicine Components. *Int. J. Pharm.* **2021**, *603*, 120709. https://doi.org/10.1016/j.ijpharm.2021.120709.

(4) Kovalchuk, N. M.; Simmons, M. J. H. Surfactant-Mediated Wetting and Spreading: Recent Advances and Applications. *Curr. Opin. Colloid Interface Sci.* **2021**, *51*, 101375. https://doi.org/10.1016/j.cocis.2020.07.004.

(5) Shao, D.; Liu, G.; Chen, H.; Xu, C.; Du, J. Combination of Surfactant Action with Peroxide Activation for Room-Temperature Cleaning of Textiles. *J. Surfactants Deterg.* **2021**, *24* (2), 357–364. https://doi.org/10.1002/jsde.12471.

(6) Quintero, L. An Overview of Surfactant Applications in Drilling Fluids for the Petroleum Industry. *J. Dispers. Sci. Technol.* **2002**, *23* (1–3), 393–404. https://doi.org/10.1080/01932690208984212.

(7) Ramprasad, C.; Philip, L. Contributions of Various Processes to the Removal of Surfactants and Personal Care Products in Constructed Wetland. *Chem. Eng. J.* **2018**, *334*, 322–333. https://doi.org/10.1016/j.cej.2017.09.106.

(8) Pettersson, A.; Adamsson, M.; Dave, G. Toxicity and Detoxification of Swedish Detergents and Softener Products. *Chemosphere* **2000**, *41* (10), 1611–1620. https://doi.org/10.1016/S0045-6535(00)00035-7.

(9) Nagtode, V. S.; Cardoza, C.; Yasin, H. K. A.; Mali, S. N.; Tambe, S. M.; Roy, P.; Singh, K.; Goel, A.; Amin, P. D.; Thorat, B. R.; Cruz, J. N.; Pratap, A. P. Green Surfactants (Biosurfactants): A Petroleum-Free Substitute for Sustainability─Comparison, Applications, Market, and Future Prospects. *ACS Omega* **2023**, *8* (13), 11674–11699. https://doi.org/10.1021/acsomega.3c00591.

(10) Badmus, S. O.; Amusa, H. K.; Oyehan, T. A.; Saleh, T. A. Environmental Risks and Toxicity of Surfactants: Overview of Analysis, Assessment, and Remediation Techniques. *Environ. Sci. Pollut. Res.* **2021**, *28* (44), 62085–62104. https://doi.org/10.1007/s11356-021-16483-w.

(11) Johnson, P.; Trybala, A.; Starov, V.; Pinfield, V. J. Effect of Synthetic Surfactants on the Environment and the Potential for Substitution by Biosurfactants. *Adv. Colloid Interface Sci.* **2021**, *288*, 102340. https://doi.org/10.1016/j.cis.2020.102340.

(12) Lindstrom, A. B.; Strynar, M. J.; Libelo, E. L. Polyfluorinated Compounds: Past, Present, and Future. *Environ. Sci. Technol.* **2011**, *45* (19), 7954–7961. https://doi.org/10.1021/es2011622.

(13) US EPA, O. *Per- and Polyfluoroalkyl Substances (PFAS)*. https://www.epa.gov/sdwa/and-polyfluoroalkyl-substances-pfas (accessed 2024-04-29).

(14) EWG. *Interactive Map: PFAS Contamination Crisis: New Data Show 6,189 Sites in 50 States*. http://www.ewg.org/interactive-maps/pfas_contamination/ (accessed 2024-06-15).

(15) González-López, A.; Costa-Rama, E.; Fernández-Abedul, M. T. Electrochemical Micropipette-Tip for Low-Cost Environmental Applications: Determination of Anionic Surfactants through Their Interaction with Methylene Blue. *Talanta* **2021**, *224*, 121732. https://doi.org/10.1016/j.talanta.2020.121732.
(16) Ostroumov, S. A. Inhibitory Analysis of Top-down Control: New Keys to Studying Eutrophication, Algal Blooms, and Water Self-Purification. *Hydrobiologia* **2002**, *469* (1), 117–129. https://doi.org/10.1023/A:1015559123646.
(17) Ostroumov, S. A. The Synecological Approach to the Problem of Eutrophication. *Dokl. Biol. Sci.* **2001**, *381* (1), 559–562. https://doi.org/10.1023/A:1013378505630.
(18) Panieri, E.; Baralic, K.; Djukic-Cosic, D.; Buha Djordjevic, A.; Saso, L. PFAS Molecules: A Major Concern for the Human Health and the Environment. *Toxics* **2022**, *10* (2), 44. https://doi.org/10.3390/toxics10020044.
(19) Galović, O.; Samardžić, M.; Hajduković, M.; Sak-Bosnar, M. A New Graphene-Based Surfactant Sensor for the Determination of Anionic Surfactants in Real Samples. *Sens. Actuators B Chem.* **2016**, *236*, 257–267. https://doi.org/10.1016/j.snb.2016.05.166.
(20) Hewitt, D. F. Geology and Scenery, Peterborough, Bancroft and Madoc Area.
(21) Government of Canada, S. C. *Focus on Geography Series, 2021 Census - Peterborough (Census metropolitan area)*. https://www12.statcan.gc.ca/census-recensement/2021/as-sa/fogs-spg/page.cfm?lang=E&topic=1&dguid=2021S0503529 (accessed 2024-04-27).
(22) Hayat, M.; Shah, A.; Nisar, J.; Shah, I.; Haleem, A.; Ashiq, M. N. A Novel Electrochemical Sensing Platform for the Sensitive Detection and Degradation Monitoring of Methylene Blue. *Catalysts* **2022**, *12* (3), 306. https://doi.org/10.3390/catal12030306.
(23) Chitikela, S.; Dentel, S. K.; Allen, H. E. Modified Method for the Analysis of Anionic Surfactants as Methylene Blue Active Substances. *Analyst* **1995**, *120* (7), 2001–2004. https://doi.org/10.1039/AN9952002001.
(24) García-González, R.; Costa-García, A.; Fernández-Abedul, M. T. Methylene Blue Covalently Attached to Single Stranded DNA as Electroactive Label for Potential Bioassays. *Sens. Actuators B Chem.* **2014**, *191*, 784–790. https://doi.org/10.1016/j.snb.2013.10.037.
(25) Canada, H. *Water talk: PFOS, PFOA and other PFAS in drinking water*. https://www.canada.ca/en/services/health/publications/healthy-living/water-talk-drinking-water-screening-values-perfluoroalkylated-substances.html (accessed 2024-04-27).
(26) *Peterborough Public Health*. https://www.peterboroughpublichealth.ca/your-health/beaches-and-pools/beach-testing-results/ (accessed 2024-06-15).

6. Chapter 4 Supporting information

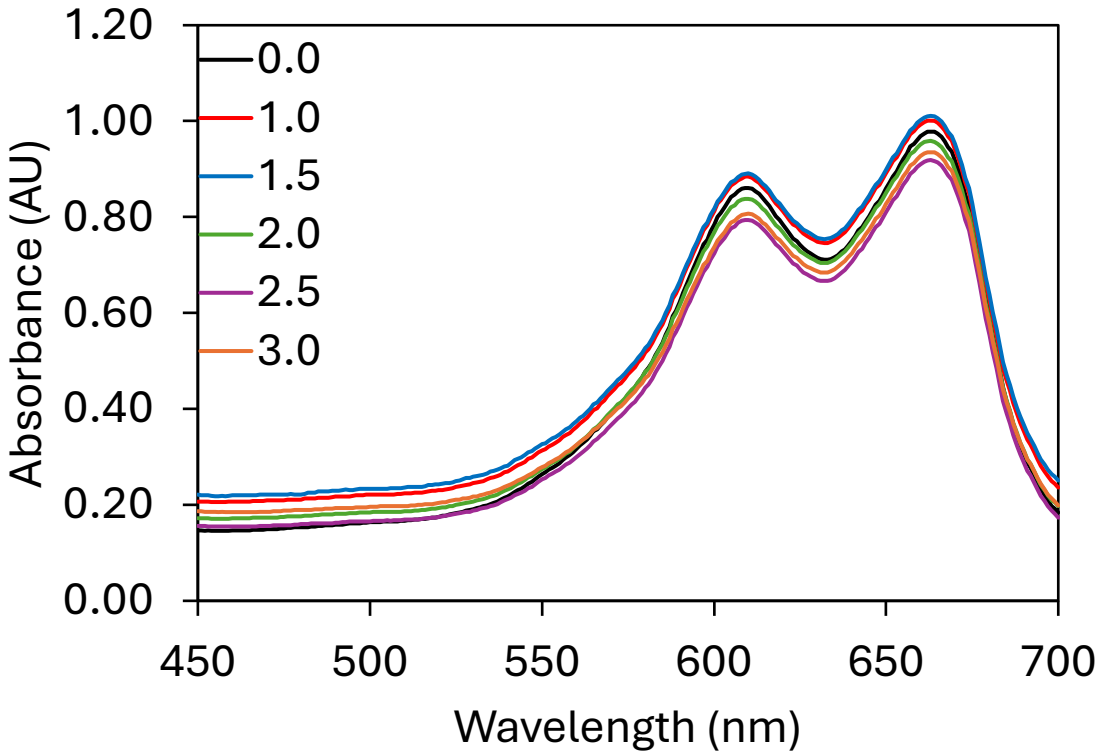

Figure S1. UV-Vis spectra of MB in aqueous phase after liquid-liquid extraction with various PFNA concentrations (0 – 3 μM).

Chapter 5 – Conclusion and Future Work

5.1 Conclusion

As demand for point of care, rapid analysis grows, there is a need to move away from traditional lab-based methods. Electrochemical sensors have proven to be a cost-effective, portable alternative across various fields. However, like traditional methods, electrochemical sensors must be optimized for each analyte of interest. Supramolecular chemistry offers a unique route to the development of a generalizable sensing platform. Host-guest chemistry is a mature area of chemistry, with vast libraries of hosts with high affinities for specific guests. By forming electroactive host-guest systems, specific, selective, rapid, and cost-effective analytical methods can be developed. Importantly, hosts can be swapped out to detect any analyte of interest allowing for a generalizable sensing platform.

The advancements in resorcinarene host molecules offer a path toward a generalizable electrochemical sensing platform. Currently, host-guest electrochemical sensors have focused on CB and CD hosts, which lack high selectivity; however, resorcinarene hosts are easily modified to impart high selectivity and sensitivity while maintaining a scalable synthesis. Recent advancements in resorcinarene modification have produced the NARX hosts which incorporate the new halide bond to fix the host structure in place and accommodate new, larger guests. The $NARCl_4$ hosts were previously reported to bind to AMP with high selectivity and sensitivity; the selective and sensitive detection of anions in solution marked a significant hurdle for supramolecular chemistry. By exploiting the halide bond to form novel supramolecular structures and non-covalent interaction with a redox probe, the NARX hosts may lead towards an ideal supramolecular assembly capable of electrochemical sensing with high affinity and little electrode modification. Results indicated that the NARX hosts formed an assembly with the Fc redox probe *exo*- to the cavity. Thus, suggesting a unique, rarely reported, bifunctionality of the host, to

encapsulate guest and simultaneously interact with a redox probe. The NARX-Fc assembly was highly stable and maintained the electron transfer kinetics of the redox probe. Investigating the NARX with higher sensitivity electrochemical pulse methods revealed previously masked electrochemical behaviour. The $NARCl_4$ sensitivity to AMP was replicated electrochemically, with modulation in signal up to a 1:1 titration.

There is also interest, in the indirect detection of guests through redox probes. Primarily, methylene blue has been used for DNA detection and more importantly anionic surfactant detection. Methylene blue, a cationic dye, is used in the EPA method 425.1 as a colorimetric test for the quantification of anionic surfactants. The methylene blue forms ion pairs with the surfactants which are separated via liquid-liquid extraction and the remaining dye in the aqueous portion can be quantified spectroscopically. However, methylene blue can be reduced to its leuco-form, suggesting that the spectroscopic method may be replaced with an electrochemical method. Given the portability, sensitivity, and cost-effectiveness of an electrochemical method, the EPA 425.1 method can be improved by a tandem electrochemical quantification step. In fact, chronoamperometric pretreatment of an unmodified GCE resulted in a nanomolar LOD, a significant improvement over the traditional spectroscopic method. The electrochemical method was also robust, detecting various anionic surfactants in RO and river water.

5.2 Significance

Chapter 2 evaluated the differential impact of resorcinarene hosts on the Fc redox couple. Previous studies have focused on less desirable CB and CD hosts, thus, the NARX hosts may be crucial for the mass adoption of host-guest electrochemical sensing. This chapter served to reveal the importance of resorcinarene modification for the interaction with Fc. No studies have investigated the NARX-Fc couple and the host's ability to form a redox active assembly. It was

revealed that the $NARCl_4$ host exhibited a rare bifunctional behaviour, with Fc interacting *exo*- to the host and shifting the Fc $E_{1/2}$ over 200 mV anodically. Therefore, the NARX hosts are promising alternatives to CB and CD hosts for the development of host-guest electrochemical sensors.

Chapter 3 focused on the direct electrochemical detection of host-guest complexation. The CV method has been previously used for monitoring host-guest interactions, however, its susceptibility to charging current can mask weaker electrochemical signals in the background noise. Furthermore, incorporating a redox probe into the supramolecular assembly to impart redox activity is not always ideal. It can limit the further modification of hosts to instead impart high affinity for guests since a compromise must be made in the host design to accommodate the redox probe. Results revealed that the background charging current in the CV was masking the phenol/phenolate signals from the resorcinarene hosts. These signals were modulated by the titration of AMP, with the $NARCl_4$ phenolate signal increasing linearly with AMP up to a full equivalent. This demonstrates an important step towards replacing traditional, cumbersome methods with electrochemical methods. The detection of the $NARCl_4$-AMP has been previously reported, however, they relied on NMR and ITC for detecting complexation. Electrochemical methods are more cost-effective and amenable to point-of-care analysis.

Chapter 4 demonstrated the value of electrochemical sensors for replacing traditional lab-based methods. Specifically, the well-established colorimetric EPA 425.1 method which relies on spectroscopy for quantification of anionic surfactants can be replaced with an electrochemical method. The method was further validated by testing river water in the Otonabee River. Electrochemical methods are cost-effective and can be miniaturized. This is an important characteristic for accessible sensing of anionic surfactants which have been linked to numerous health concerns. The PFAS molecules are a class of anionic surfactants which are notoriously toxic

and resistant to degradation; manufacturing and PFAS pollution have impacted vulnerable populations in remote and developing areas. With an unmodified glassy carbon electrode, a nanomolar LOD was achieved that withstood a complex river water media. This presents an important step towards replacing traditional cumbersome lab-based methods with simple electrochemical methods. Given the lack of electrode modification and the "off the shelf" materials used in sensing, this sensor presents a unique opportunity to bring an electrochemical sensor to market.

5.3 Future work

5.3.1 Chapter 2

1. Isolating and investigating the host-Fc complexes before and after the oxidation of Fc. This is necessary to understand the changes in the complex structure and mode of interaction. Through a softer ionizing mass spectrometry method, the weak non-covalent interactions may be investigated. DFT modelling in either oxidation state would also reveal the energies associated with the complex.
2. There is a need for kinetic information regarding the host-Fc complexes that may be acquired from rotating disk electrode studies. This would allow for the isolation of mass transport and kinetic phenomena, a limitation of traditional CV.
3. Investigating the bifunctional capabilities of the NARX host by introducing a well-known guest. EIS may serve as a better tool to monitor the change in current density at a fixed potential since guest complexation is reported to shift the redox potential. The improved sensitivity of EIS over CV offers a better method to monitor minute potential shifts as well as changes in the current density seen in direct pulse oxidation experiments.

4. Replicating experiments in an aqueous environment is crucial for biological applications. The NARX hosts are unique in their solubility in both polar and nonpolar solvents. Importantly, the $NARCl_4$ host is well-known to interact with AMP, a biological guest, therefore, an aqueous sensor is necessary. The solubility of the hosts can be tuned by their alkyl-chain and while it should not impact the Host-Fc couple, it should be investigated.
5. The NARX-Fc is a single host-guest complex, while the goal was to develop an entire sensing platform. It is of interest to investigate more resorcinarene hosts for their capability to interact and complex with Fc. This would reveal the true applicability of the class of hosts to serve as the base for a sensing platform. It would also allow for a better understanding of the requirements for host-Fc interactions. Currently, the benzyl substituents and the methylene protons appear to dictate this interaction.
6. Surface modification with the hosts would provide better quantification of complexation. Currently, the current response is reliant on the Cottrell behaviour of the redox probe and is thus limited by mass transport. Through the surface modification of an electrode through gold thiol chemistry and thiol terminated hosts, there is better control and monitoring of the extent of binding. This method is more common in literature for previous host-guest electrochemical sensors given the advantage of a known concentration of affixed host.

5.3.2 Chapter 3

1. Traditional methods to elucidate the mechanism of interaction between AMP and the $NARCl_4$ host are necessary. The electrochemical data demonstrates a linear relationship between the magnitude of the oxidation of hosts and AMP concentration. There is similar behaviour for either host with little understanding of how the host interacts with the AMP.

NMR, DFT, and MS would all allow for structural information to confirm the interaction and shed light on the electrochemical behaviour of the phenolate signal.

2. The robustness of the sensor must be tested in the presence of interferents. The $NARCl_4$ host is known to interact more favourably with pyrophosphate and weakly with other adenosine phosphate analogues. Currently, the sensor benefits from the lack of solubility of its interferents in organic solvents. However, the sensor must function in an aqueous environment for practicality.
3. Similar to Chapter 2, surface modification would greatly benefit the sensor. Again, the current is dictated by the diffusion of the host-AMP complex to the electrode surface; surface modification would eliminate this variable. Alternatively, EIS can provide a higher sensitivity signal by monitoring the Warburg diffusion. Theoretically, the diffusion coefficient decreases upon the complexation with AMP. Since CV was insufficient for detecting the host signals, the low-frequency range in an EIS would provide insight into the mass transport behaviour to quantify the extent of complexation.

5.3.3 Chapter 4

1. More river water samples are necessary to validate the sensor. The sensor had a few river water samples, tested in triplicates. These samples must be corroborated with traditional quantification methods, such as GC-MS. The electrochemical sensor is an unmodified glassy carbon electrode, which is known to lack specificity. Furthermore, MB is known to interact with a variety of anions which may confound the reported concentration of surfactants.
2. Given the high sensitivity of the electrode, it is possible to use commercially available columns for PFAS extraction. This extraction method is accepted by the EPA and avoids

the need for electrode modification to impart sensitivity. Incorporation of the extraction also improves the sensor's marketability. The sensor is unique in that it can be replicated with "off-the-shelf" parts, without complex electrode modification; by bundling all the components, the sensor has a unique marketability.

3. The sensor's reproducibility must be tested with various electrodes, potentiostat, and users. For a truly marketable sensor for surfactant detection, the calibration curve must be applicable across devices. The existing data was produced from a single electrode by a single analyst on a single electrochemical setup. Therefore, the sensor's applicability is limited unless the results can be replicated.

4. Blind samples submitted for analysis are necessary to demonstrate the sensor's reliability. To validate the electrochemical method and the MB calibration curve, blind samples must be submitted for analysis.

Appendix

License Number	5895361439938
License date	Oct 24, 2024

Printable Details

Licensed Content

Licensed Content Publisher	John Wiley and Sons
Licensed Content Publication	Wiley Books
Licensed Content Title	Electrochemical Methods: Fundamentals and Applications, 2nd Edition
Licensed Content Author	Allen J. Bard Larry R. Faulkner
Licensed Content Date	Dec 1, 2001
Licensed Content Pages	1

Order Details

Type of use	Dissertation/Thesis
Requestor type	University/Academic
Format	Print and electronic
Portion	Figure/table
Number of figures/tables	3
Will you be translating?	No

About Your Work

Title of new work	Electroactive Supramolecular Systems for Informed Electrochemical Sensor Development
Institution name	Trent University
Expected presentation date	Oct 2024

Additional Data

Portions	Figures 3.4.2, 7.3.1, 7.3.9
The Requesting Person / Organization to Appear on the License	Carlos Quintero Arias

Figure 2, 5, and 6 license

Licensed Content

Licensed Content Publisher	Elsevier
Licensed Content Publication	Journal of Molecular Liquids
Licensed Content Title	β-Cyclodextrin anchored neem carbon dots for enhanced electrochemical sensing performance of an anticancer drug, lapatinib via host-guest inclusion
Licensed Content Author	Ayyapayya S Mathad,J. Seetharamappa,Shankara S Kalanur
Licensed Content Date	Mar 15, 2022
Licensed Content Volume	350
Licensed Content Issue	n/a
Licensed Content Pages	1

Order Details

Type of Use	reuse in a thesis/dissertation
Portion	figures/tables/illustrations
Number of figures/tables/illustrations	1
Format	both print and electronic
Are you the author of this Elsevier article?	No
Will you be translating?	No

About Your Work

Title of new work	Electroactive Supramolecular Systems for Informed Electrochemical Sensor Development
Institution name	Trent University
Expected presentation date	Oct 2024

Additional Data

Portions	Figure 4
The Requesting Person / Organization to Appear on the License	Carlos Quintero Arias

Figure 4 license

Licensed Content

Licensed Content Publisher	Springer Nature
Licensed Content Publication	Journal of Food Measurement and Characterization
Licensed Content Title	Electrochemical detection of caffeine in sports drinks based on molecular imprinting technology
Licensed Content Author	Huan Li et al
Licensed Content Date	Mar 15, 2024

Order Details

Type of Use	Thesis/Dissertation
Requestor Type	academic/university or research institute
Format	print and electronic
Portion	figures/tables/illustrations
Number of figures/tables/illustrations	1
Will you be translating?	no
Circulation/distribution	1 - 29
Author of this Springer Nature content	no

About Your Work

Title of new work	Electroactive Supramolecular Systems for Informed Electrochemical Sensor Development
Institution name	Trent University
Expected presentation date	Oct 2024

Additional Data

Portions	1
The Requesting Person / Organization to Appear on the License	Carlos Quintero Arias

Figure 7 license

License Number	5895090225593
License date	Oct 23, 2024

Printable Details

Licensed Content

Licensed Content Publisher	Elsevier
Licensed Content Publication	Environmental Research
Licensed Content Title	Development of an impedimetric sensor for susceptible detection of melatonin at picomolar concentrations in diverse pharmaceutical and human specimens
Licensed Content Author	Xuru Jin,Marzieh Nodehi,Mehdi Baghayeri,Yi Xu,Zhidan Hua,Ying Lei,Minmin Shao,Pooyan Makvandi
Licensed Content Date	Dec 1, 2023
Licensed Content Volume	238
Licensed Content Issue	n/a
Licensed Content Pages	1

Order Details

Type of Use	reuse in a thesis/dissertation
Portion	figures/tables/illustrations
Number of figures/tables/illustrations	1
Format	both print and electronic
Are you the author of this Elsevier article?	No
Will you be translating?	No

About Your Work

Title of new work	Electroactive Supramolecular Systems for Informed Electrochemical Sensor Development
Institution name	Trent University
Expected presentation date	Oct 2024

Additional Data

Portions	Figure 3B
The Requesting Person / Organization to Appear on the License	Carlos Quintero Arias

Figure 10 license

License Number	5895100584896
License date	Oct 23, 2024

Printable Details

Licensed Content

Licensed Content Publisher	John Wiley and Sons
Licensed Content Publication	Chemistry - A European Journal
Licensed Content Title	Design of Organic Macrocycle-Modified Iron Oxide Nanoparticles for Drug Delivery
Licensed Content Author	Ali Trabolsi, John-Carl Olsen, Farah Benyettou, et al
Licensed Content Date	Mar 15, 2017
Licensed Content Volume	23
Licensed Content Issue	35
Licensed Content Pages	15

Order Details

Type of use	Dissertation/Thesis
Requestor type	University/Academic
Format	Print and electronic
Portion	Figure/table
Number of figures/tables	1
Will you be translating?	No

About Your Work

Title of new work	Electroactive Supramolecular Systems for Informed Electrochemical Sensor Development
Institution name	Trent University
Expected presentation date	Oct 2024

Additional Data

Portions	Figure 1
The Requesting Person / Organization to Appear on the License	Carlos Quintero Arias

Figure 11 license

License Number	5895091014380
License date	Oct 23, 2024

Printable Details

Licensed Content

Licensed Content Publisher	Springer Nature
Licensed Content Publication	Journal of Inclusion Phenomena and Macrocyclic Chemistry
Licensed Content Title	Functional modification, self-assembly and application of calix[4]resorcinarenes
Licensed Content Author	Jing-Long Liu et al
Licensed Content Date	Jan 11, 2022

Order Details

Type of Use	Thesis/Dissertation
Requestor Type	academic/university or research institute
Format	print and electronic
Portion	figures/tables/illustrations
Number of figures/tables/illustrations	2
Will you be translating?	no
Circulation/distribution	1 - 29
Author of this Springer Nature content	no

About Your Work

Title of new work	Electroactive Supramolecular Systems for Informed Electrochemical Sensor Development
Institution name	Trent University
Expected presentation date	Oct 2024

Additional Data

Portions	Figure 1 and Scheme 1
The Requesting Person / Organization to Appear on the License	Carlos Quintero Arias

Figure 12 and 13 license

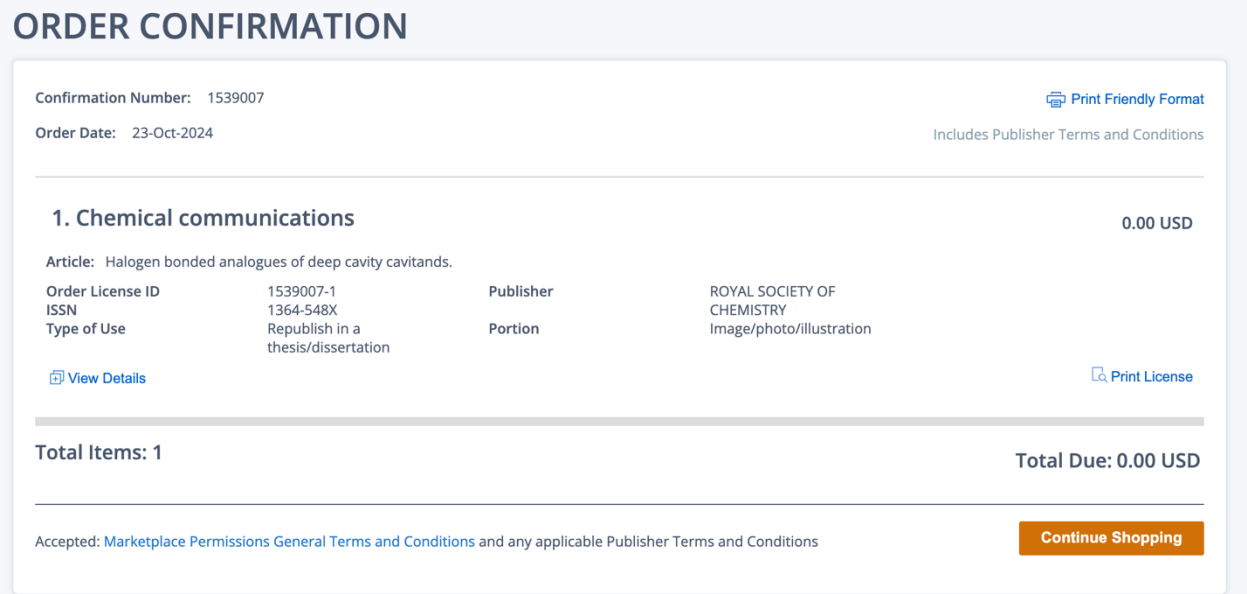

ORDER CONFIRMATION

Confirmation Number: 1539007

Order Date: 23-Oct-2024

Print Friendly Format

Includes Publisher Terms and Conditions

1. Chemical communications — 0.00 USD

Article: Halogen bonded analogues of deep cavity cavitands.

Order License ID	1539007-1	Publisher	ROYAL SOCIETY OF CHEMISTRY
ISSN	1364-548X		
Type of Use	Republish in a thesis/dissertation	Portion	Image/photo/illustration

View Details

Print License

Total Items: 1

Total Due: 0.00 USD

Accepted: Marketplace Permissions General Terms and Conditions and any applicable Publisher Terms and Conditions

Continue Shopping

Figure 15 license

License Number	5895100153284
License date	Oct 23, 2024

Printable Details

Licensed Content

Licensed Content Publisher	Elsevier
Licensed Content Publication	Current Opinion in Electrochemistry
Licensed Content Title	Harnessing host–guest chemistry for electrochemical sensing in complex matrices
Licensed Content Author	Élodie V. d'Astous,Philippe Dauphin-Ducharme
Licensed Content Date	Aug 1, 2022
Licensed Content Volume	34
Licensed Content Issue	n/a
Licensed Content Pages	1

Order Details

Type of Use	reuse in a thesis/dissertation
Portion	figures/tables/illustrations
Number of figures/tables/illustrations	1
Format	both print and electronic
Are you the author of this Elsevier article?	No
Will you be translating?	No

About Your Work

Title of new work	Electroactive Supramolecular Systems for Informed Electrochemical Sensor Development
Institution name	Trent University
Expected presentation date	Oct 2024

Additional Data

Portions	Figure 2A
The Requesting Person / Organization to Appear on the License	Carlos Quintero Arias

Figure 16 license